Prognostic factors in cochlear implantation

Gijs van Wermeskerken

Thesis University of Utrecht, Department of Otorhinolaryngology & Head and Neck Surgery, University Medical Center Utrecht, The Netherlands.

ISBN: 978-90-393-4864-2

Cover design, lay-out and print: Optima Grafische Communicatie, Rotterdam

Prognostic factors in Cochlear implantation

Prognostische factoren van cochleaire implantatie

(met een samenvatting in het Nederlands)

Proefschrift

ter verkrijging van de graad van doctor aan de Universiteit Utrecht
op gezag van de rector magnificus, prof. dr. J.C. Stoof,
ingevolge het besluit van het college voor promoties
in het openbaar te verdedigen op
dinsdag 2 september des namiddags te 12.45 uur

door

Gijsbert Karel Anne van Wermeskerken
geboren op 19 januari 1972
te Leiden

Promotoren:	Prof. dr. G.J. Hordijk
	Prof. dr. K. Graamans
Co-promotor:	Dr. A.F. van Olphen

Printing of this thesis was financially supported by:
Stichting Atze Spoor Fonds, Artu Biologicals, Atos Medical, Beltone, Beter Horen, Electro Medical Instruments, GlaxoSmithKline, GN ReSound, Meditop, Schering-Plough, Stallergenes, Veenhuis Medical Audio.

Contents

Chapter 1	Introduction and outline of the thesis	7
	1. The cochlear implant	9
	2. Electrophysiology	12
	3. Anatomy and the role of imaging techniques	16
	4. Aim of the thesis	21
Chapter 2	Intra- and postoperative electrode impedance of the straight and Contour arrays of the Nucleus 24 Cochlear Implant; relation to T and C levels *International Journal of Audiology 2006; 45(9): 537-44*	29
Chapter 3	A comparison of intra- versus postoperatively acquired electrically evoked compound action potentials *International Journal of Audiology 2006; 45(10): 589-94*	45
Chapter 4	Audiological performance after cochlear implantation: a 2-year follow-up in children with inner ear malformations *Acta Otolaryngologica 2007; 127: 252-57*	59
Chapter 5	Intracochlear assessment of electrode position after cochlear implant surgery by means of multislice computer tomography *European Archives of Otorhinolaryngology* 2007; 264(12): 405-7	73
Chapter 6	Imaging of electrode position in relation to electrode functioning after cochlear implantation *Submitted for publication*	81
Chapter 7	Summary and conclusions	93
	Samenvatting	101
	Dankwoord	109
	Curriculum vitae	113
	Publications	115
	Abbreviations	117

CHAPTER 1

Introduction and outline of the thesis

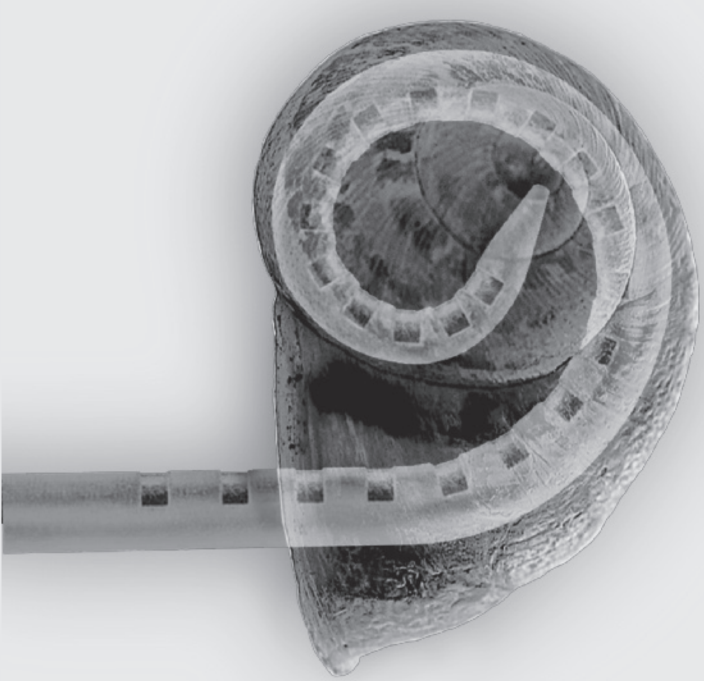

1. The cochlear implant

Highlights in the history of the cochlear implant

Around 1790, it was discovered that electrical stimulation of the auditory system can create a perception of sound. The discovery was made when Alessandro Volta placed metal rods in his own ears and connected them to a 50-volt circuit, feeling a jolt and hearing a noise "like a thick boiling soup" (1). Other experiments were sporadically performed until electrical, sound-amplifying hearing aids were developed in the 20th century.

Few people realize that cochlear implantation also has a long history, going back more than half a century. The first direct stimulation of an acoustic nerve with an electrode was performed in Paris in 1957 by two French-Algerians, André Djourno and Charles Eyriès (2). Having placed wires on nerves exposed during an operation, they reported that the patient heard sounds like "a roulette wheel" and "a cricket" when a current was applied. After implanting two patients, a dispute over the commercial development of their discovery put an abrupt end to their collaboration (3).

In the 1970s, the center of activity shifted from Paris to Los Angeles. There, in 1972, William House and Jack Urban developed the first cochlear implant, which was registered by the American Food & Drug Administration in 1979 as a clinical appliance (4). This single-channel implant permitted adequate stimulation of the cochlear nerve (5;6). The results were encouraging; by allowing patients to pick up ambient sounds, the implant served as an aid to lip-reading.

During the 1970s, Graeme Clark took the development of cochlear implants in a new direction by stimulating the cochlea at multiple points (7). The advantage of multichannel cochlear implants, which became more widely available in the 1980s, was far better speech discrimination. These implants follow the tonotopic distribution of the cochlea and the auditory nerve as described by Von Helmholtz in 1863 and Von Békésy in 1960 (8;9). The latter discovered the tonotopic tuning that exists along the length of the organ of Corti. Essentially, high-frequency sounds cause motion in the organ of Corti at the base (input end) of the cochlea, whereas low-frequency sounds cause motion at the apex of the cochlea, several centimeters down the length of the organ of Corti.

Throughout the 1990s, the external components, which had to be strapped to the body, became smaller with advances in miniaturization electronics. Today most adults and school-age children wear a little behind-the-ear (BTE) speech processor about the size of a power hearing aid.

Figure 1. Nucleus 3G microphone, transmitter and speech processor (external part).

Figure 2. Nucleus cochlear implant (internal part).

Cochlear implant systems

The cochlear implant is a system that has not changed fundamentally over the years, still consisting of an external and an internal part. Its three external components are a microphone, a speech processor, and a transmitter (Figure 1). The internal part consists of a receiver/stimulator and an electrode array (Figure 2). In modern cochlear implant systems, the array has from 12 to 22 separate electrodes. These are introduced into the scala tympani of the cochlea after a cochleostomy of 1 to 1.5 mm (Figure 3). The electrode arrays (Figure 4) may differ in number, placement, stiffness, and cross-sectional area. For a perimodiolar placement of the electrodes, the surgeon can use a contoured electrode array and a stylet (Nucleus devices) or, instead, a positioner (Clarion devices) (10-13). This placement minimizes the amount of current spreading away from the

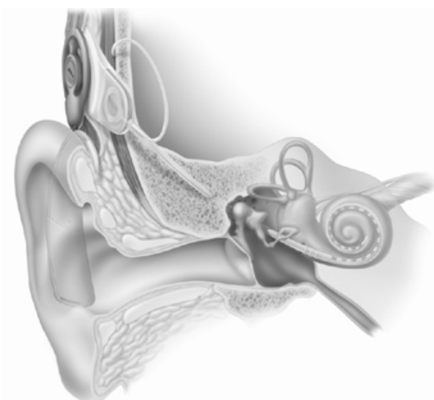

Figure 3. Overview cochlear implant.

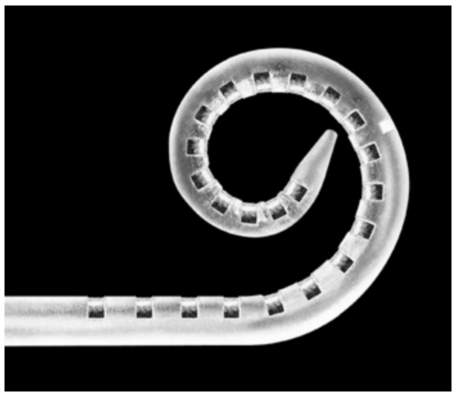

Figure 4. Nucleus Contour Advance electrode.

target spiral ganglion cells (14). The 'modiolus-hugging' electrode arrays tend to lie close to the spiral lamina. Proximity of the electrodes to the neural elements allows reduction of stimulation levels, thereby lowering the amount of power required (15).

The internal components are usually encased in biocompatible titanium silastic or ceramic casing. The electrodes are made of platinum iridium wires encased in a biocompatible silastic carrier. Magnets on either side of the intact skin hold the external transmitter and the internal receiver together. The microphone picks up ambient sounds, which are analyzed and processed by the speech processor. Both the resulting information and the necessary electrical supply are transmitted to the internal parts of the cochlear implant system. There, intracochlear electrodes are stimulated for selective triggering of auditory nerve groups. Further transport follows the usual pathways to the auditory cortex.

Cochlear implant candidacy

The main indication for cochlear implantation is severe-to-profound sensorineural hearing loss that cannot be treated adequately with conventional hearing aids. Many factors are considered when selecting cochlear implant candidates. First of all, age, emotional and cognitive abilities, cause and duration of deafness, capacity and ability to be retrained and social status should be considered. Secondly, certain anatomical and physiological conditions for proper processing of auditory signals must be met.

Decisions on cochlear implant candidacy can be very difficult, particularly regarding children and prelingually deaf adolescents. Over the past few years, pressure has been mounting to lower the minimum age for cochlear implantation in profoundly deaf children in order to improve the outcome. There is evidence that children implanted before 2 years of age achieve better open-set speech recognition than children implanted later (16;17). In recent years, implantation has been performed in children aged between 5 and 11 months (18). The neural plasticity of the auditory cortex is now widely recognized as an issue (19;20). Since hearing in two ears allows people to localize sounds and to hear better in noisy environments, bilateral implants are currently being investigated (21-23).

Outcomes in cochlear implantation

Outcomes in cochlear implantation have improved significantly over the last two decades. It is now common to expect open-set speech recognition in adults after implantation. Technological improvements, including the refinement of electrode designs and speech processing, have led to continuous gains in the performance and benefit that cochlear implant users can expect (24). Predicting the outcomes has preoccupied many researchers. Most studies have focused on preoperative variables such as audiological, cognitive, and motivational factors. But several outcome variables such as speech discrimination tests and self-reported benefit have also been studied (25-28).

2. Electrophysiology

Introduction

Positioning the electrode array close to the modiolus is presumed to lead to better-localized neural stimulation. The advantages of these so-called perimodiolar designs, include lower stimulation levels, a larger dynamic range, better channel separation, and increased speech understanding (29-32). Besides the position of the electrode array, the design of the electrode itself is very important. The electrode is the all-important interface between the electrical stimulus and the auditory nerve fibers that need to be stimulated. Telemetry can be used to measure information such as electrical impedance and intracochlear neural response recordings. In this way the state of the cochlea and electrode can be monitored.

Electrical impedance

An important aspect of the electrode design is electrical impedance, which depends on electrode surface area, morphological processes, and electrochemical processes initiated by electrical stimulation. These issues must be taken into account when developing new electrode arrays because impedance is a major factor in power consumption (33). Reducing the amount of power used by the implant would allow for further miniaturization of the processors. This, in turn, eventually would make totally implantable devices feasible (34). Measurement of electrode impedance provides an indication of the electrode's integrity, revealing, for instance, any short or open circuits. It also indicates the status of the electrode – tissue interface. Initial changes in electrode impedance may be expected prior to electrical stimulation due to morphological changes at the electrode – tissue interface (35). For example, it has been shown that after implantation the electrode array becomes encapsulated in fibrous tissue (36-39). High impedance is related to the presence of tissue and/or bone growth near the electrode array. Chow et al. suggested that intracochlear osteoneogenesis and fibrous tissue growth should be considered a pathological complication of cochlear implantation (40). A positive correlation between the grade of tissue around the electrode array and impedance was found by Clark et al. (41). An elevation of the electrically evoked compound action potential (ECAP) threshold after implantation appeared to be associated with new bone formation and fibrous tissue growth within the scala tympani (42). Pfingst demonstrated a short-term increase and subsequent decrease in the threshold during the first few months after implantation in adult macaques (43). This was followed by periods of prolonged threshold stability. In long-term implanted kittens, Ni et al. showed a steady increase in electrode impedance over the first month post-implantation (44). The impedance correlated with the degree of tissue growth observed within the scala tympani. Electrode impedance seems to be primarily related to the resistive characteristics of the fluid and tissue surrounding the electrodes (45). Electrical stimulation may also affect electrode impedance. A reduction of electrode impedance after electrical stimulation might also be explained by the formation of a hydride layer on the surface of the electrodes. This hydride layer essentially increases the surface area of the electrode, thereby reducing its impedance (46).

Electrically evoked neural responses

A significant body of research has been published on methods for measuring neural responses to electrical stimulation (47). These include the electrically evoked compound action potential (ECAP) (48;49), the electrically evoked auditory brainstem response (EABR) (50;51), the electrically evoked middle latency response (52;53), electrically evoked measures of the mismatch negativity potential (54-56), as well as electrically evoked versions of long latency potentials (57-59). A number of studies also describe potential applications for the electrically evoked stapedial reflex threshold in cochlear implant recipients (60-64). In general, all of these electrically evoked potentials have characteristics that are quite similar to their acoustically evoked counterparts (65). The major differences between the electrically and acoustically evoked neural responses are due to the fact that electrical stimulation bypasses the normal mechanical transduction mechanisms in the cochlea and stimulates the auditory nerve fibers directly. As a result, the response of the auditory nerve to electrical stimulation has a shorter latency, greater synchrony, and steeper growth characteristics than single-fiber responses evoked using acoustic stimulation (66).

Electrically evoked compound action potentials

Recording the ECAP (Figure 5) of the auditory nerve has become common practice since the introduction of neural response telemetry (NRT) by Cochlear Ltd. (Sydney, Australia) and the rather similar procedure of neural response imaging (NRI) by the Advanced Bionics Corporation (Sylmar, CA, USA). The

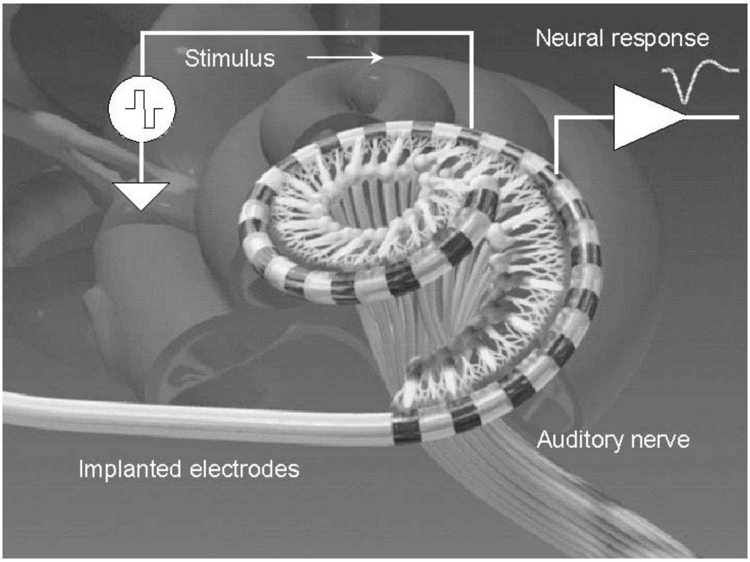

Figure 5. Measuring the ECAP.

NRT system was conceived to make intracochlear recordings of the electrically evoked compound action potentials. Intracochlear neural response recordings previously required direct access to the stimulating and recording electrodes within the cochlea, either intraoperatively or via a percutaneous connection to the electrodes. However, the Nucleus 24 Cochlear Implant System makes use of bidirectional telemetry over a transcutaneous radio frequency (RF) link. Stimulation and recording parameters are first transmitted from the speech processor to the implant in one direction. Digitally encoded information on the subsequently measured compound action potential is then transmitted from the implant back to the speech processor in the opposite direction. The NRT software communicates with the speech processor to capture, process, store, and display the measurement data. The NRT system was clinically implemented by the Cochlear Company in their Nucleus CI24M implant, which was approved in June 1998 by the American Food and Drug Administration (FDA).

ECAP recording procedure

The neural response resulting from a stimulus presented at one location within the cochlea is recorded from a neighboring location within the cochlea (67). Large stimulus artefacts impede ECAP measurements. The artefact due to the electrical stimulus is orders of magnitude larger than the response to this stimulus. In addition, the ECAP appears within 1 ms after the stimulus, a time interval within which an amplifier may not have recovered from overstimulation by the

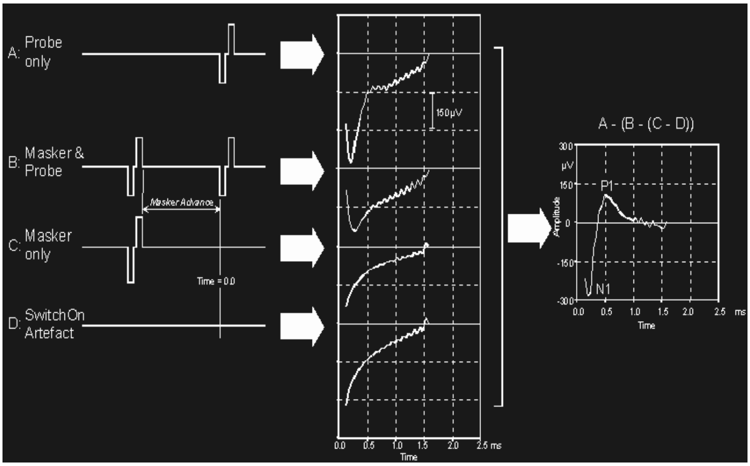

Figure 6. Complete Subtraction Paradigm (Baseline Corrected Display).
A=Probe: B=Masker+Probe: C=Masker: D=Switch-on Artefact

electrical stimulus. The NRT software uses a modified version of the forward-masking paradigm (Figure 6) that effectively copes with this problem, based on the work of Brown et al. and de Sauvage et al.(68;69). In experiments with cats, Brown and Abbas showed that uncorrupted ECAPs could be obtained by taking advantage of the refractory period of neurons (70). It is instructive to compare the response to an electrical impulse P (the probe) with the response to the probe immediately preceded by another impulse M (the masker). The response to P alone will consist of the artefact plus the response to P, while the response to the combination of probe and masker M+P will contain the artefact only. In the latter case, P does not elicit an ECAP since it was presented within the refractory period of the auditory neurons following their response to M. Thus, the difference between the two responses will reveal the ECAP.

While the ECAP is difficult or impossible to record preoperatively, it does have several advantages over the EABR or other auditory evoked potentials. For example, it is recorded from an electrode inside the cochlea rather than from surface electrodes. Therefore, the ECAP is much larger than the EABR; it is not adversely affected by muscle activity; it requires less averaging than the EABR. As a result, the subject is not required to sit still during ECAP recording sessions. Additionally, because the ECAP is a peripherally generated auditory response, it is not affected by development, anesthesia, attention, or sedation.

ECAP based speech processor fittings

ECAP-assisted fittings are particularly helpful for very young implant users. These children are unable to make reliable subjective loudness judgments for setting the map, threshold (T), and comfort (C) levels. Several studies have focused on the prediction of behavioral T and C levels from ECAP thresholds. The first large-scale studies indicated that in adults there is a significant but moderate correlation between the ECAP thresholds and the T levels (r=0.55) and C levels (r=0.57) from a conventional fitting (71). In children, Hughes et al. found somewhat higher coefficients: r=0.70 and 0.71, respectively (72). Other studies were undertaken, but all showed that the relation between the ECAP thresholds and behavioral responses were not strong enough to allow for an accurate prediction of behavioral T and C levels in individual CI users (73;74). A few ECAP-based fitting procedures have been proposed thus far (75-77). ECAP-based fittings seem to be faster and easier in the initial phase of speech processor fitting (78).

3. Anatomy and the role of imaging techniques

Introduction

Imaging performed prior to cochlear implantation provides information that may be critical to the selection of appropriate candidates and surgical techniques but also to the continuous functioning of the implanted device. Accordingly, it is important to be familiar with all current imaging modalities as they pertain to various preoperative, intraoperative, and postoperative clinical scenarios (79;80). Preoperative imaging will help the clinician identify patients with anatomic contraindications to implantation, but it will also reveal certain anatomical features that have consequences for selecting the specific device and determining which ear to implant. Furthermore, preoperative imaging may also allow the surgical team to anticipate aberrant anatomy and thus reduce the risk of surgical complications. Preoperative imaging ideally addresses several basic anatomical issues. Table 1 presents an overview of all structures and their relationships that should be evaluated preoperatively (81;82).

Nowadays, an increasing proportion of the children scheduled for cochlear implantation have congenital sensorineural hearing loss (SNHL). According to Jackler et al., 5 to 15% of these cases have malformations of the inner ear (IE) (83). With improvements in high resolution computed tomography (HRCT) and a better understanding of cochlear malformations, the number of reports on the results of cochlear implantation in malformed cochleae has risen steadily in the past decade (84-94). Research shows that various obstacles may impede hearing rehabilitation after cochlear implantation in this subgroup of patients. Difficulties may arise either intraoperatively – detected when cerebrospinal fluid (CSF) leakage, facial nerve anomalies, or electrode placement problems are noted – or

Table 1. Modified guidelines in temporal bone anatomy that have to be evaluated preoperatively in cochlear implant candidates.

	Anatomical structure	
1.	Temporal squama	- thickness
2.	Mastoid and middle ear	- extent of pneumatization
		- position of oval and round window
3.	Facial nerve	- tympanic and mastoidal course
		- size of facial recess
4.	Vascular anatomy	- relation carotid canal to cochlea
		- relation jugular bulb to round window
5.	Otic capsule	- abnormal bone density
6.	Cochlea	- patency of the scalae
		- presence of cochlear nerve
7.	Congenital abnormalities	- enlarged vestibular aqueduct
		- cochlear anomalies
		- labyrinthine anomalies
		- internal auditory canal

postoperatively, during activation and programming (95-97). Previous criteria for cochlear implantation had excluded children with IE malformations on the assumption that these children would not perform adequately after implantation. Recently published studies, however, report satisfactory hearing results in this group of patients. Their hearing outcomes are similar to those of other profoundly deaf children, with the exception of children with a common cavity type malformation (98-102). The variability in performance is considerable, however, especially in patients with severe cochlear malformations.

This chapter gives a short overview of various imaging techniques that are currently available. It also gives a detailed outline of the classification criteria for congenital IE abnormalities.

Computed tomography

HRCT has been widely accepted as the preferred imaging modality for the preoperative radiological assessment of cochlear implant candidates. Many clinicians use HRCT as the first-line (and often the only) imaging assessment in the preoperative evaluation. HRCT provides an exquisitely detailed image of all bony structures including the mastoid, middle ear, cochlea, tegmen, otic capsule, and pertinent vascular structures. Accurate measurements of the bony internal auditory canal will provide information on the likelihood of an underlying cochlear nerve abnormality. Compromise of the cochlear patency in the form of labyrintitis ossificans should be evident with HRCT, yet membranous fibrosis may not be as reliably apparent.

Magnetic resonance imaging

Magnetic resonance imaging (MRI) may currently be used to evaluate the membranous labyrinth, the internal auditory canal contents, and other pertinent structures of interest within the temporal bone by providing images with exceptional soft-tissue detail. In recent years, advances in MRI technology have compelled some cochlear implant teams to routinely order MRI scans for all implant candidates (103-105). Some centers now even use MRI as the primary means of imaging while reserving HRCT for patients with congenital malformations and anomalies in the course of the facial nerve (106). One advantage of MRI compared to HRCT is its superior efficacy in identifying abnormalities in cochlear patency. In particular, fibrosis of the membranous labyrinth is not visible with HRCT, but it may be clearly apparent as a filling defect on T2-weighted MRI images. Several cases of membranous cochlear obstruction that were missed by HRCT but discovered with MRI have been reported (107;108). It should be emphasized, however, that the results of imaging techniques are not always comparable, presumably due to differences in technical issues. For example, Bettman et al. demonstrated that CT is equivalent to MRI in predicting the cochlear patency (109).

Despite the increasing popularity of MRI, this scanning technique has some practical disadvantages. Most children and many adults undergoing MRI will need some level of sedation or, in many instances, even general anesthesia. In contrast, nearly all patients, including children, can undergo HRCT without sedation. Furthermore, the cost of HRCT is significantly less than that of a head MRI with contrast.

Functional MRI

Functional MRI attempts to provide an objective assessment of activity within the auditory cortex during electrical stimulation of the cochlea. This technique generally entails acquiring radiofrequency spoiled fast low-angle shot (FLASH) MRI sequences before and during transpromontory electrode stimulation of the cochlea. In theory, functional MRI can provide valuable information on activity along the central auditory pathway that could be helpful in selecting the best side for implantation (110). At present, however, the role and value of functional MRI in the preoperative assessment of cochlear implant candidates remains unclear.

Classification aspects in congenital inner ear malformations

Clinicians need to classify inner ear malformations in order to correlate certain of these types with surgical aspects of cochlear implantation and rehabilitation outcomes. To that end, most reports use the embryogenesis-based classification system described by Jackler et al. (111). The stage at which the embryonic development of the cochlea is arrested is related to the degree of severity of the malformation. Thus, a malformation of the cochlea may vary from total aplasia, severe cochlear hypoplasia, mild cochlea hypoplasia (basal turn only), common cavity, severe incomplete partition, and mild incomplete partition to a subnormal cochlea that does not reach the full 2.5 turns. The cochlear malformations may be present with a variety of bony abnormalities of the vestibule or semicircular canals or an enlarged vestibular aqueduct (EVA). The relative incidence of cochlear malformations is shown in Table 2 (112).

Table 2. The relative incidence of cochlear malformations reported by Jackler et al. (1987).

Malformation	*Incidence (%)*
Incomplete partition (Mondini)	55
Common cavity	26
Cochlear hypoplasia	15
Cochlear aplasia	3
Complete labyrinthine aplasia (Michel)	1

Jackler's classification system pertains to membranous as well as osseous abnormalities. The membranous malformations can only be identified in histological specimens, whereas the osseous or the combined osseous-membranous deformities are detectable by radiological techniques as well. Thus, children with congenital SNHL and radiographically normal IEs may be assumed to have anomalies limited to the membranous labyrinth or neural pathways. Many authors continue to use the term Mondini dysplasia, covering other distinct anatomic patterns of IE malformations (113). This might explain the relatively high incidence of Mondini dysplasia in the series of Jackler. More recent studies show that the EVA is the most common radiographically detectable malformation (114-120). This has become evident since HRCT made it much easier to assess the EVA in the axial plane.

Recently a more advanced classification system has been proposed by Sennaroglu and Saatci (121). Their system is based on Jackler's. They suggest the existence of two types of incomplete partition (IP): cystic cochleovestibular malformation (IP-I); and the classic Mondini deformity (IP-II). The latter has three components: a cystic apex; dilated vestibule; and a large vestibular aqueduct. A type I malformation has an empty cystic cochlea and vestibule without enlargement of the vestibular aqueduct. The Mondini deformity represents a malformation that arises in a later stage of embryogenesis, so the amount of dysplasia is much less than in type I. Table 3 gives an overview of the malformations that are

Table 3. Malformations of the membranous and osseous labyrinth.

Malformations limited to the membranous labyrinth	
1.	*Complete membranous labyrinthine dysplasia* (Siebenmann and Bing (110))
2.	*Limited membranous labyrinthine dysplasia*
	Cochleosaccular dysplasia (Scheibe (111)) – The organ of Corti is either partially or completely missing.
	Cochlear basal turn dysplasia – The basal turn of the cochlea is missing.
Malformations of the osseous and membranous labyrinth	
1.	*Complete labyrinthine aplasia* (Michel (112)) – Severest deformity, rare, absence of all cochlear and vestibular structures.
2.	*Cochlear anomalies*
	Cochlear aplasia – The cochlea is completely absent.
	Cochlear hypoplasia – A single turn cochlea or less, 15% of all cochlear anomalies. The cochlea normally measures 8 to 10 mm vertically; it is typically in the 5 to 6 mm range in cases of hypoplasia.
	Common cavity – The cochlea and vestibule are confluent. There is a cystic cavity representing the cochlea and vestibule, but without showing any differentiation into cochlea and vestibule. The position of the common cavity is predominantly anterior to the internal auditory canal on the axial plane; the dysplastic vestibular system is posterior to it.
	Incomplete partition (Mondini (113)) – A small cochlea with 1.5 turns possessing an apical scala communis due to deficiency in the osseous spiral lamina has been described (114-116).
3.	*Labyrinthine anomalies*
	Semicircular canal dysplasia – 40% of ears with a malformed cochlea will have an accompanying dysplasia of the lateral SCC (117).
	Semicircular canal aplasia –Less common, also associated with cochlear anomalies.
4.	*Aqueduct anomalies*
	Enlargement of the vestibular aqueduct (EVA) – Relatively high incidence, mostly bilateral. EVA is diagnosed when the diameter of the aqueduct exceeds 2.0 mm.
	Enlargement of the cochlear aqueduct – Not observed by Jackler, diameters highly variable, ranging from 0 to 11 mm with a mean of 4.5 mm (118).
5.	*Internal auditory canal abnormalities*
	Narrow internal auditory canal – IAC diameter less than 3 mm with normal nVII may indicate failure of the nVIII.
	Wide internal auditory canal – IAC diameter larger than 10 mm, does not correlate with hearing level.

either limited to the membranous labyrinth or found in the combined osseous and membranous labyrinth.

Inner ear malformations and cochlear implantation

IE malformations used to be classified mainly on the basis of morphological criteria. But because the aim of cochlear implantation is to restore IE function, morphological data should also be linked to data on hearing loss and outcomes of electrophysiological tests in order to refine the criteria for candidacy for cochlear implantation. Unfortunately, hardly any information is available on the relation between the nature of IE malformations and the degree of (dys)function. Given the limited number of patients with IE malformations in each cochlear implant center, it is difficult to establish criteria for eligibility. At present, there is no IE malformation classification system that includes (dys)functionality criteria.

4. Aim and outline of this thesis

The overall aim of this thesis is to investigate and to evaluate the prognostic factors of cochlear implantation. The issues that have been addressed here include electrophysiology, anatomy and imaging techniques.

Chapter 2 investigates the long-term behavior of electrode impedance. The discussion relates impedance to electrically evoked stapedius reflex measurements during surgery but also to some variables of the implant such as electrode design, stimulation mode, and threshold and comfort levels over a 9-month period after surgery.

In *Chapter 3* the electrically evoked compound action potentials are compared in the intra- versus the postoperative setting. Considering the change in the electrical pathway after cochlear implantation, it is important to know how this change would affect the timing of the recordings of threshold levels for evoked compound action potentials.

Chapter 4 analyzes audiological performance after cochlear implantation. The findings refer to a group of children with radiographically detectable malformations of the inner ear. Their results are compared to performance in prelingually deafened children at large.

Chapter 5 formulates and tests a computer tomography imaging protocol for postoperative scanning of the temporal bone in cochlear implant subjects. The chapter then discusses the feasibility of imaging the electrode position of the cochlear implant within the intracochlear spaces. The CT protocol is illustrated in both the isolated temporal bone and in a complete cadaver head.

Chapter 6 investigates the relation between eletrophysiological data such as the electrical impedance and the electrically evoked action potentials and the position of the electrode as assessed with high resolution CT-scanning.

Chapter 7 provides a summary of the thesis and offers some conclusions.

References

(1) Clark G.M., Tong Y.C., Patrick J.F. Cochlear Prosthesis. Melbourne: Churchill Livingstone; 1990.
(2) Djourno A., Eyriès C., Vallancien B. Electric excitation of the cochlear nerve in man by induction at a distance with the aid of micro-coil included in the fixture. C R Seances Soc Biol Fil 1957;151:423-5.
(3) Graham JM. Graham Fraser Memorial Lecture 2002. From frogs' legs to pieds-noirs and beyond: some aspects of cochlear implantation. J Laryngol Otol 2003 September;117(9): 675-85.
(4) House WF, Urban J. Long term results of electrode implantation and electronic stimulation of the cochlea in man. Ann Otol Rhinol Laryngol 1973 July;82(4):504-17.
(5) House LR. Cochlear implant: the beginning. Laryngoscope 1987 August;97(8 Pt 1):996-7.
(6) House W. Cochlear implants: past, present and future. Adv Otorhinolaryngol 1993;48:1-3.
(7) Clark GM, Hallworth RJ. A multiple-electrode array for a cochlear implant. J Laryngol Otol 1976 July;90(7):623-7.
(8) Békésy G von. Experiments in hearing. New York: McGraw-Hill; 1960.
(9) Helmholtz HLF. Die Lehre von den Tonempfindungenals physiologische Grundlage für die Theorie der Musik. Braunschweig: Vieweg Verlag; 1863.
(10) Balkany TJ, Eshraghi AA, Yang N. Modiolar proximity of three perimodiolar cochlear implant electrodes. Acta Otolaryngol 2002 June;122(4):363-9.
(11) Tykocinski M, Cohen LT, Pyman BC, Roland T, Jr., Treaba C, Palamara J et al. Comparison of electrode position in the human cochlea using various perimodiolar electrode arrays. Am J Otol 2000 March;21(2):205-11.
(12) Saunders E, Cohen L, Aschendorff A, Shapiro W, Knight M, Stecker M et al. Threshold, comfortable level and impedance changes as a function of electrode-modiolar distance. Ear Hear 2002 February;23(1 Suppl):28S-40S.
(13) Richter B, Aschendorff A, Lohnstein P, Husstedt H, Nagursky H, Laszig R. Clarion 1.2 standard electrode array with partial space-filling positioner: radiological and histological evaluation in human temporal bones. J Laryngol Otol 2002 July;116(7):507-13.
(14) Parkinson AJ, Arcaroli J, Staller SJ, Arndt PL, Cosgriff A, Ebinger K. The nucleus 24 contour cochlear implant system: adult clinical trial results. Ear Hear 2002 February;23(1 Suppl): 41S-8S.
(15) Wackym PA, Firszt JB, Gaggl W, Runge-Samuelson CL, Reeder RM, Raulie JC. Electrophysiologic effects of placing cochlear implant electrodes in a perimodiolar position in young children. Laryngoscope 2004 January;114(1):71-6.
(16) O'Neill C, O'Donoghue GM, Archbold SM, Nikolopoulos TP, Sach T. Variations in gains in auditory performance from pediatric cochlear implantation. Otol Neurotol 2002 January; 23(1):44-8.
(17) Waltzman SB, Cohen NL. Cochlear implantation in children younger than 2 years old. Am J Otol 1998 March;19(2):158-62.
(18) Lenarz T, Lesinski-Scheidat RD, Battmer RD. Cochlear implants in childen under the age of one. 2000.
(19) Robinson K. Implications of developmental plasticity for the language acquisition of deaf children with cochlear implants. Int J Pediatr Otorhinolaryngol 1998 November 15;46(1-2): 71-80.

(20) Baumgartner WD, Pok SM, Egelierler B, Franz P, Gstoettner W, Hamzavi J. The role of age in pediatric cochlear implantation. Int J Pediatr Otorhinolaryngol 2002 February 25;62(3): 223-8.
(21) Galvin KL, Mok M, Dowell RC. Perceptual benefit and functional outcomes for children using sequential bilateral cochlear implants. Ear Hear 2007 August;28(4):470-82.
(22) Grantham DW, Ashmead DH, Ricketts TA, Labadie RF, Haynes DS. Horizontal-plane localization of noise and speech signals by postlingually deafened adults fitted with bilateral cochlear implants. Ear Hear 2007 August;28(4):524-41.
(23) Wolfe J, Baker S, Caraway T, Kasulis H, Mears A, Smith J et al. 1-year postactivation results for sequentially implanted bilateral cochlear implant users. Otol Neurotol 2007 August;28(5): 589-96.
(24) David EE, Ostroff JM, Shipp D, Nedzelski JM, Chen JM, Parnes LS et al. Speech coding strategies and revised cochlear implant candidacy: an analysis of post-implant performance. Otol Neurotol 2003 March;24(2):228-33.
(25) Gantz BJ, Woodworth GG, Knutson JF, Abbas PJ, Tyler RS. Multivariate predictors of audiological success with multichannel cochlear implants. Ann Otol Rhinol Laryngol 1993 December; 102(12):909-16.
(26) Nadol JB, Jr., Young YS, Glynn RJ. Survival of spiral ganglion cells in profound sensorineural hearing loss: implications for cochlear implantation. Ann Otol Rhinol Laryngol 1989 June; 98(6):411-6.
(27) Pisoni DB. Cognitive factors and cochlear implants: some thoughts on perception, learning, and memory in speech perception. Ear Hear 2000 February;21(1):70-8.
(28) Tait M, Lutman ME, Robinson K. Preimplant measures of preverbal communicative behavior as predictors of cochlear implant outcomes in children. Ear Hear 2000 February;21(1):18-24.
(29) Blamey PJ, Pyman BC, Gordon M, Clark GM, Brown AM, Dowell RC et al. Factors predicting postoperative sentence scores in postlinguistically deaf adult cochlear implant patients. Ann Otol Rhinol Laryngol 1992 April;101(4):342-8.
(30) Finley CF WBWM. Models of neural responsiveness to electrical stimulation. In: Miller JM SF, editor. Cochlear Implants: Models of the Electrically Stimulated Ear.New York: Springer-Verlag; 1990. p. 55-93.
(31) Shepherd RK, Hatsushika S, Clark GM. Electrical stimulation of the auditory nerve: the effect of electrode position on neural excitation. Hear Res 1993 March;66(1):108-20.
(32) Frijns JH, Briaire JJ, Grote JJ. The importance of human cochlear anatomy for the results of modiolus-hugging multichannel cochlear implants. Otol Neurotol 2001 May;22(3):340-9.
(33) Gaddes LA. Historical evolution of circuit models for the electrode-electrolyte interface. Ann Biomed Eng 1997;25:1-14.
(34) Tykocinski M, Duan Y, Tabor B, Cowan RS. Chronic electrical stimulation of the auditory nerve using high surface area (HiQ) platinum electrodes. Hear Res 2001 September;159(1-2): 53-68.
(35) Hughes ML, Vander Werff KR, Brown CJ, Abbas PJ, Kelsay DM, Teagle HF et al. A longitudinal study of electrode impedance, the electrically evoked compound action potential, and behavioral measures in nucleus 24 cochlear implant users. Ear Hear 2001 December;22(6):471-86.
(36) Peeters S, Van Immerseel L, Zarowski A, Houben V, Govaerts P, Offeciers E. New developments in cochlear implants. Acta Otorhinolaryngol Belg 1998;52(2):115-27.
(37) Walsh SM, Leake-Jones PA. Chronic electrical stimulation of auditory nerve in cat: Physiological and histological results. Hear Res 1982 August;7(3):281-304.

(38) Kawano A, Seldon HL, Clark GM, Ramsden RT, Raine CH. Intracochlear factors contributing to psychophysical percepts following cochlear implantation. Acta Otolaryngol 1998 June;118(3): 313-26.
(39) Li L, Parkins CW, Webster DB. Does electrical stimulation of deaf cochleae prevent spiral ganglion degeneration? Hear Res 1999 July;133(1-2):27-39.
(40) Chow JK, Seldon HL, Clark GM. Experimental animal model of intracochlear ossification in relation to cochlear implantation. Ann Otol Rhinol Laryngol Suppl 1995 September;166:42-5: 42-5.
(41) Clark GM, Shute SA, Shepherd RK, Carter TD. Cochlear implantation: osteoneogenesis, electrode-tissue impedance, and residual hearing. Ann Otol Rhinol Laryngol Suppl 1995 September;166:40-2:40-2.
(42) Pfingst BE. Changes over time in thresholds for electrical stimulation of the cochlea. Hear Res 1990 December;50(1-2):225-36.
(43) Ni D, Shepherd RK, Seldon HL, Xu SA, Clark GM, Millard RE. Cochlear pathology following chronic electrical stimulation of the auditory nerve. I: Normal hearing kittens. Hear Res 1992 September;62(1):63-81.
(44) Swanson B, Seligman P, Carter P. Impedance measurement of the Nucleus 22-electrode array in patients. Ann Otol Rhinol Laryngol Suppl 1995 September;166:141-4.
(45) Brummer SB, Turner MJ. Electrochemical considerations for safe electrical stimulation of the nervous system with platinum electrodes. IEEE Trans Biomed Eng 1977 January;24(1):59-63.
(46) Cullington HT. Cochlear Implants: Objective Measures. London: Whurr; 2003.
(47) Brown CJ, Abbas PJ, Gantz B. Electrically evoked whole-nerve action potentials: data from human cochlear implant users. J Acoust Soc Am 1990 September;88(3):1385-91.
(48) Brown CJ, Abbas PJ. Electrically evoked whole-nerve action potentials: parametric data from the cat. J Acoust Soc Am 1990 November;88(5):2205-10.
(49) Abbas PJ, Brown CJ. Electrically evoked auditory brainstem response: growth of response with current level. Hear Res 1991 January;51(1):123-37.
(50) van den HC, Stypulkowski PH. Characterization of the electrically evoked auditory brainstem response (ABR) in cats and humans. Hear Res 1986;21(2):109-26.
(51) Kileny PR, Kemink JL. Electrically evoked middle-latency auditory potentials in cochlear implant candidates. Arch Otolaryngol Head Neck Surg 1987 October;113(10):1072-7.
(52) Shallop JK, Beiter AL, Goin DW, Mischke RE. Electrically evoked auditory brain stem responses (EABR) and middle latency responses (EMLR) obtained from patients with the nucleus multi-channel cochlear implant. Ear Hear 1990 February;11(1):5-15.
(53) Kileny PR, Boerst A, Zwolan T. Cognitive evoked potentials to speech and tonal stimuli in children with implants. Otolaryngol Head Neck Surg 1997 September;117(3 Pt 1):161-9.
(54) Kraus N, Micco AG, Koch DB, McGee T, Carrell T, Sharma A et al. The mismatch negativity cortical evoked potential elicited by speech in cochlear-implant users. Hear Res 1993 February; 65(1-2):118-24.
(55) Ponton CW, Don M. The mismatch negativity in cochlear implant users. Ear Hear 1995 February;16(1):131-46.
(56) Kaga K, Kodera K, Hirota E, Tsuzuku T. P300 response to tones and speech sounds after cochlear implant: a case report. Laryngoscope 1991 August;101(8):905-7.
(57) Micco AG, Kraus N, Koch DB, McGee TJ, Carrell TD, Sharma A et al. Speech-evoked cognitive P300 potentials in cochlear implant recipients. Am J Otol 1995 July;16(4):514-20.

(58) Battmer RD, Laszig R, Lehnhardt E. Electrically elicited stapedius reflex in cochlear implant patients. Ear Hear 1990 October;11(5):370-4.
(59) Hodges AV, Balkany TJ, Ruth RA, Lambert PR, Dolan-Ash S, Schloffman JJ. Electrical middle ear muscle reflex: use in cochlear implant programming. Otolaryngol Head Neck Surg 1997 September;117(3 Pt 1):255-61.
(60) Shallop JK, Ash KR. Relationships among comfort levels determined by cochlear implant patient's self-programming, audiologist's programming, and electrical stapedius reflex thresholds. Ann Otol Rhinol Laryngol Suppl 1995 September;166:175-6.
(61) Spivak LG, Chute PM. The relationship between electrical acoustic reflex thresholds and behavioral comfort levels in children and adult cochlear implant patients. Ear Hear 1994 April; 15(2):184-92.
(62) Stephan K, Welzl-Muller K, Stiglbrunner H. Acoustic reflex in patients with cochlear implants (analog stimulation). Am J Otol 1991;12 Suppl:48-51.
(63) Abbas PJ, Brown CJ. Utility of electrically evoked potentials in cochlear implant users. Cochlear Implants: A Practical Guide.London: Whurr; 2006. p. 245-73.
(64) Kiang NY, Moxon EC. Physiological considerations in artificial stimulation of the inner ear. Ann Otol Rhinol Laryngol 1972 October;81(5):714-30.
(65) Lai W. An NRT cookbook. Guidelines for making NRT measurements. Basel: Cochlear AG; 1999.
(66) de Sauvage RC, Cazals Y, Erre JP, Aran JM. Acoustically derived auditory nerve action potential evoked by electrical stimulation: an estimation of the waveform of single unit contribution. J Acoust Soc Am 1983 February;73(2):616-27.
(67) Brown CJ, Hughes ML, Luk B, Abbas PJ, Wolaver A, Gervais J. The relationship between EAP and EABR thresholds and levels used to program the nucleus 24 speech processor: data from adults [see comments]. Ear Hear 2000 April;21(2):151-63.
(68) Hughes ML, Brown CJ, Abbas PJ, Wolaver AA, Gervais JP. Comparison of EAP thresholds with MAP levels in the nucleus 24 cochlear implant: data from children. Ear Hear 2000 April;21(2): 164-74.
(69) Gordon KA, Ebinger KA, Gilden JE, Shapiro WH. Neural response telemetry in 12- to 24-month-old children. Ann Otol Rhinol Laryngol Suppl 2002 May;189:42-8.:42-8.
(70) Thai-Van H, Chanal JM, Coudert C, Veuillet E, Truy E, Collet L. Relationship between NRT measurements and behavioral levels in children with the Nucleus 24 cochlear implant may change over time: preliminary report. Int J Pediatr Otorhinolaryngol 2001 April 27;58(2): 153-62.
(71) Almqvist, B. The Almqvist/Lund procedure for adjusting a speech processor for a congenitally deaf child using objective measurements. 2004. Report No.: July/August.
(72) Seyle K, Brown CJ. Speech perception using maps based on neural response telemetry measures. Ear Hear 2002 February;23(1 Suppl):72S-9S.
(73) Smoorenburg GF, Willeboer C, van Dijk JE. Speech perception in nucleus CI24M cochlear implant users with processor settings based on electrically evoked compound action potential thresholds. Audiol Neurootol 2002 November;7(6):335-47.
(74) Willeboer C, Smoorenburg GF. Comparing cochlear implant users' speech performance with processor fittings based on conventionally determined T and C levels or on compound action potential thresholds and live-voice speech in a prospective balanced crossover study. Ear Hear 2006 December;27(6):789-98.

(75) Marsot-Dupuch K, Meyer B. Cochlear implant assessment: imaging issues. Eur J Radiol 2001 November;40(2):119-32.
(76) Witte RJ, Lane JI, Driscoll CL, Lundy LB, Bernstein MA, Kotsenas AL et al. Pediatric and adult cochlear implantation. Radiographics 2003 September;23(5):1185-200.
(77) Frau GN, Luxford WM, Lo WW, Berliner KI, Telischi FF. High-resolution computed tomography in evaluation of cochlear patency in implant candidates: a comparison with surgical findings. J Laryngol Otol 1994 September;108(9):743-8.
(78) Driscoll CL, Gluth MB. Radiological evaluation in cochlear implantation. In: Cooper HR, Craddock LC, editors. Cochlear Implants: A Practical Guide. Second Edition ed. London: Whurr; 2006. p. 199-202.
(79) Jackler RK, Luxford WM, House WF. Congenital malformations of the inner ear: a classification based on embryogenesis. Laryngoscope 1987 March;97(3 Pt 2 Suppl 40):2-14.
(80) Eisenman DJ, Ashbaugh C, Zwolan TA, Arts HA, Telian SA. Implantation of the malformed cochlea. Otol Neurotol 2001 November;22(6):834-41.
(81) Hoffman RA, Downey LL, Waltzman SB, Cohen NL. Cochlear implantation in children with cochlear malformations. Am J Otol 1997 March;18(2):184-7.
(82) Jackler RK, Luxford WM, House WF. Sound detection with the cochlear implant in five ears of four children with congenital malformations of the cochlea. Laryngoscope 1987 March;97(3 Pt 2 Suppl 40):15-7.
(83) Luntz M, Balkany T, Hodges AV, Telischi FF. Cochlear implants in children with congenital inner ear malformations. Arch Otolaryngol Head Neck Surg 1997 September;123(9):974-7.
(84) McElveen JT, Jr., Carrasco VN, Miyamoto RT, Linthicum FH, Jr. Cochlear implantation in common cavity malformations using a transmastoid labyrinthotomy approach. Laryngoscope 1997 August;107(8):1032-6.

(85) Molter DW, Pate BR, Jr., McElveen JT, Jr. Cochlear implantation in the congenitally malformed ear. Otolaryngol Head Neck Surg 1993 February;108(2):174-7.
(86) Mylanus EA, Rotteveel LJ, Leeuw RL. Congenital malformation of the inner ear and pediatric cochlear implantation. Otol Neurotol 2004 May;25(3):308-17.
(87) Slattery WH, III, Luxford WM. Cochlear implantation in the congenital malformed cochlea. Laryngoscope 1995 November;105(11):1184-7.
(88) Tucci DL, Telian SA, Zimmerman-Phillips S, Zwolan TA, Kileny PR. Cochlear implantation in patients with cochlear malformations. Arch Otolaryngol Head Neck Surg 1995 August;121(8):833-8.
(89) Weber BP, Dillo W, Dietrich B, Maneke I, Bertram B, Lenarz T. Pediatric cochlear implantation in cochlear malformations. Am J Otol 1998 November;19(6):747-53.
(90) Woolley AL, Jenison V, Stroer BS, Lusk RP, Bahadori RS, Wippold FJ. Cochlear implantation in children with inner ear malformations. Ann Otol Rhinol Laryngol 1998 June;107(6):492-500.
(91) Arnoldner C, Baumgartner WD, Gstoettner W, Egelierler B, Czerny C, Steiner E et al. Audiological performance after cochlear implantation in children with inner ear malformations. Int J Pediatr Otorhinolaryngol 2004 April;68(4):457-67.
(92) van Wermeskerken GK, Dunnebier EA, Van Olphen AF, Van Zanten BA, Albers FW. Audiological performance after cochlear implantation: a 2-year follow-up in children with inner ear malformations. Acta Otolaryngol 2007 March;127(3):252-7.
(93) Baumgartner WD, Youssefzadeh S, Hamzavi J, Czerny C, Gstoettner W. Clinical application of magnetic resonance imaging in 30 cochlear implant patients. Otol Neurotol 2001 November;22(6):818-22.

(94) Gleeson TG, Lacy PD, Bresnihan M, Gaffney R, Brennan P, Viani L. High resolution computed tomography and magnetic resonance imaging in the pre-operative assessment of cochlear implant patients. J Laryngol Otol 2003 September;117(9):692-5.
(95) Sennaroglu L, Saatci I, Aralasmak A, Gursel B, Turan E. Magnetic resonance imaging versus computed tomography in pre-operative evaluation of cochlear implant candidates with congenital hearing loss. J Laryngol Otol 2002 October;116(10):804-10.
(96) Ellul S, Shelton C, Davidson HC, Harnsberger HR. Preoperative cochlear implant imaging: is magnetic resonance imaging enough? Am J Otol 2000 July;21(4):528-33.
(97) Arriaga MA, Carrier D. MRI and clinical decisions in cochlear implantation. Am J Otol 1996 July;17(4):547-53.
(98) Klein HM, Bohndorf K, Hermes H, Schutz WF, Gunther RW, Schlondorff G. Computed tomography and magnetic resonance imaging in the preoperative work-up for cochlear implantation. Eur J Radiol 1992 July;15(1):89-92.
(99) Bettman R, Beek E, Van OA, Zonneveld F, Huizing E. MRI versus CT in assessment of cochlear patency in cochlear implant candidates. Acta Otolaryngol 2004 June;124(5):577-81.
(100) Berthezene Y, Truy E, Morgon A, Giard MH, Hermier M, Franconi JM et al. Auditory cortex activation in deaf subjects during cochlear electrical stimulation. Evaluation by functional magnetic resonance imaging. Invest Radiol 1997 May;32(5):297-301.
(101) Schuknecht HF. Mondini dysplasia; a clinical and pathological study. Ann Otol Rhinol Laryngol Suppl 1980 January;89(1 Pt 2):1-23.
(102) Arcand P, Desrosiers M, Dube J, Abela A. The large vestibular aqueduct syndrome and sensorineural hearing loss in the pediatric population. J Otolaryngol 1991 August;20(4):247-50.
(103) Jackler RK, De La CA. The large vestibular aqueduct syndrome. Laryngoscope 1989 December;99(12):1238-42.
(104) Levenson MJ, Parisier SC, Jacobs M, Edelstein DR. The large vestibular aqueduct syndrome in children. A review of 12 cases and the description of a new clinical entity. Arch Otolaryngol Head Neck Surg 1989 January;115(1):54-8.
(105) Mafee MF, Charletta D, Kumar A, Belmont H. Large vestibular aqueduct and congenital sensorineural hearing loss. AJNR Am J Neuroradiol 1992 March;13(2):805-19.
(106) Okumura T, Takahashi H, Honjo I, Takagi A, Mitamura K. Sensorineural hearing loss in patients with large vestibular aqueduct. Laryngoscope 1995 March;105(3 Pt 1):289-93.
(107) Valvassori GE, Clemis JD. The large vestibular aqueduct syndrome. Laryngoscope 1978 May;88(5):723-8.
(108) Valvassori GE, Clemis JD. Abnormal vestibular aqueduct in cochleovestibular disorders. Adv Otorhinolaryngol 1978;24:100-5.
(109) Sennaroglu L, Saatci I. A new classification for cochleovestibular malformations. Laryngoscope 2002 December;112(12):2230-41.
(110) Siebenmann F, Bing R. Über den labyrinth und hirnbefund bei einem an retinitis pigmentosa erblindeten angeboren taubstummen. Z Hals Nasen Ohrenheilkunde 1907;54:265-80.
(111) Scheibe A. Ein fall von taubstummheit mit acusticusatrophie und bildungsanomalien in hautigen labyrinth beiderseits. Z Hals Nasen Ohrenheilkunde 1892;22:11-23.
(112) Michel EM. Gas med strasbourg. Arch F Ohrenheilk 1864;1:353-4.
(113) Mondini C. Anatomica surdi nati sectio: de Bononiensi scientiarum et artium institutoatque academia commentarii, Bononiae 7. 1791. p. 419-31.
(114) Beal DD, Davey PR, Lindsay JR. Inner ear pathology of congenital deafness. Arch Otolaryngol 1967 February;85(2):134-42.

(115) Johnsson LG, Hawkins JE, Jr., Rouse RC, Kingsley TC. Four variations of the Mondini inner ear malformations as seen in microdissections. Am J Otolaryngol 1984 July;5(4):242-57.
(116) Paparella MM. Mondini's deafness. A review of histopathology. Ann Otol Rhinol Laryngol Suppl 1980 March;89(2 Pt 3):1-10.
(117) Jackler RK, Luxford WM, House WF. Congenital malformations of the inner ear: a classification based on embryogenesis. Laryngoscope 1987 March;97(3 Pt 2 Suppl 40):2-14.
(118) Jackler RK, Hwang PH. Enlargement of the cochlear aqueduct: fact or fiction? Otolaryngol Head Neck Surg 1993 July;109(1):14-25.

CHAPTER 2

Intra- and postoperative electrode impedance of the straight and Contour arrays of the Nucleus 24 Cochlear Implant; relation to T and C levels

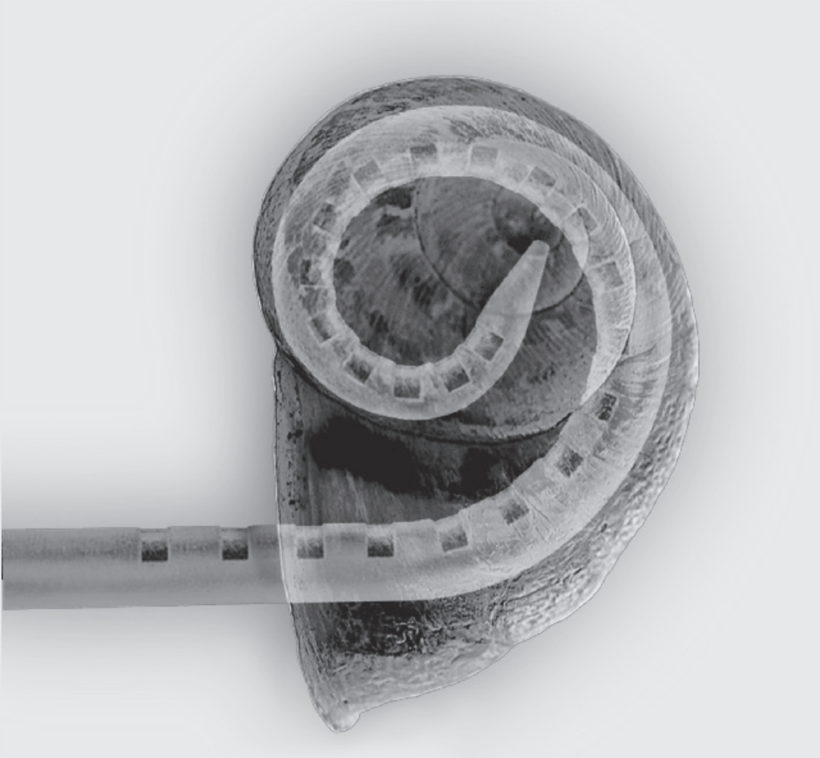

G.K.A. van Wermeskerken
A.F. van Olphen
G.F. Smoorenburg

International Journal of Audiology 2006 Sep;45(9):537-44

Abstract

Objective: The objective of this study was to investigate electrode impedance in cochlear implant recipients in relation to electrically evoked stapedius reflex measurements during surgery and to electrode design, stimulation mode, and T and C levels over a 9 month period after surgery.

Methods: Seventy-five implant recipients, implanted with a Nucleus straight electrode array or a Contour array, were included.

Results: The results show that 1) during surgery electrode impedance decreases markedly after electrically evoked stapedius reflex measurements, 2) after surgery, during the period without stimulation until speech processor switch-on, impedance increases, 3) after processor switch-on impedance decreases.

Conclusions: The lower impedance values after a period of stimulation are found at the higher T and C levels. Impedances of the straight array electrodes are lower than those of the Contour array. The difference corresponds mainly to their respective surface areas. In addition, the straight array shows a larger increase of impedance in the apical direction than the Contour array, probably because of the larger fluid environment around the basal electrodes of the straight array.

Introduction

The design of the electrode is one of the most challenging issues in developing cochlear implants. The electrode is the all-important interface between the electrical stimulus and the auditory nerve fibers that need to be stimulated. An important aspect of its design is electrical impedance, which depends on electrode surface area, morphological processes and electrochemical processes initiated by electrical stimulation. Electrode impedance is an important consideration in developing new electrode arrays because it is a major factor in power consumption (1). Reducing the amount of power used by the implant would allow for further miniaturization of the processors so that totally implantable devices can be produced (2). Measurement of electrode impedance provides an indication of electrode integrity, such as short or open circuits. It also provides an indication of the status of the electrode-tissue interface. Initial changes in electrode impedance, before electrical stimulation, may be expected due to morphological changes at the electrode-tissue interface (3). For example, it has been shown that after implantation the electrode array becomes encapsulated in fibrous tissue (4-7). High impedance is related to the presence of tissue and/or bone growth near the electrode array. Chow suggested that intracochlear osteoneogenesis and fibrous tissue growth should be considered a pathological complication of cochlear implantation (8). A positive correlation between the grading of tissue around the electrode array and impedance was found by Clark (9). An elevation of the electrically evoked compound action potential (ECAP) threshold after implantation appeared to be associated with new bone formation and fibrous tissue growth within the scala tympani (3). Electrical stimulation may also affect electrode impedance. Pfingst demonstrated a short-term increase and subsequent decrease in threshold during the first few months after implantation in adult macaques (10). This was followed by periods of long-term threshold stability. In chronically implanted kittens, Ni et al. showed a steady increase of the electrical impedance over the first month post-implantation (11). The electrode impedance correlated with the degree of tissue growth observed within the scala tympani. Electrode impedance seems to be primarily related to the resistive characteristics of the fluid and tissue surrounding the electrodes (12). In addition, a reduction in electrode impedance after electrical stimulation might be explained by the formation of a hydride layer on the surface of the electrodes. This hydride layer essentially increases the surface area of the electrode, thus reducing the impedance (13).

There have been few reports of changes in electrode impedance after implantation. A recent retrospective study in 25 children using the Nucleus 24 straight array electrode showed a decrease in impedance within a one-month period after electrical stimulation. Subsequently, a gradual but non-significant increase was evident (14).

In view of the limited amount of literature, the objective of the present study was to investigate short- and long-term impedance behavior and possible differences between the Nucleus 24 straight electrode array and the Nucleus 24 Contour array. The aspects considered are:

- Effect of electrically evoked stapedius reflex (ESR) measurements during surgery on electrode impedance
- Effect of a period without stimulation after surgery on electrode impedance
- Effects of electrode design on impedance
- Effect of mode of stimulation (impulse repetition frequency and choice of reference electrode configuration) on electrode impedance
- Possible correlation between electrical impedance on the one hand and hearing threshold and maximum loudness comfort levels (T and C levels) on the other hand.

Materials and Methods

Subjects

Seventy-five implant recipients were included in this study. All subjects were implanted between March 1999 and January 2002 at the University Medical Center Utrecht. Of these, 23 received a Nucleus 24 straight-array cochlear implant and 52 a Nucleus 24 Contour cochlear implant (Cochlear Corp., Lane Cove, Australia). In all subjects, the electrodes were fully inserted without surgical complications. Subject characteristics are shown in Table 1. The various causes of deafness are listed in Table 2.

Table 1 – Subject characteristics.

	Contour (n=52)	Straight array (n=23)
Male / Female	17 / 35	14 / 9
Children	29	9
- mean age implantation (range)	4.8 (2-12)	4.3 (2-15)
- mean age deafness	2.3 (0-15)	2.3 (0-15)
Adults	23	14
- mean age implantation (range)	57.8 (39-74)	49.8 (33-68)
- mean age deafness	36.0 (0-73)	38.9 (0-60)

Table 2 - Etiology of deafness.

	Contour (n=52)		Straight array (n=23)	
	Adults (n=23)	Children (n=29)	Adults (n=14)	Children (n=9)
Congenital	2	17	1	3
Unknown	13	1	9	1
Meningitis	3	5	-	5
Hereditary	1	4	1	-
Chronic otitis	2	-	-	-
Otosclerosis	1	-	3	-
Radiotherapy	1	-	-	-
Enlarged vestibular aqueduct	-	1	-	-
Mondini dysplasia	-	1	-	-

Implant design

The Nucleus 24 straight-array cochlear implant has 22 circular platinum band electrodes. Electrode width decreases from 0.62 to 0.40 mm in a basal to apical direction, with electrode 22 being the most apically positioned one. The diameter of the electrode also decreases in an apical direction. Consequently, the geometric surface area decreases from 0.58 mm^2 basally to 0.38 mm^2 apically.

The Nucleus 24 Contour cochlear implant also has 22 platinum band electrodes, but each electrode spans only half a circle. The semicircular band electrodes are oriented toward the modiolus, thus minimizing current spread away from the target spiral ganglion cells (15). The Contour array is designed to assume a perimodiolar position after surgical insertion. The diameter decreases in an apical direction in a fashion similar to the straight electrode array, from 0.62 mm to 0.40 mm. However, the geometric surface decreases much less, from 0.31 mm^2 basally to 0.28 mm^2 apically.

The Nucleus 24 multiple electrode cochlear implant system has a telemetry facility that can be used to measure electrode impedance. Impedance can be measured in a clinical setting to check for normal electrode functioning and to identify any electrodes with a short or open circuit (16). This is used in configuring the electrode array.

Electrical impedance is expected to be lower for the straight-array electrode due to the larger surface area than for the Contour electrode. In addition, the strong reduction in the surface area of the electrodes in the straight array, when moving apically, will lead to a systematic increase in impedance in this direction.

Electrode impedance measurement

The device was activated using the Windows-based Diagnostic and Programming System software (Win-DPS, release versions 116 and 126) provided by the

Table 3 – Time of impedance measurements.

Time interval	Description	Contour (n=52)	Straight array (n=23)
M1 (implantation)	After electrode insertion	52	23
M2 (implantation)	After determining the ESR threshold	39	
M3 (6 weeks)	Before switch-on of the implant	49	23
M4 (9 months)	Post fitting	30	11

manufacturer (Cochlear Corp., Lane Cove, Australia). The stimuli consisted of biphasic current impulses presented at a level of 100 clinical current units, which is approximately 76 μA, and impulse duration of 25 μs/phase. In the present study electrode impedances was measured in common ground (CG) mode and in monopolar 1 (MP1) mode. In CG mode the impedance is measured between an intracochlear electrode and all other intracochlear electrodes coupled in parallel. In MP1 mode the impedance is measured between the intracochlear electrode and a reference ball electrode situated underneath the temporal muscle. Short-cut or open-circuit electrodes were not considered for data analysis. According to the specifications of the manufacturer this implied the exclusion of data with impedances below 0.7 and above 20 kOhm, respectively.

Impedance was measured at the following points in time: M1, intraoperatively, immediately after electrode insertion; M2, intraoperatively after electrical stimulation to determine the ESR threshold (only in those subjects receiving the Contour electrode); M3, before the first fitting at six weeks after implantation without any prior electrical stimulation; and, M4, nine months after implantation (Table 3).

Visually determined threshold of the electrically evoked stapedius reflex

ESR thresholds were obtained by visual inspection of the reflex in only those subjects who received the Contour electrode. Thresholds were determined by the surgeon intraoperatively by watching the stapedius tendon under microscopic view while stimulating four electrodes numbered 5, 10, 15, and 20. The stimulation was carefully adjusted to the current level at which the reflex was just visible.

Psychophysical measurements

Threshold (T) and maximum comfortable loudness (C) stimulation levels were measured with stimuli consisting of biphasic impulse trains and impulse duration of 25 μs/phase. Implant recipients using either SPEAK or ACE strategy were included. When using SPEAK strategy, T and C levels were measured at a stimulation rate of 250 impulses/s, when using ACE strategy the rate applied lay between 720 and 1200 impulses/s. The duration of the impulse train was 500 ms, separated by silent intervals of about 500 ms. During the silent interval the subject could indicate the perception of a sound. With both strategies the stimulation mode in this psychophysical measurement was monopolar (MP1). The stimulation amplitude is expressed in current level (CL), a quantity defined by Cochlear Ltd. The CL ranges from 1 to 255 current units, which corresponds to electrical currents from 10 μA to 1.75 mA. The relation between current units and electrical current in mA is approximately logarithmic, with 34 current units corresponding to a factor 2 in electrical current or 6 dB. Measurements were performed at the third fitting within about two weeks after switch-on of the cochlear implant and at nine months post implantation, after stabilization of the T and C levels.

Statistical analysis

The data were subjected to analysis of variance (ANOVA) for repeated variables (Statistica V 6.1, Statsoft Inc.).

Results

Analysis of variance of the impedance data

Analysis of variance (ANOVA) covered three between-subject variables: AGE (child or adult); STRATEGY (either the SPEAK or ACE stimulation strategy, as defined for the Nucleus implant); and ELECTRODE (either the straight or Contour electrode). It also covered three within-subject variables: MODE (either Common Ground, CG, or monopolar using the reference ball electrode, MP1); NUMBER (electrode number); and TIME (time of measurement, M1-M4).

AGE did not appear to be a statistically significant variable at the 5% level, neither as a main effect nor in any interaction with the other variables. Thus, the statistical model was redefined excluding this variable.

Likewise, STRATEGY did not show a significant main effect or first-order interactions. Thus, the impulse rate (250 Hz for SPEAK and about 720-1200 Hz for ACE) had a limited effect on electrode impedance. The only significant interaction found for STRATEGY was in relation to NUMBER and TIME. After nine months in the ACE mode, the apical electrodes showed lower impedances (Figure 1). This could be a result of the higher impulse rate in the ACE mode. The two most basal electrodes showed rather high impedance after nine months, reflecting the fact that these electrodes often are not switched on.

Figure 1 also shows a clear effect of the ESR measurement, particularly when using ACE mode. The impedances at electrodes 5, 10, 15, and 20 are markedly lower at M2, the impedance measurement made shortly after the ESR measurement. This effect could be larger for ACE than for SPEAK because of the higher impulse rate used in the ESR measurement when ACE mode was the anticipated strategy.

However, ESR measurements were not conducted in all cochlear implant recipients. Thus, this difference between the SPEAK and ACE modes could be due to differences in the percentage of measurements preceded by an ESR measurement. Therefore, we selected only those M2 impedance measurements preceded by the ESR test and compared the impedance of the electrodes that were included in the ESR measurement (5,10,15, and 20) with the impedance of the two neighboring electrodes. After the ESR test we found an average decrease in the impedance of 1.5 kOhm for ACE and 1.1 kOhm for SPEAK. We also checked whether or not the larger decrease in impedance found for ACE could be due to possibly higher stimulation levels applied in the ESR measurements when anticipating ACE mode. On average, however, the ESR thresholds were about equal in the two modes. In conclusion, the impulse rate during the

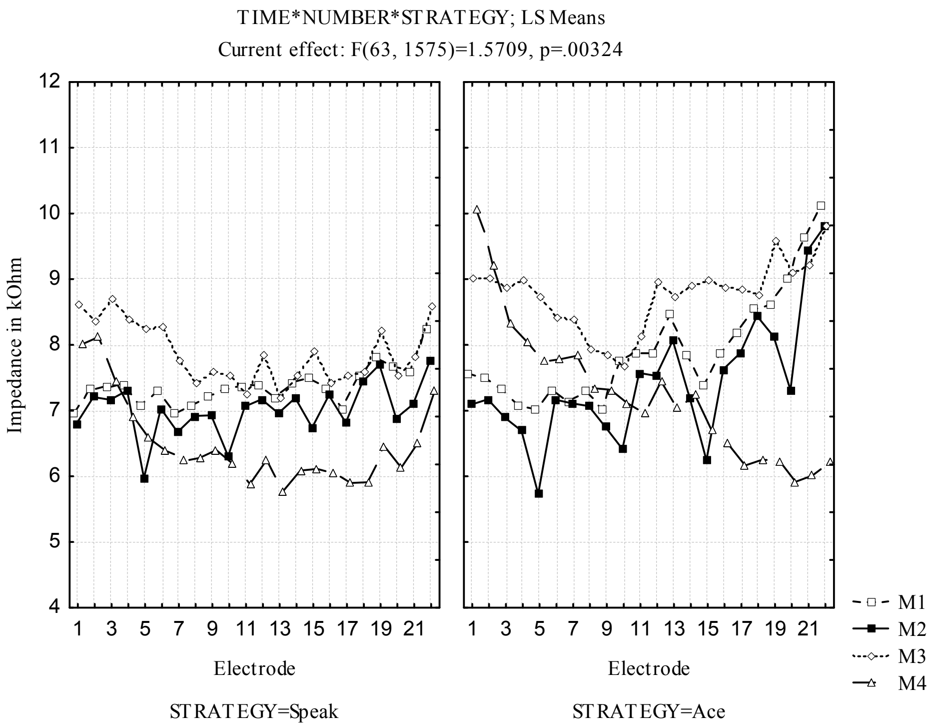

Figure 1 - Interaction for STRATEGY in relation to NUMBER and TIME.

ESR measurement was probably the principal factor affecting the extent of the decrease in impedance measured shortly after the ESR test.

Highly significant (p<0.005) main effects were found for the third between-subject variable ELECTRODE and the within-subject variables MODE, NUMBER, and TIME.

Moreover, ELECTRODE shows significant first-order interactions with NUMBER and TIME and second-order interactions with NUMBER*MODE and TIME*MODE. Figure 2 shows the means corresponding to ELECTRODE*NUMBER*MODE. The main effect of ELECTRODE is immediately apparent. On average, the Contour electrodes have higher impedances than the straight electrodes. The means are 8.8 kOhm for the Contour and 6.2 kOhm for the straight electrode. The main effect of MODE is also very clear. In common ground (CG) we find smaller impedances than in monopolar (MP1). The means are 6.2 kOhm in CG mode and 8.8 kOhm in MP1 mode. The significant first-order interaction of ELECTRODE and NUMBER is interesting. The impedance of the electrodes of the straight array increases from base to apex (number 1 to 22), whereas the impedance of the Contours decreases in this direction. This will be discussed in the next section. There was no significant first-order effect of ELECTRODE*MODE. The difference

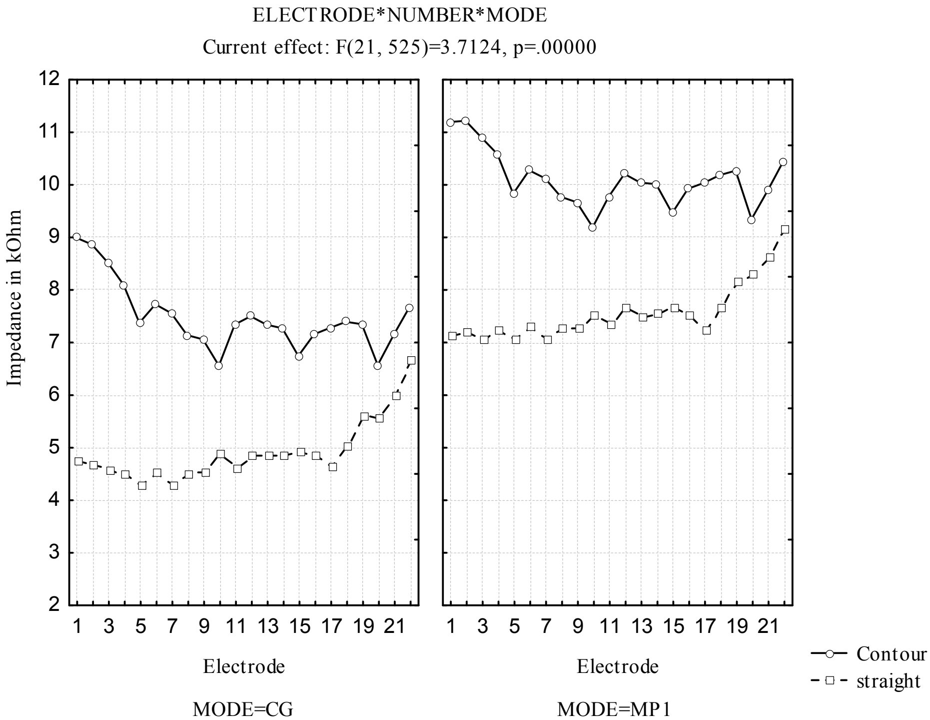

Figure 2 - Interaction for ELECTRODE in relation to NUMBER and MODE.

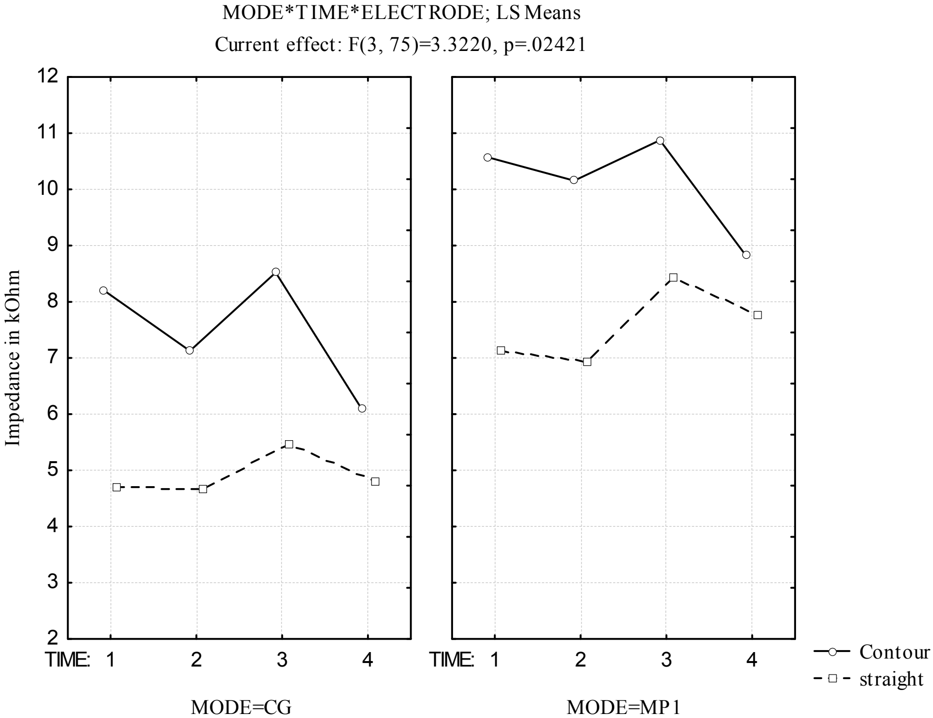

Figure 3 - Interaction for ELECTRODE in relation to TIME and MODE.

between the impedances for CG and MP1, averaged across the electrode array, do not depend on the type of electrode. The significant second-order interaction ELECTRODE*NUMBER*MODE indicates that the impedance profiles across the electrode array depend not only on the electrode (straight or Contour) but also on the way the impedance was measured, in CG or MP1. However, Figure 2 shows no marked effect of MODE on the profiles across the electrode array. Figure 2 suggests that the effect of MODE is largely a simple difference in impedance of 2.6 kOhm for both electrode arrays and each individual electrode.

Figure 3 shows the means corresponding to the significant second-order interaction of ELECTRODE*TIME*MODE. As before, we note that the impedances of the Contour electrodes are higher than those of the straight electrodes and that the impedances measured in CG are lower than those measured in MP1. With time, Figure 3 shows a small decrease of the impedance of the Contour electrode, averaged across the electrode array, which is not found for the straight electrode.

Impedance in relation to electrode surface area

The area of the surface of the straight electrodes decreases from 0.58 mm^2 basally to 0.38 mm^2 apically, whereas the surface of the Contour electrodes changes little: from 0.31 mm^2 basally to 0.28 mm^2 apically. Thus, the overall difference in impedance between these two types of electrodes and the different change in impedance with electrode number could well be related to these differences in electrode surface area. Figure 4 shows the impedance, averaged across subjects, of the straight and Contour electrodes measured at M1 in CG mode. A third curve represents the impedance of the straight electrode when it is adjusted assuming an inversely proportional relation between impedance and surface area. The result indicates that the differences in impedance are primarily due to differences in surface area. We used the data at M1 in order to avoid any effects of electrical stimulation on these impedance values. Moreover, the impedance was measured in CG mode in order to minimize the effect of the reference electrode.

Impedance in relation to T and C levels

A common question is whether or not impedance values are related to T and C levels. Therefore, we analyzed the correlations between the impedances measured at M1, M3, and M4 on the one hand and the T and C levels measured within two weeks after switch-on (thus shortly after M3, indicated by T3 and C3) and those measured after nine months (T4 and C4). We did not use the T and C

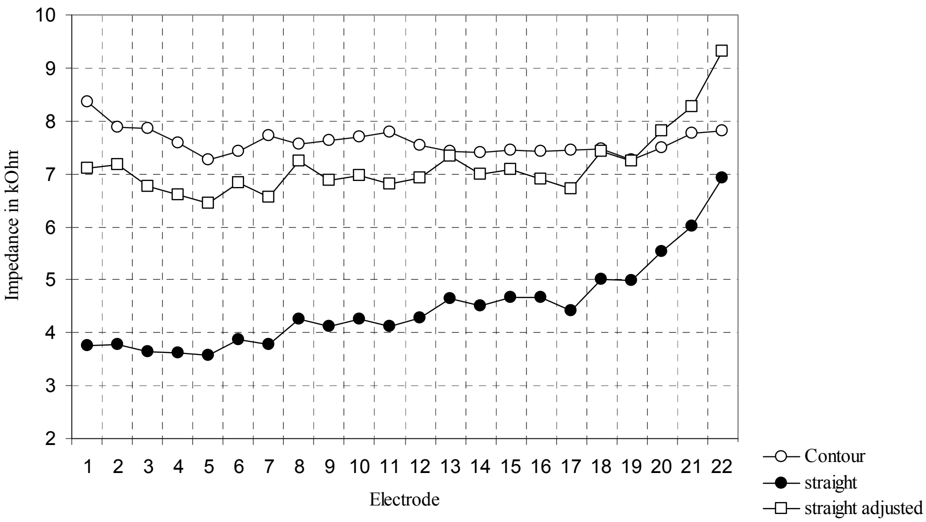

Figure 4 – Recalculated surface area for the straight array electrode directly post implantation (M1).

Table 4 – Correlation threshold / comfort levels and electrode impedance.

electrode	T3/M4	n=	C3/M4	n=	T4/M4	n=	C4/M4	n=
1	0.07	12	0.13	12	-0.72*	9	-0.41	11
2	0.13	18	0.03	18	-0.61*	13	-0.35	14
3	-0.36	30	-0.43*	30	-0.55*	36	-0.53*	38
4	-0.38*	30	-0.38*	30	-0.61*	41	-0.48*	42
5	-0.51*	34	-0.53*	34	-0.62*	43	-0.48*	43
6	-0.41*	31	-0.35	31	-0.60*	42	-0.46*	42
7	-0.34	32	-0.44*	32	-0.54*	42	-0.51*	42
8	-0.46*	38	-0.42*	38	-0.50*	42	-0.44*	42
9	-0.43*	30	-0.43*	30	-0.59*	43	-0.50*	43
10	-0.40*	34	-0.28	34	-0.52*	42	-0.38*	43
11	-0.50*	31	-0.48*	31	-0.65*	42	-0.45*	42
12	-0.54*	37	-0.50*	37	-0.56*	43	-0.39*	43
13	-0.48*	31	-0.45*	31	-0.58*	43	-0.40*	43
14	-0.36*	33	-0.29	33	-0.50*	42	-0.39*	42
15	-0.31	34	-0.31	34	-0.41*	42	-0.34*	42
16	-0.34	34	-0.37*	34	-0.46*	42	-0.43*	42
17	-0.21	32	-0.29	32	-0.46*	41	-0.44*	41
18	-0.14	36	-0.22	37	-0.37*	43	-0.25	43
19	-0.22	31	-0.30	31	-0.39*	43	-0.37*	43
20	-0.24	38	-0.32*	39	-0.40*	42	-0.30	42
21	-0.20	29	-0.31	29	-0.32*	40	-0.21	40
22	-0.30	36	-0.28	36	-0.33*	40	-0.28	40

levels from the first fitting but those measured within two weeks because it was not always possible to fit all the electrodes at the first fitting session. We used the impedances measured in CG mode because most data were available for that mode. The results showed no correlation between M3 and T3 or between M3 and C3. Thus, the impedance measured shortly before the first measurements of the T and C levels cannot be used to estimate these levels. There was a positive correlation, although not statistically significant ($r = 0.1$-0.3), between M1 and T3 and, particularly, between M1 and T4. This is noted without further discussion. A large negative correlation was found between M4 and T3 and C3 and an even stronger one between M4 and T4 and C4 (see Table 4). Thus, lower impedances are found with the higher T and C levels.

Discussion

The effect of electrical stimulation during surgery was immediately clear when we compared the impedances before (M1) and after (M2) the ESR threshold measurement. The electrodes used for this reflex measurement (5, 10, 15, and

20) showed a decrease in impedance of 1.5 kOhm when using the ACE strategy and 1.1 kOhm using SPEAK. As mentioned in the introduction, this decrease in impedance could be attributed to the formation of a hydride layer on the surface of the electrodes during stimulation. This layer effectively increases the surface of the electrodes and consequently results in a lower impedance (13). The higher impulse repetition frequency used during the ESR test when ACE mode was the anticipated strategy probably explains the larger decrease in impedance found for ACE.

Impedance increased considerably during the six-week period after surgery in which there had been no stimulation, as shown in Figure 1. Also, the effect of previous stimulation during the ESR test disappeared. At M3 the impedances of the electrodes 5, 10, 15, and 20 are not any lower than those of the neighboring electrodes. Thus, the effect of the electrolytic reaction at the surface of the electrodes during stimulation vanished after a period without stimulation. The increase in impedance across the whole array of electrodes is attributed to growth of fibrous tissue around the electrodes, as has been shown by other research groups and was mentioned in the introduction. In Figure 3 we note that the difference between the impedances measured at M1 and M3 is somewhat larger for the straight electrode than for the Contour. This may also be related to fibrous tissue growth. The electrodes in the straight array are mainly surrounded by conductive fluid. In contrast, the 'modiolus-hugging' Contour electrodes are situated close to bone and tissue with less space in between the electrodes and the tissue filled by fluid. Thus, growth of less conductive fibrous tissue into the fluid spaces will increase the impedances of the electrodes of the straight array to a larger extent than the impedances of the electrodes of the Contour array. Hughes reported different impedance changes over time for children versus adults, with increasing electrode impedances over time in the whole electrode array in children (3). Some authors have suggested that more bone and tissue growth along the entire electrode array in children could be responsible for the higher electrode impedance. It has been reported that excessive scarring after surgical procedures or injury is more common in children and adolescents than in adults (17;18). In our data, however, we did not find significant differences in impedance measurements between children and adults. AGE was not a statistically significant variable at the 5% level, neither as a main effect nor in any interaction with the other variables. Hence we assume that the amount of fibrous tissue growth after implantation is equal in both children and adults.

Figure 3 also showed that at any moment, from M1 through M4, we find considerably higher impedances for the Contour than for the straight electrode. This could be due to the fluid environment of the straight electrode, as discussed above. However, most of the discrepancy is caused by the difference in surface area of the two types of electrodes. In the introduction we mentioned that the area of the straight electrodes changes from 0.58 mm^2 basally to 0.38 mm^2 apically while the area of the Contour changes from 0.31 mm^2 basally to 0.28 mm^2 apically. Figure 4 showed that when we adjust the impedances of the electrodes of the straight array assuming that the change in impedance is inversely proportional to the surface area, we find for equal surface areas impedances that are close to but a little smaller than those of the Contour electrodes. Thus, the major part of the difference between the straight and Contour impedances is due to their respective surface areas. The remaining small difference between the adjusted values for the electrodes of the straight array and the Contour electrodes may be due to the fluid environment of the straight electrodes.

Figure 3 and Figure 2 show that the impedance measured in common ground (CG) mode is smaller than the monopolar measurement with the reference electrode situated underneath the temporal muscle. In CG mode the impedance of a particular electrode is measured with respect to all other electrodes, thereby yielding a lower total impedance than when measured in series with the impedance of a single reference electrode (MP1). In the latter case the measured impedance reflects essentially the sum of the impedances of the electrodes of the array and the reference electrode. In CG mode one may expect an increase of the measured impedance for the most basally and apically placed electrodes because for those locations the current flows only to the middle of the array and not laterally. However, Figure 2 shows no clear change of impedance with electrode position in line with this assumption. Both graphs – the pair of curves for the straight and the pair for the Contour array – show a parallel shift when comparing CG to MP1 mode.

Finally, we investigated whether or not there is a relation between and T and C levels. We found a slight, although statistically insignificant, trend of higher T levels for higher impedances measured during surgery. However, the principal finding was a strong negative correlation between the T and C levels measured either shortly after switch-on or nine months later and the impedance after nine months. We conclude that the higher stimulation levels during nine months result in lower impedances. The impedance reflects the stimulation. Early impedance measurements cannot serve as an indicator of the T and C levels to be expected.

Conclusions

The present study demonstrates that electrical stimulation results in a lower electrical impedance, probably due to the formation of a hydride layer, effectively increasing the surface area of the electrode. During a period without stimulation we find an increase of impedance, probably due to fibrous tissue growth. This is found in particular for the straight electrode. A larger effect of tissue growth may be expected for the straight electrode because it is surrounded by a larger volume of fluid. The difference between the impedances of the straight array and the Contour array is primarily due to their respective surface areas. We found a significant correlation between the T and C levels and the electrode impedance nine-month post-implantation but no significant relation between the T and C levels and the impedance measured shortly after implantation. This shows that impedance cannot serve as an indicator of the T and C levels to be expected but, vice versa, after stimulation impedance reflects the stimulation levels.

Acknowledgments

None

References

(1) Gaddes LA. Historical evolution of circuit models for the electrode-electrolyte interface. Ann Biomed Eng 1997;25:1-14.

(2) Tykocinski M, Duan Y, Tabor B, Cowan RS. Chronic electrical stimulation of the auditory nerve using high surface area (HiQ) platinum electrodes. Hear Res 2001 September;159(1-2):53-68.

(3) Hughes ML, Vander Werff KR, Brown CJ, Abbas PJ, Kelsay DM, Teagle HF et al. A longitudinal study of electrode impedance, the electrically evoked compound action potential, and behavioral measures in nucleus 24 cochlear implant users. Ear Hear 2001 December;22(6):471-86.

(4) Peeters S, Van Immerseel L, Zarowski A, Houben V, Govaerts P, Offeciers E. New developments in cochlear implants. Acta Otorhinolaryngol Belg 1998;52(2):115-27.

(5) Walsh SM, Leake-Jones PA. Chronic electrical stimulation of auditory nerve in cat: Physiological and histological results. Hear Res 1982 August;7(3):281-304.

(6) Kawano A, Seldon HL, Clark GM, Ramsden RT, Raine CH. Intracochlear factors contributing to psychophysical percepts following cochlear implantation. Acta Otolaryngol 1998 June;118(3): 313-26.

(7) Li L, Parkins CW, Webster DB. Does electrical stimulation of deaf cochleae prevent spiral ganglion degeneration? Hear Res 1999 July;133(1-2):27-39.

(8) Chow JK, Seldon HL, Clark GM. Experimental animal model of intracochlear ossification in relation to cochlear implantation. Ann Otol Rhinol Laryngol Suppl 1995 September;166:42-5: 42-5.

(9) Clark GM, Shute SA, Shepherd RK, Carter TD. Cochlear implantation: osteoneogenesis, electrode-tissue impedance, and residual hearing. Ann Otol Rhinol Laryngol Suppl 1995 September;166:40-2:40-2.

(10) Pfingst BE. Changes over time in thresholds for electrical stimulation of the cochlea. Hear Res 1990 December;50(1-2):225-36.

(11) Ni D, Shepherd RK, Seldon HL, Xu SA, Clark GM, Millard RE. Cochlear pathology following chronic electrical stimulation of the auditory nerve. I: Normal hearing kittens. Hear Res 1992 September;62(1):63-81.

(12) Swanson B, Seligman P, Carter P. Impedance measurement of the Nucleus 22-electrode array in patients. Ann Otol Rhinol Laryngol Suppl 1995 September;166:141-4.

(13) Brummer SB, Turner MJ. Electrochemical considerations for safe electrical stimulation of the nervous system with platinum electrodes. IEEE Trans Biomed Eng 1977 January;24(1):59-63.

(14) Henkin Y, Kaplan-Neeman R, Muchnik C, Kronenberg J, Hildesheimer M. Changes over time in electrical stimulation levels and electrode impedance values in children using the Nucleus 24M cochlear implant. Int J Pediatr Otorhinolaryngol 2003 August;67(8):873-80.

(15) Parkinson AJ, Arcaroli J, Staller SJ, Arndt PL, Cosgriff A, Ebinger K. The nucleus 24 contour cochlear implant system: adult clinical trial results. Ear Hear 2002 February;23(1 Suppl):41S-8S.

(16) Carter P. Determining electrode faults using different stimulation modes. In Clark GM (eds) Cochlear implants: Proceedings of the XVI World Congress of Otorhinolaryngology, Head and Neck Surgery. Bologna:Monduzzi editore, 69-73. 1997.

(17) Bardach J, Hurwitz DJ. Pediatric plastic and reconstructive surgery of the head and neck. In: Bluestone CD, Stool SE, Kenna MA, editors. Pediatric Otolaryngology Vol.1. 3rd ed. ed. Philadelphia: WB Saunders Company; 1983. p. 805-30.

(18) Linares HA, Kischer CW, Dobrkovsky M, Larson DL. The histiotypic organization of the hypertrophic scar in humans. J Invest Dermatol 1972 October;59(4):323-31.

CHAPTER 3

A comparison of intra- versus postoperatively acquired electrically evoked compound action potentials

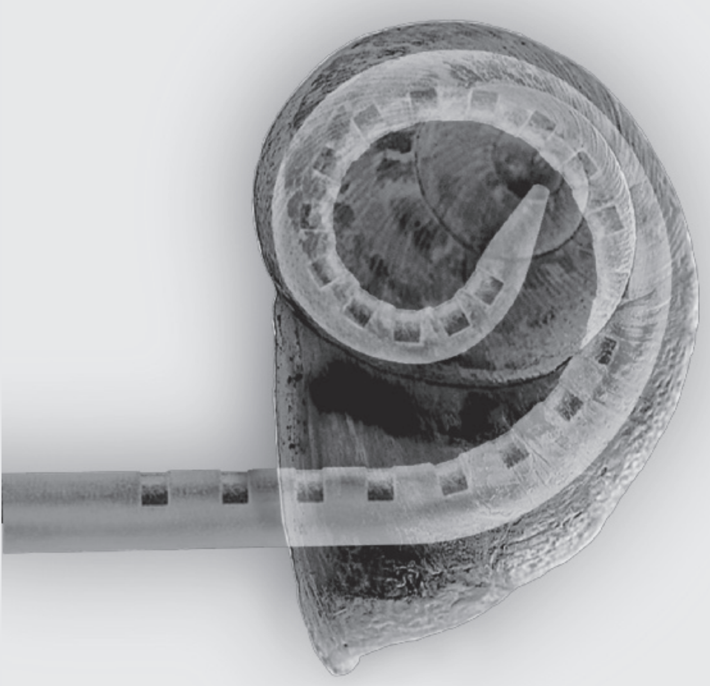

G.K.A. van Wermeskerken
A.F. van Olphen
G.A. van Zanten

International Journal of Audiology 2006 Oct;45(10):589-94

Abstract

Objective: The objective of this study was to compare the electrically evoked compound action potentials, intra- versus post-operatively, in cochlear implant patients.

Study design: Prospective study design.

Methods: Twenty-five consecutively implanted adult patients received a multi-channel cochlear implant. In all patients, electrically evoked compound action potentials were recorded immediately after cochlear implantation and in a post-operative setting nine months later. The threshold of the electrically evoked compound action potential was determined in both settings.

Results: A high success rate (97.4%) was found in the intra-operative setting when recording the electrically evoked compound action potential threshold per patient. The success rate per patient was significantly lower (53.4%) in the post-operative setting. Correlations between the intra- versus the post-operative ECAP thresholds were statistically significant for all electrodes tested. The ECAP thresholds were not significantly different for the two settings.

Conclusion: The intra-operative setting is preferable for acquisition of the ECAP threshold.

Introduction

The Neural Response Telemetry (NRT) system has become an easy-to-use tool for measuring the electrically evoked compound action potential (ECAP) generated by the auditory nerve following electrical stimulation of the cochlea via an electrode of the cochlear implant (1). The data it yields are currently applied in various methods of fitting speech processors (2-5). An interesting perspective is to what extent these objective measures are applicable when fitting children. Children cannot make reliable assessments of subjective loudness, while such judgments are needed to set the Threshold (T) and Comfort (C) levels. Sometimes, clinicians let the children get used to their new hearing capacity by gradually increasing the stimulation levels over a number of sessions. The levels vary from soft to rather loud. If the level is too high, the stimulation could cause discomfort and thus induce rejection of the cochlear implant. A gradual adjustment requires an extended fitting procedure in children. The ECAP thresholds determined with NRT software provide a good starting point for locating the behavioral T and C levels. This allows for a faster fitting procedure using higher stimulation levels than previously (4).

ECAP recordings can be made in different settings: directly after implantation, intra-operatively, or post-operatively. When done immediately after implantation, the subject is still under general anesthesia. This allows the clinician to apply high stimulation levels, which results in a high success rate of recording ECAP responses. However, this time-consuming procedure adds 40 minutes to the duration of general anesthesia. In the post-operative setting, high stimulation levels might cause discomfort by exceeding the patient's subjectively determined loudest acceptable level (6). This discomfort may lower the success rate of recording ECAP responses.

Changes in the electrical pathway can and do occur after cochlear implantation. Various authors have evaluated how such changes affect the function of the implanted electrodes (7-9). As yet, no studies have been done on how the timing of the recordings affects the ECAP threshold levels. We need to understand the role of time to assess the validity of intra-operatively acquired NRT data for setting the speech processor.

The aim of this study was to find out whether changes did occur in ECAP threshold levels after use of the cochlear implant, and whether there was a difference between the data acquired intra- versus post-operatively. To that end, we compared the ECAP measurements acquired intra-operatively and post-operatively in a sample of patients. The ECAP measurements were obtained with the NRT software and were judged by experts, who assessed the success rate of the recordings and determined their threshold level.

Patients and Methods

Patient characteristics

Twenty-five adult patients were included in this study. All were consecutively implanted between January 2001 and March 2002 at the University Medical Center of Utrecht. Two of these patients were implanted with a Nucleus 24 straight-array cochlear implant. The other 23 were implanted with a Nucleus 24 Contour array (Cochlear Corp., Lane Cove, Australia). In all 25, the electrodes were fully inserted without surgical complications. The patient characteristics are shown in Table 1, and the various causes of deafness are listed in Table 2.

Table 1 - Patient characteristics.

Male / Female	10 / 15
Mean age at implantation (age)	54 (31-74)
Years of deafness	19.8, SD 19.0 years
CI system Nucleus 24 straight array	2 (8%)
Nucleus 24 Contour	23 (92%)

Table 2 - Etiology of deafness.

Unknown	11
Meningitis	4
Otosclerosis	3
Chronic otitis	3
Congenital	2
Hereditary	1
Radiotherapy	1

Test procedure

The ECAP responses were recorded twice for each subject by the first author. The initial examination took place intra-operatively immediately after implantation. Nine months later, a subsequent examination took place in a post-operative setting. The ECAP responses were recorded using a portable personal computer equipped with NRT software, versions 2.04 or 3.0, distributed by the Cochlear Corporation. We used a modified version of the protocol described by Abbas et al. (10). Our test parameters are presented in Table 3. The stimulation mode was monopolar (MP1 mode, using the extra cochlear ball reference electrode). Masker advance, which is the masker-probe interval, was fixed at 500 μs. As a rule, the

Table 3 - Test parameters.

Stimulation rate	80 Hz
Pulse width	25 μs
Masker level	+5 CL above probe level
Masker probe interval	500 μs
Gain / number of sweeps	60 dB / 100 or 40 dB / 200
Delay	100 μs

sampling delay – i.e., the interval between stimulation and initiation of sampling – was set at 100 μs. In the event of amplifier saturation, the delay was adjusted until a satisfactory response was obtained. The amplifier gain was set at 60 dB but was decreased to 40 dB in cases of amplifier saturation. We set the number of sweeps at 100, whereas Abbas set it at 50. In conformance with the Abbas protocol, we set the pulse duration at 25 μs per phase. The stimulation levels are described in terms of Current Level (CL), a quantity defined by the Cochlear Company. The CL ranges from 1 to 255 Current Units (CU), which corresponds to electrical currents from 10μA to 1.75 mA. Our aim was to test 20 electrodes (electrodes 3-22) intra-operatively as well as post-operatively. The electrodes selected for recording were two positions above the stimulation electrode. Thus, for each patient, we selected the second electrode, N+2, from the stimulation electrode, N, in the apical direction. An exception was made for electrodes 21 and 22, for which the recording electrodes were 19 and 20, respectively.

In the intra-operative setting, the test stimulus was set at 200 CU or higher until a clear supra-threshold response was noticed. Since the patient was under anaesthesia, we did not have to worry about the subjective loudness of the stimuli. Then the CL was gradually decreased in steps of 5 CU until the threshold level was found. In the post-operative setting, stimulation started at a CL of 150 CU and was gradually increased. To avoid a subjective loudness that was too high for the patients, we asked them to indicate the maximum stimulation level they could tolerate. In children, we would expect few responses and possibly some negative associations with cochlear implant use. Therefore, we chose to work with adult patients. To be able to compare the ECAP data intra- and post-operatively, it was mandatory to keep the stimulation and recording conditions identical. Nonetheless, the delay and gain parameters were optimized for each recording session.

Response identification, amplitude growth function, and threshold

Interpretation of the ECAP recordings was based on subjective visual inspection by the first author. This entailed identifying a clear negative peak (N1) response followed by a positive peak (P1), as described by Killian (11). The amplitude

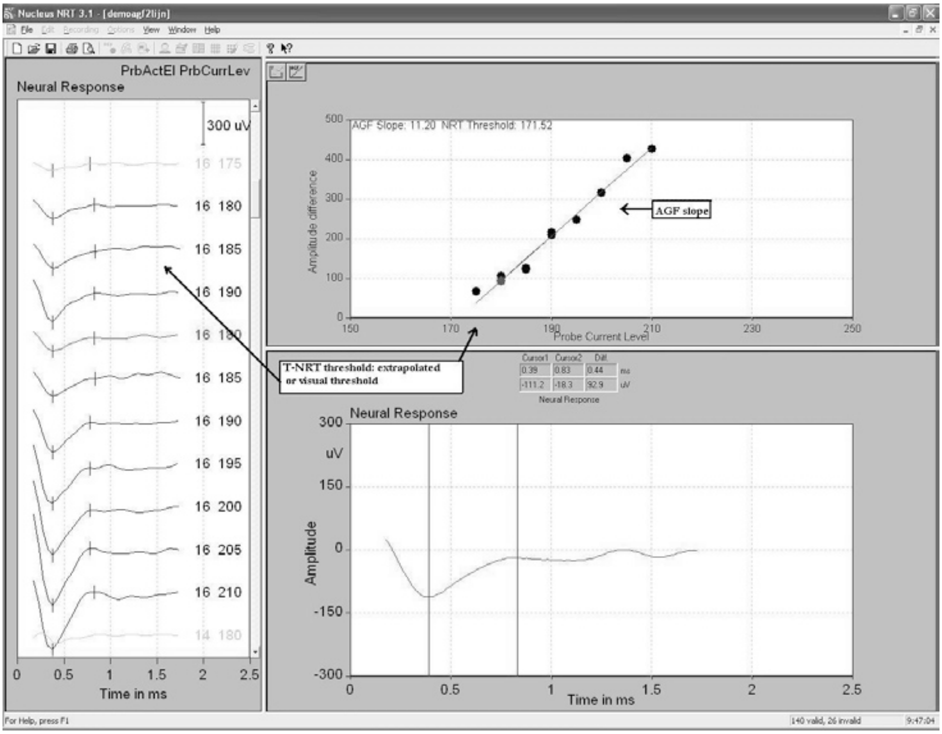

Figure 1 - Examples of ECAP waveform shown in the left panel, ECAP threshold, AGF, and AGF slope. On the left side, an increasing negative N1 peak is shown with an increase in CL. On the right side, an example is shown of the AGF and the extrapolated ECAP threshold.

growth function (AGF) was approximated as a straight-line function relating the neural response amplitude to the probe current level (6;8). The AGF for the ECAP at each electrode pair was determined by the N1-P1 peak-to-peak amplitude measured for at least 3 different current levels. Only those measurements with a clear N1 peak were included in the calculation of the AGF slope. Peak-to-peak amplitudes of less than 20 μV were considered to be likely within the noise floor. Therefore, they were excluded from the AGF calculation. The ECAP threshold, often referred to as 'T-NRT', was estimated by linearly extrapolating the AGF down to zero. An example is shown in Figure 1. There, on the left, the visual threshold is shown with all the N1-P1 peaks marked; on the right, the AGF is plotted.

Psychophysical measurements

The C level is defined as the highest electrical stimulation level per electrode that does not produce an uncomfortable loudness sensation. To measure C levels, we applied stimuli consisting of biphasic impulse trains with an impulse duration of 25 μs/phase. The measurements were conducted on patients who use either the

SPEAK or the ACE strategy. The C levels were used for the post-operative ECAP threshold measurement at nine months post-implantation.

Statistics

All analyses were carried out with SPSS statistical software (version 12.0.1). The Success Rate of recording per Patient (SRP) was defined as the percentage of electrodes on which an ECAP threshold could be calculated per patient. The Success Rate of recording per Electrode (SRE) was defined for each electrode as the percentage of patients for whom ECAP thresholds were successfully determined. A paired *t* test and correlations were used to compare ECAP threshold values obtained intra- versus post-operatively. Box plots were used to show the average differences in ECAP threshold values, calculated as the intra- minus the post-operative value.

Results

Success rate ECAP threshold per patient (SRP)

The SRP in the intra-operative setting showed a range of 65 to 100%. Out of a total of 500 electrodes tested intra-operatively, 473 were successfully tested (97.4%). The SRP in the post-operative setting showed a range of 0 to 100% per patient. Out of the 500 electrodes tested post-operatively, 267 were successfully tested (53.4%). Figure 2 shows the results for each patient. Note the strong variability in the SRP in the post-operative setting.

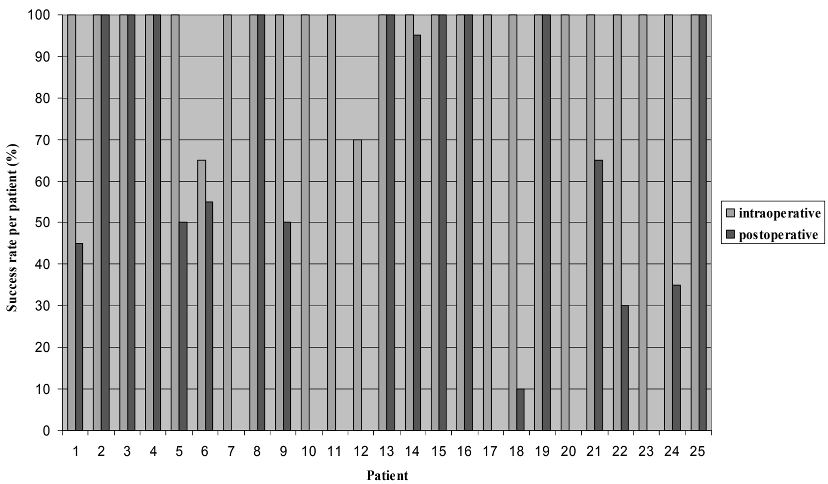

Figure 2 - Percentage of valid ECAP threshold measurements over all patients.

Success rate ECAP threshold per electrode (SRE)

The SRE in the intra-operative setting showed a range of 92 to 100%. In the post-operative setting, a range of 44 to 60% was found. Figure 3 shows the results for each electrode. Note the small variability between the different electrodes post-operatively. There is no specifically worse electrode or group of electrodes within the array.

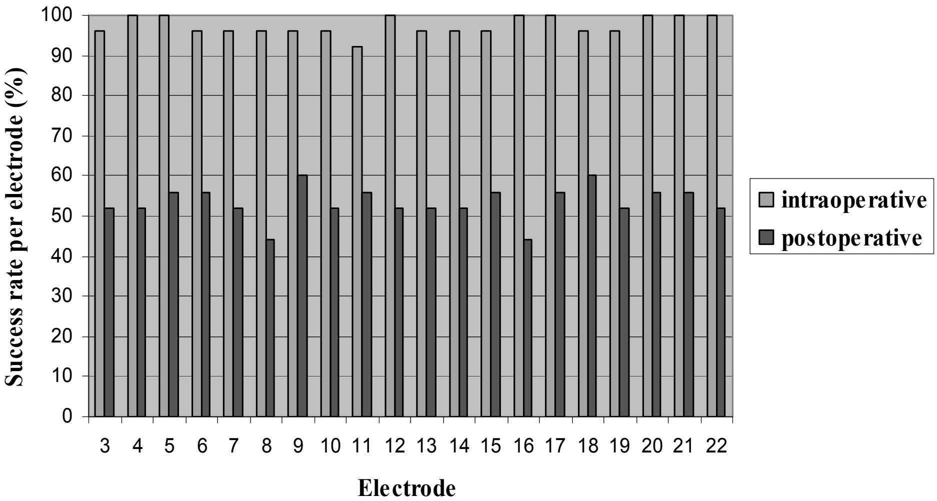

Figure 3 - Percentage of valid ECAP threshold measurements over the electrode array.

Threshold difference of ECAP threshold intra- versus post-operatively

With an overall lower number of valid ECAP thresholds in the post-operative setting, the number of valid paired comparisons is limited. On average, 13.1 valid pairs (range 11-14) were available for comparison. With paired sample *t* testing, the mean ECAP threshold in the intra-operatively setting was not significantly different from the post-operative result (mean difference 0.7 (SD 7)). This was valid for all electrodes. In Figure 4 the differences are shown in the box plot.

In Figure 5 the intra-operative result is plotted against the post-operative ECAP threshold for all electrodes. A strongly significant correlation of 0.88 was found. Also for each separate electrode, the correlation between the intra- and post-operative results was highly significant (range 0.84-0.94; for all electrodes $p<0.05$).

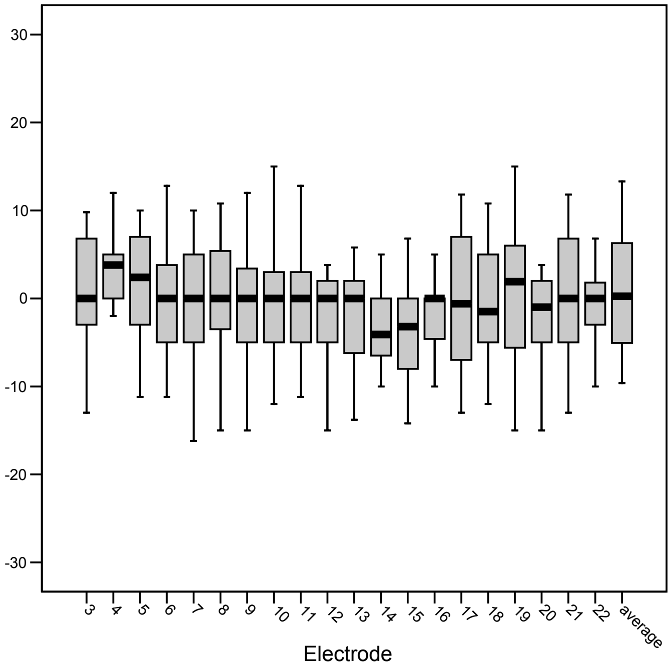

Figure 4 - Difference in current units of the ECAP threshold between the intra- minus the post-operatively recorded values.

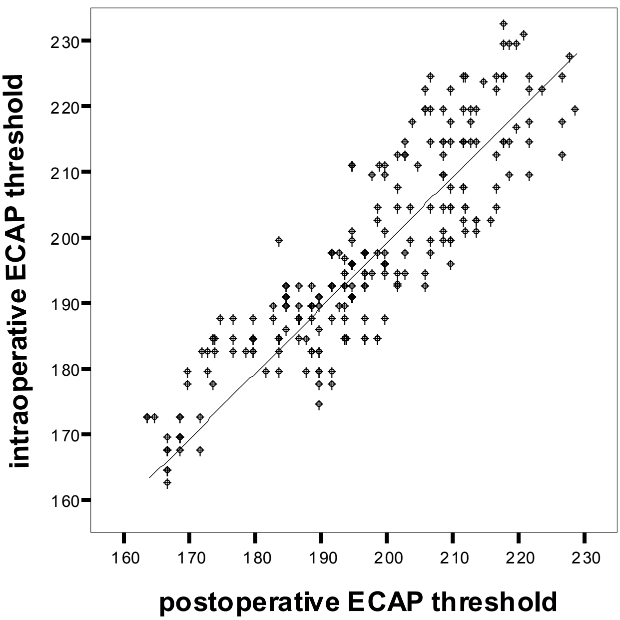

Figure 5 - Scatterplot of intra- against post-operative ECAP thresholds for all electrodes.

Discussion

Intra-operative ECAP thresholds provide a good starting point for locating the behavioral C levels (4). At this moment though, fully automatic setting of speech processor maps based on intra-operative NRT data, without any behavioral feedback, is not recommended (8). In the present study, we compared the ECAP measurements acquired intra- and post-operatively by NRT software for 25 patients. We showed a high success rate per patient (SRP) of 97.4% in the intra-operative setting. The SRP in the post-operative setting was much lower, at 53.4%. Thus, acquisition of the ECAP threshold in an intra-operative setting is preferable. This finding is supported by the larger inter- and intra-subject variability seen post-operatively. One explanation of this lower success rate in the post-operative setting is the high stimulation level required. The stimulation can produce too much subjective loudness in the patients, thereby causing the ECAP measurements to fail. A recent multi-center study by Cafarelli et al. showed a higher SRP, namely 87%. However, this multi-center study tested a minimum of only 5 instead of 20 electrode pairs per patient. Moreover, a large number of patients were excluded from the analysis (12). If we recalculate the SRP for only 5 electrode pairs our success rate is 68%.

Recently, an automated ECAP recording system was introduced by Nucleus: the AutoNRT© system. Acquisition of data is faster with this system, and the ECAP recordings can be performed by less-skilled staff. These features will encourage more extensive use of ECAP recordings. As ECAP measurements are increasingly used to program speech processor settings, we felt it was important to demonstrate the stability of intra-operatively acquired ECAP measurements compared to those obtained post-operatively. One possible difference would be in the changes to the auditory neural periphery resulting from the implant surgery. For instance, the electrode array might become encapsulated in fibrous tissue after implantation (13-15). Our study demonstrated the stability in ECAP measurements by comparing the ECAP thresholds intra-operatively and post-operatively. We found highly significant correlations on all electrodes tested (see Figures 4 and 5). Furthermore, we found small differences in ECAP thresholds intra- versus post-operatively, as shown in Figure 4. Overall, we did not find any systemic change in the ECAP threshold level in either setting. The effects of changes to the auditory neural periphery are not noticeable in the ECAP threshold level.

A limitation of our analysis was that we could not obtain ECAP measurements for all patients post-operatively. To ascertain the presence of biasing factors, we analyzed the differences between three subgroups as to the intra-operative ECAP threshold level and the post-operative C levels. The first group we defined was the post-operative-fail group; no ECAP measurement could be recorded on any electrodes in patients in this group. Secondly, we defined the partial-fail group; an ECAP threshold could be recorded on a subset of electrodes in patients in this group. Finally, we defined the post-operative-success group; an ECAP threshold was successfully determined on all electrodes in patients in this group. For these three groups, as mentioned above, no significant differences were found in *t* testing on their mean respective C levels and their intra- and post-operative ECAP threshold level (p>0.05). Next we decided to exclude the partial-fail group from the complete dataset. We did this so we could compare the two most 'extreme' groups: the post-operative-success and the post-operative-fail group. Again, no significant differences were found in *t* testing on their mean respective C and ECAP threshold levels (p>0.05).

In the most recent studies available, the results of the ECAP measurements might be of limited use. The problem lies in the poorer signal quality in the previous generation of amplifiers of the cochlear implant. This is due to the noise characteristics of the amplifier. In our study, we excluded peak amplitudes of less than 20 μV, since these were considered to be likely within the noise floor. They were excluded from the AGF calculation (12). With the availability of better quality electronics in the latest generation of cochlear implants, the noise floor has decreased significantly, as we have experienced with the results of the ECAP measurements in the Nucleus Freedom cochlear implants in our department. Because of this improvement, the non-linear part of the entire AGF curve may become visible at low current levels. Both the automated ECAP recording system and the new amplifier in the latest generation of Nucleus cochlear implants will lead to more precise data acquisition in the future. Whether this will affect the present results is not yet known. We doubt it, though, since the improvement will affect both the intra- and the post-operative measurements.

Conclusion

Acquisition of ECAP threshold measurements is preferable in the intra-operative setting, because of a higher success rate per patient and the equal outcome compared to the post-operative setting. In view of the development of automated ECAP measurement systems, intra-operative use of this system is advised.

Acknowledgments

None.

References

(1) Lai WK, Dillier N, Laszig R, Fisch U. Results from a pilot study using the nucleus CI24M/SP5 cochlear implant system. Am J Otol 1997 November;18(6 Suppl):S35-S36.

(2) Brown CJ, Hughes ML, Luk B, Abbas PJ, Wolaver A, Gervais J. The relationship between EAP and EABR thresholds and levels used to program the nucleus 24 speech processor: data from adults [see comments]. Ear Hear 2000 April;21(2):151-63.

(3) Seyle K, Brown CJ. Speech perception using maps based on neural response telemetry measures. Ear Hear 2002 February;23(1 Suppl):72S-9S.

(4) Smoorenburg GF, Willeboer C, van Dijk JE. Speech perception in nucleus CI24M cochlear implant users with processor settings based on electrically evoked compound action potential thresholds. Audiol Neurootol 2002 November;7(6):335-47.

(5) Thai-Van H, Chanal JM, Coudert C, Veuillet E, Truy E, Collet L. Relationship between NRT measurements and behavioral levels in children with the Nucleus 24 cochlear implant may change over time: preliminary report. Int J Pediatr Otorhinolaryngol 2001 April 27;58(2): 153-62.

(6) Dillier N, Lai WK, Almqvist B, Frohne C, Muller-Deile J, Stecker M et al. Measurement of the electrically evoked compound action potential via a neural response telemetry system. Ann Otol Rhinol Laryngol 2002 May;111(5 Pt 1):407-14.

(7) Hughes ML, Vander Werff KR, Brown CJ, Abbas PJ, Kelsay DM, Teagle HF et al. A longitudinal study of electrode impedance, the electrically evoked compound action potential, and behavioral measures in nucleus 24 cochlear implant users. Ear Hear 2001 December;22(6):471-86.

(8) Lai WK, Aksit M, Akdas F, Dillier N. Longitudinal behaviour of neural response telemetry (NRT) data and clinical implications. Int J Audiol 2004 May;43(5):252-63.

(9) Pfingst BE. Changes over time in thresholds for electrical stimulation of the cochlea. Hear Res 1990 December;50(1-2):225-36.

(10) Abbas PJ, Brown CJ, Shallop JK, Firszt JB, Hughes ML, Hong SH et al. Summary of results using the nucleus CI24M implant to record the electrically evoked compound action potential. Ear Hear 1999 February;20(1):45-59.

(11) Killian MJ, Klis SF, Smoorenburg GF. Adaptation in the compound action potential response of the guinea pig VIIIth nerve to electric stimulation. Hear Res 1994 December;81(1-2):66-82.

(12) Cafarelli DD, Dillier N, Lai WK, von WE, van DB, Akdas F et al. Normative findings of electrically evoked compound action potential measurements using the neural response telemetry of the Nucleus CI24M cochlear implant system. Audiol Neurootol 2005 March;10(2):105-16.

(13) Kawano A, Seldon HL, Clark GM, Ramsden RT, Raine CH. Intracochlear factors contributing to psychophysical percepts following cochlear implantation. Acta Otolaryngol 1998 June;118(3): 313-26.

(14) Li L, Parkins CW, Webster DB. Does electrical stimulation of deaf cochleae prevent spiral ganglion degeneration? Hear Res 1999 July;133(1-2):27-39.

(15) Walsh SM, Leake-Jones PA. Chronic electrical stimulation of auditory nerve in cat: Physiological and histological results. Hear Res 1982 August;7(3):281-304.

CHAPTER 4

Audiological performance after cochlear implantation: a 2 year follow-up in children with inner ear malformations

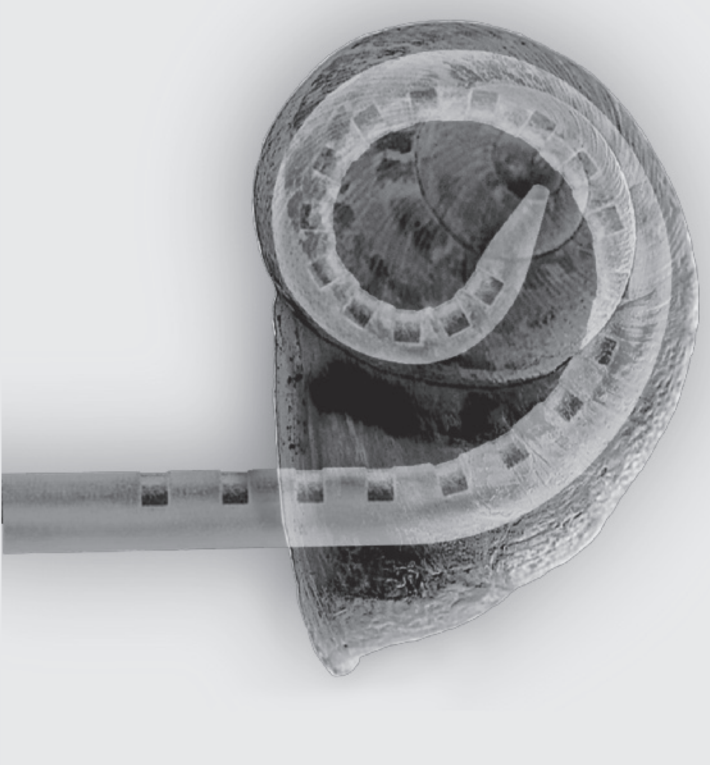

G.K.A. van Wermeskerken
E.A. Dunnebier
A.F. van Olphen
G.A. van Zanten
F.W.J. Albers

Acta Otolaryngologica 2007; 127: 252-57

Abstract

Objective: The objective was to analyze audiological performance after cochlear implantation in a sample of children with radiographically detectable malformations of the inner ear compared to performance in prelingually deafened children at large.

Methods: Nine children with osseous inner ear malformations were compared to 22 congenitally deaf children, all of whom underwent cochlear implantation. All subjects were tested on their electrical compound action potential. Speech perception tests were performed using the monosyllabic trochee polysyllabic test without visual support and the open-set monosyllabic wordlist.

Results: Twenty percent of the congenitally deaf children in our center study have inner ear abnormalities. Inner ear malformations were limited to incomplete partition of the cochlea, none of the subjects had common cavity malformations. Electrical compound action potentials were successfully recorded in both groups intraoperatively. Speech perception tests on open-set speech yielded an average of 48.8% (SD 21.2%) in the group of children with inner ear malformations vs. 54.5% (SD 21.1%) in congenitally deaf children. In four out of nine cases with an inner ear malformation we encountered a minor CSF leak.

Conclusion: Open-set speech perception in children with an inner ear malformation is equal to that of congenitally deaf children after an average of 2 years follow-up.

Introduction

Although early criteria for cochlear implantation had excluded children with inner ear (IE) malformations, presuming malperformance after implantation, recently published studies report satisfactory hearing results in this group of patients. Their audiological performance is comparable to that of other profoundly deaf children, with the exception of those with a common cavity malformation (1-3).

Abnormality of the IE has to be considered an important limiting factor for a successful cochlear implant outcome, but duration of deafness and preoperative speech perception have been indicated to play major roles as variables (4). Since radiologically detectable IE malformations have been reported to occur in approximately 5-15% of cases of congenital sensorineural hearing loss (SNHL), it is of significant interest to investigate the audiological performance of this group of children (5).

Jackler et al. proposed a classification of congenital malformations of the IE based on embryogenesis, which is still widely accepted (5). According to that classification, IE malformations represent a continuum ranging from severe to mild, depending on the stage at which development is arrested. The membranous malformations of this classification are based on histopathological changes of the inner ear, whereas the osseous or the combined osseous-membranous deformities are detectable by radiological techniques. Children with congenital SNHL and radiographically normal IE's may be assumed to have anomalies limited to the membranous labyrinth or neural pathways.

The neural response telemetry (NRT) system has become an easy-to-use tool for measuring the electrically evoked compound action potential (ECAP) generated by the auditory nerve following electrical stimulation of the cochlea via an electrode of the cochlear implant (6). The data it yields are currently applied in various methods of fitting speech processors (7-10). NRT-assisted fittings are particularly helpful for very young implant users, as these children are unable to make reliable subjective loudness judgments for setting the map, threshold (T) and comfort (C) levels. Overall, the ECAP thresholds determined with the NRT software provide a good starting point for locating the behavioral T and C levels after switch on of the cochlear implant. This allows for a faster fitting procedure using higher stimulation levels than previously (9). When NRT data are collected directly after implantation, we are much better informed about the ability to stimulate spiral ganglion cells. This information might help us verify the position and function of the implanted electrodes in a malformed IE.

The aim of our study was to analyze the audiological performance postoperatively and analyze the intraoperatively tested ECAP measurements in a sample of children with radiographically detectable malformations of the IE and to compare these findings with implantation results reported for other prelingually deafened children at large. The audiological performance was evaluated via speech discrimination tests, while the ECAP measurements were acquired by the NRT software.

Materials and Methods

Patient selection and characteristics

The database of our cochlear implant center of the Department of Otorhinolaryngology of the University Medical Center of Utrecht included 51 congenital deaf children on a total number of 75 cochlear implantations in children between January 2001 and April 2004. Inner ear malformations were reported in 16 congenitally deaf children; the other 35 congenitally deaf children served as controls. We systematically analyzed the clinical records, computer tomography (CT) scans, and NRT data. Of the group with suspected IE malformations in our database, seven children were diagnosed as normal on the grounds of CT scans and were thus excluded from the study. Of the control group, 13 were excluded because of incomplete NRT data. The children were either implanted with a Nucleus 24 Contour or Nucleus 24 Contour Advance cochlear implant (Cochlear Corp., Lane Cove, Australia). The patient characteristics are summarized in Table 1.

Table 1. Patient characteristics.

	With IE malformations (n=9)	Without IE malformations (n=22)	*p* value
Male / Female	5 / 4	11 / 11	
Mean age at implantation (age)	3.9 (2-6), SD 1.5 years	2.8 (1.5-6), SD 1.1 years	0.13
CI system Nucleus Contour	6 (66%)	20 (91%)	
Nucleus Contour Advance	3 (33%)	2 (9%)	
Average follow up-period (months)	23.3 (6-48)	28.6 (6-48)	0.28
Percentage of total number of children operated on (n=75)	12%		
Percentage of total number of congenitally deaf children (n=35)	20%		

Classification system of congenital inner ear malformations

In 1987, Jackler proposed a classification of congenital malformations of the IE based on embryogenesis (5). Depending on the various stages when development is arrested, IE malformations represent a continuum ranging from severe to mild malformation. In 2002, Sennaroglu and Saatci proposed a refinement of Jackler's system (11). They suggested distinguishing between two types of incomplete partition (IP): cystic cochleovestibular malformation (IP-I), and the classic Mondini deformity (IP-II). All CT scans were reviewed blindly by an experienced otologist and neuroradiologist.

Imaging technique

As part of the standard evaluation for cochlear implantation, the patients had undergone high-resolution CT scanning. All CT scans were performed in the axial plane, in accordance with our protocol (12). Multiplanar reformatting (MPR) was used to visualize the semilongitudinal plane.

ECAP measurements

After introducing the electrode array into the cochlea, the integrity of the implant, the electrode array, and the reference electrode were tested by measuring the electrode impedance, The ECAP responses were recorded using a portable personal computer equipped with NRT software, version 2.04 or 3.0, which is distributed by the Cochlear Corporation. We used a modified version of the protocol described by Abbas et al. (13).

The stimulation mode was monopolar (MP1 mode, using the extra cochlear ball reference electrode). Masker advance, which is the masker-probe interval, was fixed at 500 μs. As a rule, the sampling delay -i.e., the interval between stimulation and initiation of sampling - was set at 100 μs. If amplifier saturation occurred, the delay was adjusted until a satisfactory response was obtained. The amplifier gain was set at 60 dB but it was decreased to 40 dB in cases of amplifier saturation. The number of sweeps was set at 100, instead of 50 as in the protocol of Abbas. In conformance with Abbas, the pulse duration was set at 25 μs per phase. The objective parameter in this study is the NRT threshold (TNRT). This is estimated by linearly extrapolating the amplitude growth function (AGF) down to zero. The AGF plots the neural response amplitude as a function of the probe current level, which is approximated as a straight-line function (14).

Speech discrimination tests

For each child a battery of speech perception tests was selected on the basis of age, language ability, and participation level. Postoperative testing was administered at 6 and 12 months and annually thereafter. The maximum follow-up period was 48 months after implantation (range 12-48 months). The closed-set tests included the monosyllabic trochee polysyllabic test (MTP, 12 words), without visual support. The open-set tests included a monosyllabic word test by means of a Dutch phonetically balanced monosyllabic word test (NVA wordlist) (15).

Data analysis and statistical processing

Statistical analysis with a paired *t* test was performed using Statistica v 6.1 (Statsoft Inc., Tulsa, OK, U.S.A.).

Results

Classification of inner ear malformations

After reviewing the CT scans the following IE malformations according to the classification system were observed: one case of IP-I, 5 cases of IP-II, 5 cases of enlarged vestibular aqueduct (EVA), 3 cases of semicircular canal dysplasia (SCD), and 2 cases of widened internal auditory canal (WIAC) were found. Most deformities were associated with another and only a minority was isolated (see Table 2 and Figures 1 and 2).

Table 2. Speech perception tests and NRT measurements in children with IE malformations.

Patient	Implant type	Malformation	MTP test, auditive response (%)	Auditive response, open-set speech, NVA wordlist (%)	Valid number of NRT measurements on electrodes tested (%)	Follow up (months)
1	Contour	IP-II / EVA	89	38	3/5 (60)	24
2	Contour	IP-II	100	67	11/11 (100)	24
3	Contour Advance	WIAC	Not testable		22/22 (100)	24
4	Contour	EVA	75	21	22/22 (100)	12
5	Contour	IP-II / EVA / SCD	Refused to use CI		18/18 (100)	36
6	Contour Advance	IP-II / EVA / SCD	100	80	19/22 (86)	12
7	Contour	IP-I / SCD / WIAC	33		Not tested	36
8	Contour Advance	IP-II	75	45	22/22 (100	6
9	Contour	EVA	80	42	20/22 (91)	24

NRT, neural response telemetry; IE, inner ear; MTP, monosyllabic trochee polysyllabic; IP I, incomplete partition type I (cystic cochleovestibular malformation); IP-II, incomplete partition type II (Mondini dysplasia); EVA, enlarged vestibular aqueduct; SCD, semicircular canal dysplasia; WIAC, wide internal auditory canal.

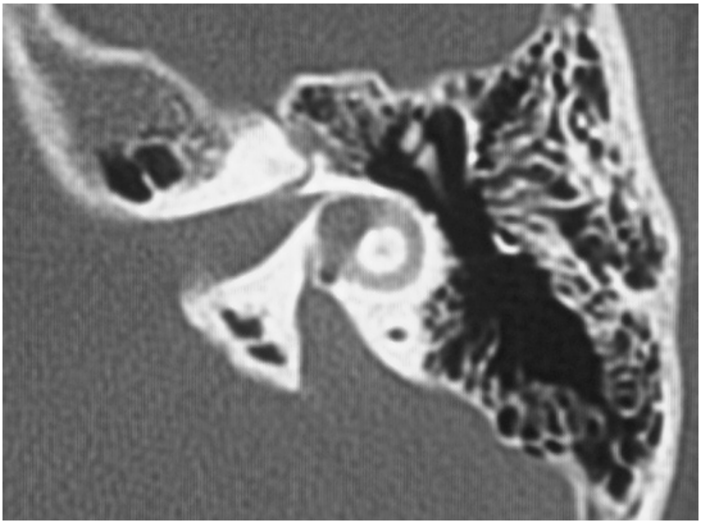

Figure 1. Enlarged vestibular aqueduct and semicircular canal dysplasia.

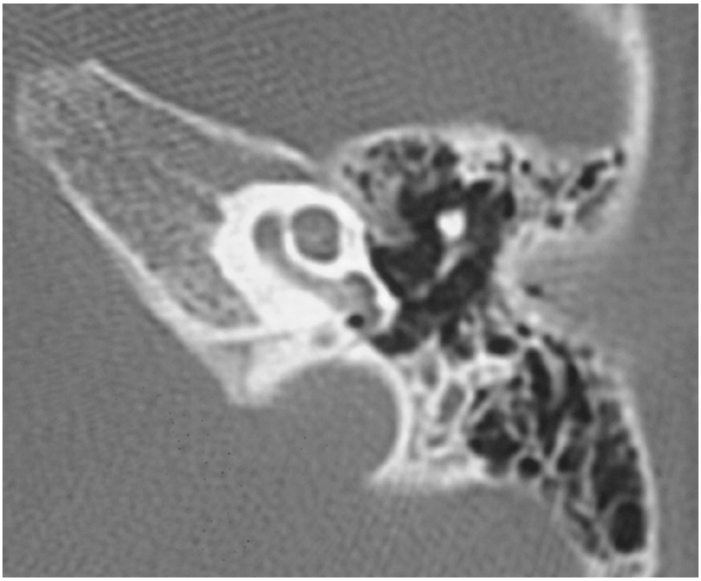

Figure 2. Incomplete partition type II (Mondini).

ECAP measurements

NRT responses in the group of children with IE malformations were measured in eight of the nine patients. The success rates of the NRT responses on the tested electrodes are shown in Table 2. Of the 144 electrodes tested intraoperatively, 137 electrodes (95.1%) showed a valid TNRT. The success rates varied from 60 to 100%. In the case of patient no. 1, no valid NRT responses were found in

Table 3 – Speech perception tests and NRT measurements in children without IE malformations.

Patient	Implant type	MTP test, auditive response (%)	Auditive response, open- set speech, NVA wordlist (%)	Valid number of NRT measurements on no. of electrodes (%)	Follow up (months)
1	Contour	100	84	11/11 (100)	48
2	Contour	100	85	22/22 (100)	48
3	Contour			22/22 (100)	6
4	Contour	100	49	22/22 (100)	36
5	Contour	100	39	20/20 (100)	36
6	Contour		50	5/5 (100)	24
7	Contour			11/11 (100)	24
8	Contour	75	45	11/11 (100)	24
9	Contour	100	48	11/11 (100)	24
10	Contour	100	39	16/20 (80)	24
11	Contour	33		22/22 (100)	24
12	Contour	42		21/22 (95)	24
13	Contour	75	30	22/22 (100)	12
14	Contour Advance	42		15/15 (100)	12
15	Contour Advance	75	45	22/22 (100)	12
16	Contour	89	21	22/22 (100)	36
17	Contour	100	73	22/22 (100)	36
18	Contour	100	73	22/22 (100)	36
19	Contour		24	22/22 (100)	24
20	Contour		61	22/22 (100)	24
21	Contour	100	76	22/22 (100)	48
22	Contour	100	82	17/22 (77.3)	48

the apical part of the electrode array. However, it should be noted that only five electrodes were tested across the electrode array. NRT responses were measured in all of the congenitally deaf children. Of the 412 electrodes measured, 402 electrodes (97.6%) showed a valid TNRT (Table 3).

Speech discrimination tests

Depending on the stage of development, different audiological tests were used to measure the speech perception. Soon after implantation, these were mainly closed-set tests such as the MTP test. With the MTP, the auditory response without visual support was variable, ranging from 33 to 100% (average 80.0%, SD 35.0%) word recognition in children with IE malformations. We could not perform a standardized test on patient no. 3, even though the child seemed to have some auditory response. Patient no. 5 refused to wear the cochlear implant and instead used a contralaterally positioned conventional hearing aid. As the children started to develop their speech abilities, we switched to the open-set test, the NVA wordlist. The results in children with IE malformations varied from 21 to 80% (average 48.8%, SD 21.2%). No results of this test were obtained for

3 children. Besides the 2 patients described above (no. 3 and no. 5), another one (no. 7) received very little auditory support from the cochlear implant.

The results on the MTP test for the congenitally deaf group are comparable to those for the group with IE abnormalities. The responses by the congenitally deaf children ranged from 33 to 100% (average 81.5%, SD 23.7%). There were some dropouts. Patient no. 3 had moved abroad, so no speech test could be performed. Patient no. 7 is spastic and reacts to auditory input but is not testable.

The results of the NVA wordlist testing showed performances ranging from 21 to 85% (average 54.5%, SD 21.1%). Patients 3 and 7, as mentioned above, could not be tested. Nor could patients 11, 12, and 14 (only using the cochlear implant during school hours); in all three cases, the speech development was very limited.

Surgical complications

No insertion problems were encountered after cochleostomy. The electrode array was fully inserted in all children. In four out of nine patients with IE malformations, complications arose during surgery. In all 4, there was minor leakage of cerebrospinal fluid (CSF). These leaks were successfully managed intraoperatively by applying conservative packing. No further treatment was needed. The CSF leaks occurred in two patients with a wide internal auditory canal and two with an EVA. No complications were found in the control group. Neither group showed any other postoperative complication such as meningitis.

Discussion

We determined the results in audiological performance after cochlear implantation in a group of children with IE abnormalities compared to a group of congenitally deaf children without radiologically detectable malformations. In our cochlear implant program the group of children with IE malformations comprised 20 % of the total number of congenitally deaf children. This share is slightly larger than that reported by Jackler et al., whose figures ranged from 5 to 15% (5). There was a relatively high incidence of incomplete partition in our series, mainly concerning IP-II. In the majority of the IP-II there was an association with another deformity, such as an EVA or SCD. We did not find the more severe malformations of the inner ear, such as the common cavity.

Studies published on this subject are rare and mostly based on small series. The definition of radiographically detectable IE abnormalities has not been applied strictly by other investigators. Luntz et al. and Arnoldner et al., for instance, included subjects with clinically determined malformations such as CSF leaks in the group of children with IE abnormalities (1;3). In contrast, Eisenman et al. only included patients whose malformations were limited to the cochlea (2).

The audiological performance in this study is described by postoperative speech discriminations tests. There is a substantial variability in these tests in patients with IE abnormalities, but overall results are encouraging. Several factors are critical to the success of cochlear implantation. Thee factors include the age at implantation, the duration of deafness, the mode of communication, and the participation and support of the child's family during rehabilitation(16-19). In our study six out of nine children with an IE malformations really benefited from cochlear implantation, demonstrated by their ability to develop open-set speech perception skills. In the group of congenitally deaf children, at least 18 out of 22 children showed positive results in this regard. Performance of open-set speech perception skills varied strongly among the patients. Overall, the variance among the group of children with IE malformations is comparable to the variance in performance by congenitally deaf children.

The intraoperatively tested ECAP measurements were described by the NRT software with a high success rate. In our series, we found a rate of 95.1% in the group with IE malformations and 97.6% in the group of congenitally deaf children. We should expect a much lower percentage of valid TNRT responses in the postoperative setting due to unacceptable subjective loudness for the patient. Besides the high success rates, this gives us valuable information on the amount of functioning electrodes directly after implantation.

Conclusion

Audiological performance after cochlear implantation in radiographically malformed inner ears is comparable to that found in other congenitally deaf patients. However, the inner ear malformations were limited to incomplete partition of the cochlea, whereas none of the patients had common cavity malformations. The ability to develop open-set speech perception is equal after an average follow-up period of 2 years. The risk of a CSF leak is associated with IE abnormalities and should be anticipated during surgery.

Acknowledgements

None

References

(1) Arnoldner C, Baumgartner WD, Gstoettner W, Egelierler B, Czerny C, Steiner E et al. Audiological performance after cochlear implantation in children with inner ear malformations. Int J Pediatr Otorhinolaryngol 2004 April;68(4):457-67.

(2) Eisenman DJ, Ashbaugh C, Zwolan TA, Arts HA, Telian SA. Implantation of the malformed cochlea. Otol Neurotol 2001 November;22(6):834-41.

(3) Luntz M, Balkany T, Hodges AV, Telischi FF. Cochlear implants in children with congenital inner ear malformations. Arch Otolaryngol Head Neck Surg 1997 September;123(9):974-7.

(4) Rubinstein JT, Parkinson WS, Tyler RS, Gantz BJ. Residual speech recognition and cochlear implant performance: effects of implantation criteria. Am J Otol 1999 July;20(4):445-52.

(5) Jackler RK, Luxford WM, House WF. Congenital malformations of the inner ear: a classification based on embryogenesis. Laryngoscope 1987 March;97(3 Pt 2 Suppl 40):2-14.

(6) Lai WK, Dillier N, Laszig R, Fisch U. Results from a pilot study using the nucleus CI24M/SP5 cochlear implant system. Am J Otol 1997 November;18(6 Suppl):S35-S36.

(7) Brown CJ, Hughes ML, Luk B, Abbas PJ, Wolaver A, Gervais J. The relationship between EAP and EABR thresholds and levels used to program the nucleus 24 speech processor: data from adults [see comments]. Ear Hear 2000 April;21(2):151-63.

(8) Seyle K, Brown CJ. Speech perception using maps based on neural response telemetry measures. Ear Hear 2002 February;23(1 Suppl):72S-9S.

(9) Smoorenburg GF, Willeboer C, van Dijk JE. Speech perception in nucleus CI24M cochlear implant users with processor settings based on electrically evoked compound action potential thresholds. Audiol Neurootol 2002 November;7(6):335-47.

(10) Thai-Van H, Chanal JM, Coudert C, Veuillet E, Truy E, Collet L. Relationship between NRT measurements and behavioral levels in children with the Nucleus 24 cochlear implant may change over time: preliminary report. Int J Pediatr Otorhinolaryngol 2001 April 27;58(2):153-62.

(11) Sennaroglu L, Saatci I. A new classification for cochleovestibular malformations. Laryngoscope 2002 December;112(12):2230-41.

(12) Bettman RH, Van Olphen AF, Zonneveld FW, Huizing EH. Preoperative imaging protocol for cochlear implant candidates. Acta Otolaryngol 2004 November;124(9):1028-32.

(13) Abbas PJ, Brown CJ, Shallop JK, Firszt JB, Hughes ML, Hong SH et al. Summary of results using the nucleus CI24M implant to record the electrically evoked compound action potential. Ear Hear 1999 February;20(1):45-59.

(14) Lai WK, Aksit M, Akdas F, Dillier N. Longitudinal behaviour of neural response telemetry (NRT) data and clinical implications. Int J Audiol 2004 May;43(5):252-63.

(15) Bosman AJ. Speech Perception by the Hearing Impaired. Utrecht: State University of Utrecht; 1989.

(16) Baumgartner WD, Pok SM, Egelierler B, Franz P, Gstoettner W, Hamzavi J. The role of age in pediatric cochlear implantation. Int J Pediatr Otorhinolaryngol 2002 February 25;62(3):223-8.

(17) Gstoettner WK, Hamzavi J, Egelierler B, Baumgartner WD. Speech perception performance in prelingually deaf children with cochlear implants. Acta Otolaryngol 2000 March;120(2):209-13.

(18) Hamzavi J, Baumgartner WD, Egelierler B, Franz P, Schenk B, Gstoettner W. Follow up of cochlear implanted handicapped children. Int J Pediatr Otorhinolaryngol 2000 December 22; 56(3):169-74.

(19) Tucci DL, Telian SA, Zimmerman-Phillips S, Zwolan TA, Kileny PR. Cochlear implantation in patients with cochlear malformations. Arch Otolaryngol Head Neck Surg 1995 August;121(8): 833-8.

CHAPTER 5

Intracochlear assessment of electrode position after cochlear implant surgery by means of multislice computer tomography

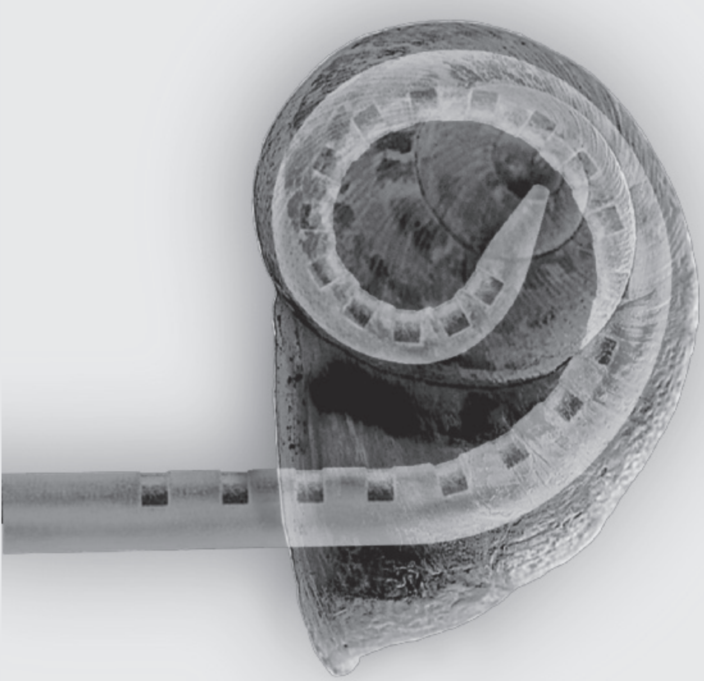

G.K.A. van Wermeskerken
M. Prokop
A.F. van Olphen
F.W.J. Albers

European Archives of Otorhinolaryngology 2007 Dec;264(12): 405-7

Abstract

Objective: In this study we formulated and tested a CT imaging protocol for postoperative scanning of the temporal bone in cochlear implant subjects.

Methods: Both a fresh human temporal bone and a fresh human cadaver head were implanted with a cochlear implant. Multislice CT was performed for adequate depiction of the cochlear implant. All scans were analyzed on a viewing workstation.

Results: After mid-modiolar reconstruction we were able to identify the intracochlear electrode position relative to the scala tympani and scala vestibuli. This was possible in both the implanted isolated temporal bone and the fresh human cadaver head.

Conclusion: The feasibility of imaging the electrode position of the cochlear implant within the intracochlear spaces is shown with multislice CT. An imaging protocol is suggested.

Introduction

Cochlear implants (CI) are widely used for auditory rehabilitation in congenital and acquired deafness. Research in the field of speech processing and electrode design has resulted in better speech quality after implantation. Over the past few years, the literature has drawn attention to the importance of intracochlear positioning and diminishing intracochlear trauma after insertion of the implant (1).

The position of the electrode array close to the modiolus, the inner wall of the cochlea, is presumed to lead to a better-localized neural stimulation. The advantages of these so-called perimodiolar designs include lower stimulation levels, a larger dynamic range, better channel separation and increase of speech understanding (2-4). Despite the advantages of perimodiolar designs, the recent concern about post-implant meningitis has prompted studies on reassessment of the electrode position after implantation (5).

Since 1999 a new treatment modality has been introduced for patients with preserved low-frequency hearing: combined electric and acoustic stimulation (EAS) (6). To ensure hearing preservation during implantation, an atraumatic electrode insertion is fundamental (7). New electrode carriers have been tested, and the electrode positions were histologically evaluated. Intracochlear positioning of the individual electrodes by radiological techniques has not yet been shown.

Several radiological techniques are available to assess the position of the electrode array after cochlear implantation, the main ones being 2-D X-ray approaches, rotational tomography (RT), and computer tomography (CT). Xu has demonstrated the utility of the plain cochlear view in a 2-D setting for evaluating the depth and angle of insertion (8). Rotational tomography is a relatively new technique. A feasibility study by Aschendorff et al. showed that RT permitted a definite allocation of electrodes. The high resolution and the low impact of the electrode artifact, compared to single- and older multislice CT scanners, allowed RT images to be matched with histological slices. However, Aschendorff et al. have questioned its status as the definitive standard for evaluating newly developed electrode arrays. They recently found a higher rate of dislocation of the Contour electrode array from scala tympani to the scala vestibuli than expected on the grounds of various studies of the human temporal bone (9). CT is an important tool in temporal-bone imaging (10). By now, conventional CT has been replaced by helical or spiral CT, which allow rapid acquisition of volumetric data set as 2-D or high-quality 3-D reformations (11;12). The advantages of spiral CT include the elimination of respiratory misregistration, decrease of motion artifact, and an obvious improvement in patient comfort by shortening the examination time (13). With the recent introduction of the 64-slice CT scan, thin-slice coverage has improved the quality of the diagnostic image, with a possible smaller electrode artifact.

We performed a feasibility study using a fresh human temporal bone and a fresh human cadaver head to determine the minimum dose required to examine the implanted patients in the future.

Materials and methods

Material

Both a fresh human temporal bone and a fresh human cadaver head were implanted with a Nucleus 24 Contour and a Nucleus 24 Contour Advance cochlear implant (Cochlear Corp., Lane Cove, Australia). The fresh temporal bone was fixed in a 4% phosphate buffered formaldehyde solution directly after electrode insertion. It was then dehydrated using an ascending alcohol series (70-100% ethanol). Afterwards the temporal bone was embedded in methylmethacrylate (MMA). The fresh cadaver head was implanted with a cochlear implant within 24 hours postmortem. Directly after cochlear implantation it was transported to the CT scanner.

Imaging

Multislice CT was performed using the Philips Brilliance 64-slice CT (Philips Medical Systems, Cleveland, OH, USA). The temporal bone was scanned with the following parameters: 140 kV; effective tube current–time product of 260 milliamperes per seconds (mAs); rotation time 0.5 second. In order to maximize spatial resolution the collimation was reduced to 2 x 0.5 mm. To reduce aliasing artifacts a low pitch factor of 0.35 was used. The cadaver head was scanned with the same settings except for effective mAs. In order to evaluate the minimal dose required for adequate depiction of the cochlear implant, we chose the mAs settings that were increased and decreased stepwise by approximately 30% starting at 260 mAs. As a result, we obtained a total of seven datasets at the following settings: at 62, 89, 127, 182, 260, 338 and ending at 413 mAs due to the technical limitations of the CT scanner. The corresponding measures of local exposure dose (CT dose indices, CTDI) varied between 58 and 136 mGy.

An ultrahigh resolution mode was used for image acquisition. A corresponding ultrahigh resolution filter was applied for image reconstruction. In order to further optimize resolution, a field of view of 51 mm was chosen, resulting in a pixel size of 0.1 mm. Datasets were transferred to a workstation (Easyvision; Philips, Best, The Netherlands) where 3-D reconstructions were created using multiplanar reformation (MPR), i.e. calculating slices along arbitrary sections.

Results

The results for the scanned temporal bone gave a good overview of the insertion depth of the implanted electrodes, all of which were inserted completely. With our multislice CT scanning technique, we were able to identify each electrode individually. Because the electrode artifact was small, we were able to identify the intracochlear electrode position relative to the scala tympani and scala vestibuli. This was possible after mid-modiolar reconstruction (Figure 1).

The overview of the electrodes implanted in the cadaver head was also good. All electrodes were inserted completely. Two observers (GvW, MP) independently judged the most acceptable thresholds of image quality with a variable mAs setting. A setting of 260 mAs was judged to give the best image quality, with a CDTI of 136. The electrode artifact in the cadaver head was slightly larger than the one in the smaller temporal bone. Nonetheless, the individual electrode

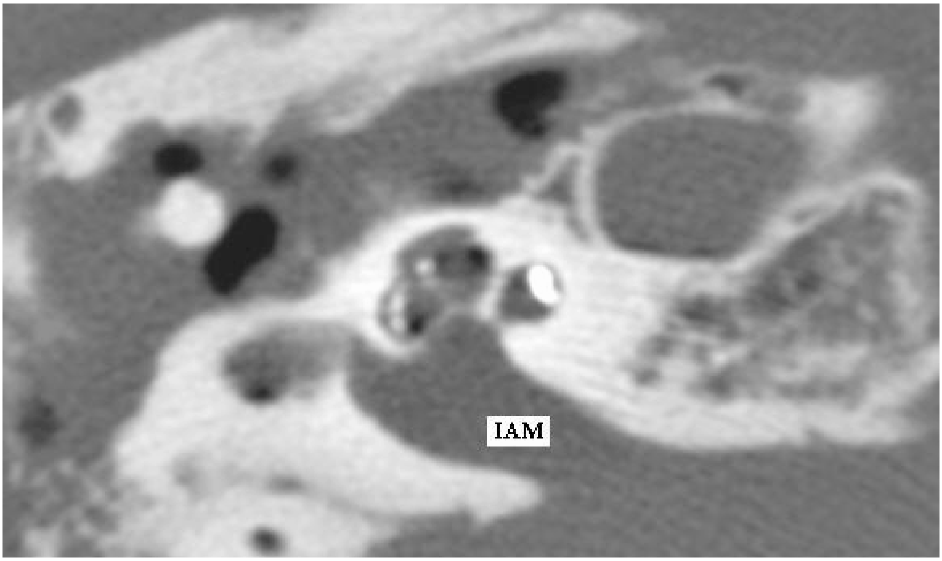

Figure 1. Mid-modiolar reconstruction showing the position of the Contour array in the human temporal bone, IAM = internal auditory meatus.

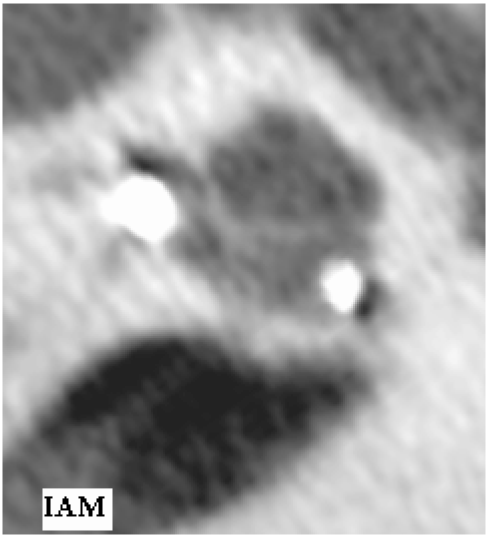

Figure 2. Mid-modiolar reconstruction showing the position of the Contour Advance array in the cadaver head.

position could still be visualized after mid-modiolar reconstruction within the cochlea (Figure 2).

Discussion

This study demonstrates the feasibility of imaging the electrode position within the intracochlear spaces with multislice CT scanning, as shown in both the isolated temporal bone and in the complete cadaver head. In earlier studies the postoperative use of CT scans for this purpose has been questioned by some authors (14;15). The electrode artifact in this latest generation of CT scanners is much smaller than in previous single-/multislice CT scanners which enables a good visualization of the individual electrode within the cochlea.

The new generation of multislice CT scanners may be used in future assessments of the electrode position in patients. Because multislice CT scanning gathers more detailed information on intracochlear electrode positioning, it may assist in estimating intracochlear trauma after implantation, which can severely damage the modiolar wall (16;17). Multislice CT scanning can also play a role in the development of new electrodes, as the devices must not only allow for atraumatic insertion and positioning but also for safe explantation and reimplantation (18).

These results provide a baseline for a subsequent study to verify the estimated electrode positioning.

Acknowledgments

We would like to thank the department of Anatomy of the University Medical Center of Utrecht for their help in preparing the study material.

References

(1) Richter B, Aschendorff A, Lohnstein P, Husstedt H, Nagursky H, Laszig R. The Nucleus Contour electrode array: a radiological and histological study. Laryngoscope 2001 March;111(3):508-14.

(2) Finley CF WBWM. Models of neural responsiveness to electrical stimulation. In: Miller JM SF, editor. Cochlear Implants: Models of the Electrically Stimulated Ear.New York: Springer-Verlag; 1990. p. 55-93.

(3) Shepherd RK, Hatsushika S, Clark GM. Electrical stimulation of the auditory nerve: the effect of electrode position on neural excitation. Hear Res 1993 March;66(1):108-20.

(4) Blamey PJ, Pyman BC, Gordon M, Clark GM, Brown AM, Dowell RC et al. Factors predicting postoperative sentence scores in postlinguistically deaf adult cochlear implant patients. Ann Otol Rhinol Laryngol 1992 April;101(4):342-8.

(5) Reefhuis J, Honein MA, Whitney CG, Chamany S, Mann EA, Biernath KR et al. Risk of bacterial meningitis in children with cochlear implants. N Engl J Med 2003 July 31;349(5):435-45.

(6) Von Ilberg C, Kiefer J, Tillein J, Pfenningdorff T, Hartmann R, Sturzebecher E et al. Electric-acoustic stimulation of the auditory system - New technology for severe hearing loss. Orl-Journal for Oto-Rhino-Laryngology and Its Related Specialties 1999 November;61(6):334-40.

(7) Adunka O, Kiefer J, Unkelbach MH, Lehnert T, Gstoettner W. Development and evaluation of an improved cochlear implant electrode design for electric acoustic stimulation. Laryngoscope 2004 July;114(7):1237-41.

(8) Xu J, Xu SA, Cohen LT, Clark GM. Cochlear view: postoperative radiography for cochlear implantation. Am J Otol 2000 January;21(1):49-56.

(9) Aschendorff A, Kubalek R, Turowski B, Zanella F, Hochmuth A, Schumacher M et al. Quality control after cochlear implant surgery by means of rotational tomography. Otol Neurotol 2005 January;26(1):34-7.

(10) Chakares DW, Augustyn MA. Temporal Bone Imaging. In: Som PM, Curtin HD, editors. Head and Neck Imaging. 4th ed. ed. St. Louis, MO: Mosby; 2003. p. 1093-108.

(11) Hu H. Multi-slice helical CT: scan and reconstruction. Med Phys 1999 January;26(1):5-18.

(12) Klingenbeck-Regn K, Schaller S, Flohr T, Ohnesorge B, Kopp AF, Baum U. Subsecond multi-slice computed tomography: basics and applications. Eur J Radiol 1999 August;31(2):110-24.

(13) GA Valvassori. Imaging of the temporal bone. In: MF Mafee, GE Valvassori, M Becker, editors. Imaging of the head and neck. 2nd ed. ed. Stuttgart: Georg Thieme Verlag; 2005. p. 30.

(14) Skinner MW, Ketten DR, Holden LK, Harding GW, Smith PG, Gates GA et al. CT-derived estimation of cochlear morphology and electrode array position in relation to word recognition in Nucleus-22 recipients. J Assoc Res Otolaryngol 2002 September;3(3):332-50.

(15) Aschendorff A, Kubalek R, Hochmuth A, Bink A, Kurtz C, Lohnstein P et al. Imaging procedures in cochlear implant patients--evaluation of different radiological techniques. Acta Otolaryngol Suppl 2004 May;(552):46-9.

(16) Richter B, Jaekel K, Aschendorff A, Marangos N, Laszig R. Cochlear structures after implantation of a perimodiolar electrode array. Laryngoscope 2001 May;111(5):837-43.

(17) Tykocinski M, Cohen LT, Pyman BC, Roland T, Jr., Treaba C, Palamara J et al. Comparison of electrode position in the human cochlea using various perimodiolar electrode arrays. Am J Otol 2000 March;21(2):205-11.

(18) Glueckert R, Pfaller K, Kinnefors A, Rask-Andersen H, Schrott-Fischer A. The human spiral ganglion: new insights into ultrastructure, survival rate and implications for cochlear implants. Audiol Neurootol 2005 September;10(5):258-73.

CHAPTER 6

Imaging of electrode position in relation to electrode functioning after cochlear implantation

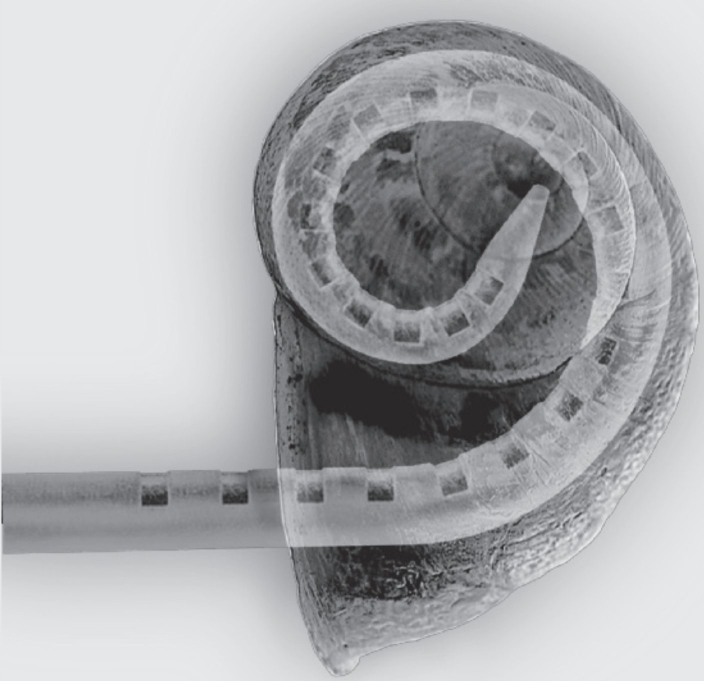

G.K.A. van Wermeskerken
A.F. van Olphen
K. Graamans

Submitted for publication

IAbstract

Objective: To assess the electrode position in cochlear implant patients and to evaluate the extent to which the electrode position is determinative in the electrophysiological functioning of the cochlear implant system.

Methods: Five consecutively implanted adult patients received a multichannel cochlear implant. In all patients, the electrical impedance and the electrically evoked compound action potentials were recorded immediately after implantation. Multislice computer tomography was performed six weeks postoperatively before switch-on of the cochlear implant. The electrode position relative to the modiolus was assessed and correlated to the electrophysiological measurements.

Results: All electrodes were fully inserted; this was confirmed by computer tomography. The individual electrode distance towards the modiolus could be most precisely analyzed for the basal part of the electrode array. It was thus decided to study the data of electrodes one, four, and seven. No correlation was found between electrical impedance and electrode distance. A significant correlation was found between electrode distance and the electrically evoked compound action potentials, with a 96% probability using Kendall's rank correlation.

Conclusion: The electrode – modiolus distance is of importance to the stimulation of auditory nerve fibers. Future developments in imaging will further improve and refine our insight in the relation between electrode positioning and electrophysiological functioning.

Introduction

In cochlear implant patients a large proportion of the success or failure depends on the transfer of stimulating signals from the electrode towards the auditory nerve fibers. An important aspect of the electrode design is electrical impedance, which depends on electrode surface area, morphological processes, and electrochemical processes initiated by electrical stimulation. The development of a new generation of cochlear implant devices as well as modern surgical techniques has to a great extent been aimed at improving stimulus-transferring mechanisms. In line with this trend, in the past years the development of electrode arrays has been focused on the 'modiolus-hugging' type of electrodes. The advantages of these so-called perimodiolar designs include lower stimulation levels, a larger dynamic range, better channel separation, and improvement of speech understanding (1-3). Despite the advantages of perimodiolar designs, concern about post-implant meningitis has prompted studies reassessing the electrode position after implantation (4). Thus, there are multiple incentives to strive for an exact documentation of the position of the individual electrode in relation to cochlear structures and the insertion depth of the electrode array (5).

The aim of this study is first to meticulously assess the electrode position in cochlear implant recipients. Formerly the plain X-ray Stenvers projection was used, but for obvious reasons this method has been abandoned (6;7). The study considers the benefits of high-resolution CT (HRCT) scanning as a more exact method to visualize the structures of the temporal bone. The advantages of HRCT include the elimination of respiratory misregistration, decrease of other motion artifacts, and an obvious improvement in patient comfort by reducing the examination time (8). The main disadvantage of HRCT in the postoperative assessment of a cochlear implant is image degradation, due to partial voluming and the metallic artifacts that may interfere with the visibility of individual electrodes (9-11). We recently demonstrated the feasibility of imaging the electrode position within the intracochlear spaces on both an implanted temporal bone and a fresh human cadaver head (12). So we assume that locating the electrode will be possible with HRCT and that this visualization will allow us to measure the distance to important landmarks in the cochlea, such as the modiolus. Therefore this study was expected to achieve a standardized HRCT-based assessment of the distance between the electrode and the modiolus.

The second aim of this study is to investigate the possible relations between this morphological parameter and electrophysiological characteristics, that is the electrical impedance (EI) and the electrically evoked compound action potential (ECAP), as measured with neural response telemetry (NRT). The NRT system has become an easy-to-use tool for measuring the ECAP generated by the auditory nerve following electrical stimulation of the cochlea via an electrode of the cochlear implant (13). The data it yields are currently applied in various methods of fitting speech processors (14-17). When NRT data are collected directly after implantation, we are much better informed about the ability to stimulate spiral ganglion cells. This information might help us verify the position and function of the implanted electrodes.

The main question that is addressed in this study is to what extent the electrode position is determinative in the electrophysiological functioning of the cochlear implant system.

Materials and Methods

Subjects

Five adult patients were included in this study. All of them were subsequently implanted with a Nucleus Contour cochlear implant (Cochlear Corp., Lane Cove, Australia) between October 2005 and November 2005 at the University Medical Center Utrecht. In all patients, the electrodes were inserted as planned, that is according to the insertion depth that had been set out. There were no surgical problems or complications. The patient characteristics are shown in Table 1. The causes of deafness in these patients were meningitis, a congenital and hereditary etiology, and trauma. In one patient no etiology could be identified.

Table 1 – Patient characteristics.

Male / Female	2 / 3
Mean age at implantation (range)	58.8 (45-75)
Mean age of deafness (range)	28.3 (4-45)

Electrode impedance measurement

The device was activated using the Windows-based Diagnostic and Programming System software (Win-DPS, release version 126) provided by the manufacturer (Cochlear Corp., Lane Cove, Australia). The stimuli consisted of biphasic current pulses presented at a level of 100 clinical current units, which is approximately 76 μA, and an impulse duration of 25 μs/phase. In the present study the EI was measured in common ground (CG) mode intra-operatively. In this mode the impedance is measured between an intracochlear electrode and all other intracochlear electrodes coupled in parallel. Shortcut or open-circuit electrodes were not considered for data analysis. According to the specifications of the manufacturer this implied the exclusion of data with impedances below 0.7 and above 20 kOhm, respectively.

ECAP measurement

The registration procedure of the ECAP responses was identical to the one we used in previous experiments (18). The initial examination took place intra-operatively immediately after implantation. The ECAP responses were recorded using a computer equipped with NRT software, version 3.0, distributed by the Cochlear Corporation. We used a modified version of the protocol described by Abbas et al. (19). Our test parameters are presented in Table 2. The stimulation mode was monopolar (MP1 mode), using the extra cochlear ball reference electrode. Masker advance, which is the masker-probe interval, was fixed at 500 μs. As a rule, the sampling delay – i.e., the interval between stimulation and initiation of sampling – was set at 100 μs. In the event of amplifier saturation, the delay was adjusted until a satisfactory response was obtained. The amplifier gain was set at 60 dB but was decreased to 40 dB in cases of amplifier saturation. We set the number of sweeps at 100, whereas Abbas set it at 50. In conformance with the Abbas protocol, we set the pulse duration at 25 μs per phase. The stimulation levels are described in terms of Current Level (CL), a quantity defined by the Cochlear Company. The CL ranges from 1 to 255 Current Units (CU), which corresponds to electrical currents from 10μA to 1.75 mA. Our aim was to test 22 electrodes (electrodes 1-22) intra-operatively. The electrodes selected for recording were two positions above the stimulation electrode. Thus, for each patient, we selected the second electrode, N+2, from the stimulation electrode, N, in the apical direction. An exception was made for electrodes 21 and 22, for which the recording electrodes were 19 and 20, respectively.

Table 2 – ECAP test parameters.

Stimulation rate	80 Hz
Pulse width	25 μs
Masker level	+5 CL above probe level
Masker probe interval	500 μs
Gain / number of sweeps	60 dB / 100 or 40 dB / 200
Delay	100 μs

Imaging

Multislice CT was performed six weeks after implantation but before the first fitting of the speech processor, using the Philips Brilliance 64-slice CT (Philips Medical Systems, Cleveland, OH, USA). The patients were scanned with the following parameters, according to the imaging protocol we used in previous experiments (20): 140 kV; effective tube current–time product of 260 milliamperes per seconds (mAs); rotation time 0.5 second. In order to maximize spatial resolution the collimation was reduced to 2 x 0.5 mm. To reduce aliasing artifacts a low pitch factor of 0.35 was used. The corresponding measures of local exposure dose (CT dose indices, CTDI) was 136 mGy. An ultrahigh resolution mode was used for image acquisition. A corresponding ultrahigh resolution filter was applied for image reconstruction. In order to further optimize resolution, a field of view of 51 mm was chosen, resulting in a pixel size of 0.1 mm. Datasets were transferred to a workstation (Easyvision; Philips, Best, The Netherlands) where 3-D reconstructions were created using multiplanar reformation (MPR), i.e. calculating slices along arbitrary sections. In our study an MPR was made parallel to the basal turn of the cochlea and perpendicular to the modiolus and thus in the plane of the electrode array. Window width and window level were adjusted until both the cochlear tissues and the individual electrodes could be visualized.

Statistical analysis

All analyses were carried out with Wessa statistical software (21). The Kendall tau rank correlation was used analyzing the correlation between the ECAP, electrode impedance versus electrode distance.

Results

In all five patients the electrode arrays were fully inserted, and this was confirmed by HRCT (Figure 1). After initial data analysis the distance of the apical electrodes to the modiolus could not be visualized. The distance of the more basally located electrodes could be reliably assessed, however. In general, about half of all the electrodes inserted could be identified separately (range: eight to fourteen). With the limitation of not being able to analyze the more apical part of the array, it was decided to restrict our investigation to the data of electrodes one, four, and seven, as these electrodes could be clearly distinguished in all five patients. Moreover, possible differences between electrophysiological parameters presumably are more apparent with a larger inter-electrode distance.

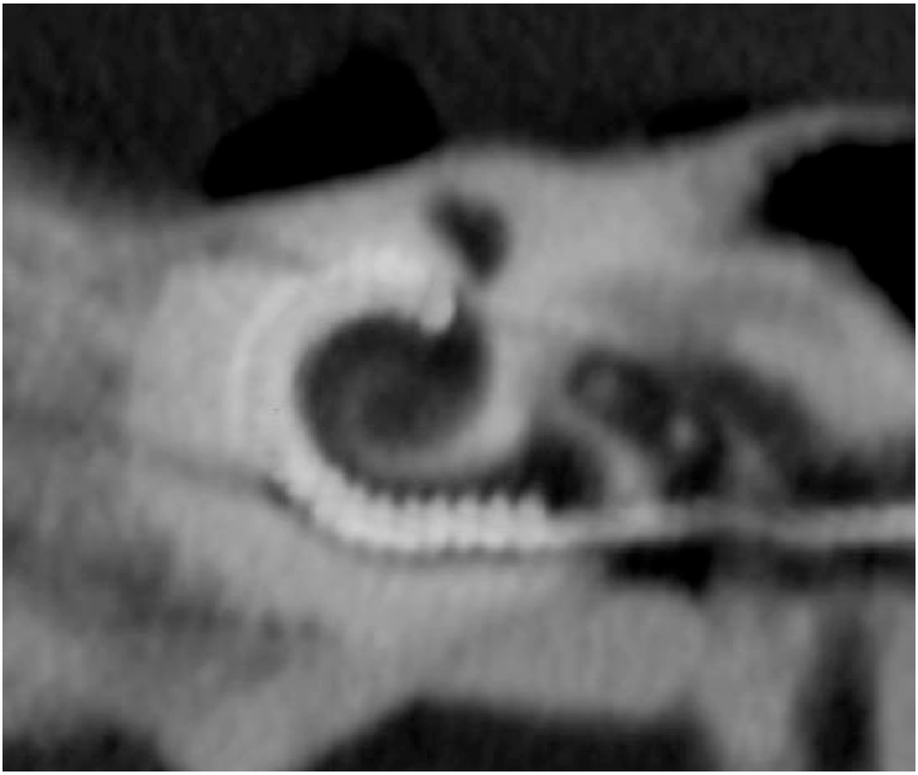

Figure 1 – HRCT image with an MPR in the plane of the electrode array.

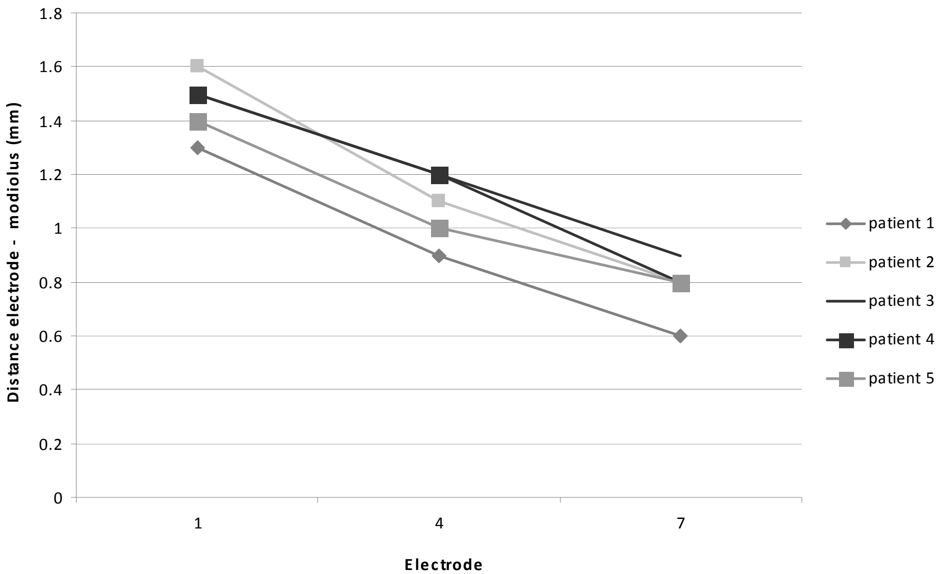

Figure 2 – Distance electrode – modiolus.

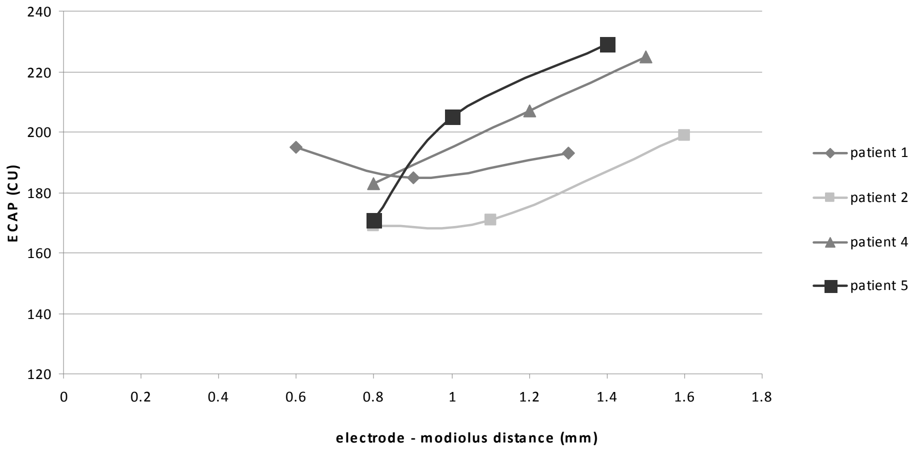

Figure 3 – Electrode – modiolus distance versus ECAP.

The distance from the three examined electrodes towards the modiolus is illustrated in Figure 2. Note that in all five patients a decrease in electrode distance is clearly visible.

Secondly we investigated the relationship between the electrode position, the EI, and the ECAP. No shortcut or open-circuit electrodes were measured. In Patient 3, no ECAP recordings could be obtained on the study electrodes since the surgical procedure had to be shortened for various reasons. No correlation was found between the EI and electrode position. A correlation was found between the electrode distance and the ECAP with a 96% probability using Kendall's rank correlation. In Figure 3 the electrode – modiolus distance is plotted against the ECAP levels.

Discussion

In this study we examined the value of HRCT in assessing the electrode position of cochlear implant recipients. Using an MPR in the plane of the electrode array enabled us to count the number of implanted electrodes in all patients. HRCT seems to have a clear advantage over the previously used plain film radiography with the standard Stenvers projection. With modern multislice CT scanning, more detailed information can be gathered on the intracochlear electrode position. Thus it may be helpful in the assessment of intracochlear damage after implantation, such as degradation of the modiolar wall (22). When determining the exact position of the electrode in the cochlea, it was difficult to identify the separate electrodes in relation to the modiolus. This was mainly due to image degradation caused by partial volume effects, but metallic artifacts of the electrode array also posed a problem (23-25). The window depth in our software configuration limited us in visualizing the three extreme contrasts we wanted to investigate: the fluid compartment of the cochlea; the bony structures of the cochlea and modiolus; and the radiopaque electrode array. In the future, technical improvements in both soft- and hardware will further improve the spatial resolution in HRCT under such extreme contrast conditions.

The second part of this study addressed the relation between electrode distance and electrophysiological parameters. First of all we evaluated the possible relationship between the EI and the electrode – modiolus distance. We could not demonstrate such a relationship. A limitation of our study was the small number of electrodes that we measured. In an earlier study we analyzed the electrical impedance in 52 Nucleus Contour electrode arrays. This showed us a small decrease in electrical impedance in the apical direction. This decrease was especially notable in the first five electrodes (26). One explanation of this observation is that the more basally located electrodes are less ‘modiolus-hugging’ than the apical ones. The higher electrical impedance can be explained by the larger fluid compartment, which leads to the growth of less conductive fibrous tissue.

A significant correlation was found between the electrode – modiolus distance and the ECAP. Our data suggest that a higher electrode – modiolus distance leads to a higher ECAP. Again the small number of electrodes that could be investigated was a limitation in our analysis. Electrode stimulation led to selective triggering of auditory nerve groups. In this process, many factors are important; the electrode – modiolus distance is just one part of this complex process.

In conclusion, the results of this study suggest that electrode – modiolus distance is of importance in the stimulation of the auditory nerve fibers. In the development of new cochlear implant systems, optimizing the electrode positioning in relation to the modiolus may influence the functional outcome. Further development in HRCT will help us analyze the electrode positioning postoperatively. This should further improve and refine our insight in the importance of electrode positioning in relation to aspects of electrophysiological functioning.

Acknowledgements

None

References

(1) Blamey PJ, Pyman BC, Gordon M, Clark GM, Brown AM, Dowell RC et al. Factors predicting postoperative sentence scores in postlinguistically deaf adult cochlear implant patients. Ann Otol Rhinol Laryngol 1992 April;101(4):342-8.

(2) Finley CF at al. Models of neural responsiveness to electrical stimulation. In: Miller JM SF, editor. Cochlear Implants: Models of the Electrically Stimulated Ear.New York: Springer-Verlag; 1990. p. 55-93.

(3) Shepherd RK, Hatsushika S, Clark GM. Electrical stimulation of the auditory nerve: the effect of electrode position on neural excitation. Hear Res 1993 March;66(1):108-20.

(4) Reefhuis J, Honein MA, Whitney CG, Chamany S, Mann EA, Biernath KR et al. Risk of bacterial meningitis in children with cochlear implants. N Engl J Med 2003 July 31;349(5):435-45.

(5) Verbist BM, Frijns JH, Geleijns J, van Buchem MA. Multisection CT as a valuable tool in the postoperative assessment of cochlear implant patients. AJNR Am J Neuroradiol 2005 February; 26(2):424-9.

(6) Bettman RH, Van Olphen AF, Zonneveld FW, Huizing EH. Electrode insertion depth in cochlear implantees estimated during surgery, on plain film radiographs and with electrode function testing. Eur Arch Otorhinolaryngol 2003 November;260(10):536-40.

(7) Xu J, Xu SA, Cohen LT, Clark GM. Cochlear view: postoperative radiography for cochlear implantation. Am J Otol 2000 January;21(1):49-56.

(8) Valvassori GA. Imaging of the temporal bone. In: Mafee MF, Valvassori GE, Becker M, editors. Imaging of the head and neck. 2nd ed. ed. Stuttgart: Georg Thieme Verlag; 2005. p. 30.

(9) Ketten DR, Skinner MW, Wang G, Vannier MW, Gates GA, Neely JG. In vivo measures of cochlear length and insertion depth of nucleus cochlear implant electrode arrays. Ann Otol Rhinol Laryngol Suppl 1998 November;175:1-16.

(10) Whiting BR, Bae KT, Skinner MW. Cochlear implants: three-dimensional localization by means of coregistration of CT and conventional radiographs. Radiology 2001 November;221(2):543-9.

(11) Xu J, Xu SA, Cohen LT, Clark GM. Cochlear view: postoperative radiography for cochlear implantation. Am J Otol 2000 January;21(1):49-56.

(12) van Wermeskerken GK, Prokop M, Van Olphen AF, Albers FW. Intracochlear assessment of electrode position after cochlear implant surgery by means of multislice computer tomography. Eur Arch Otorhinolaryngol 2007 December;264(12):1405-7.

(13) Lai WK, Dillier N, Laszig R, Fisch U. Results from a pilot study using the nucleus CI24M/SP5 cochlear implant system. Am J Otol 1997 November;18(6 Suppl):S35-S36.

(14) Brown CJ, Hughes ML, Luk B, Abbas PJ, Wolaver A, Gervais J. The relationship between EAP and EABR thresholds and levels used to program the nucleus 24 speech processor: data from adults [see comments]. Ear Hear 2000 April;21(2):151-63.

(15) Seyle K, Brown CJ. Speech perception using maps based on neural response telemetry measures. Ear Hear 2002 February;23(1 Suppl):72S-9S.

(16) Smoorenburg GF, Willeboer C, van Dijk JE. Speech perception in nucleus CI24M cochlear implant users with processor settings based on electrically evoked compound action potential thresholds. Audiol Neurootol 2002 November;7(6):335-47.

(17) Thai-Van H, Chanal JM, Coudert C, Veuillet E, Truy E, Collet L. Relationship between NRT measurements and behavioral levels in children with the Nucleus 24 cochlear implant may change over time: preliminary report. Int J Pediatr Otorhinolaryngol 2001 April 27;58(2): 153-62.

(18) Van Wermeskerken GK, Van Olphen AF, van Zanten GA. A comparison of intra- versus post-operatively acquired electrically evoked compound action potentials. Int J Audiol 2006 October;45(10):589-94.

(19) Abbas PJ, Brown CJ, Shallop JK, Firszt JB, Hughes ML, Hong SH et al. Summary of results using the nucleus CI24M implant to record the electrically evoked compound action potential. Ear Hear 1999 February;20(1):45-59.

(20) van Wermeskerken GK, Prokop M, Van Olphen AF, Albers FW. Intracochlear assessment of electrode position after cochlear implant surgery by means of multislice computer tomography. Eur Arch Otorhinolaryngol 2007 December;264(12):1405-7.

(21) Wessa, P. Free statistics software, office for research development and education. http://www.wessa.net [computer program]. Version 1.1.22-r6 2008.

(22) Richter B, Jaekel K, Aschendorff A, Marangos N, Laszig R. Cochlear structures after implantation of a perimodiolar electrode array. Laryngoscope 2001 May;111(5):837-43.

(23) Ketten DR, Skinner MW, Wang G, Vannier MW, Gates GA, Neely JG. In vivo measures of cochlear length and insertion depth of nucleus cochlear implant electrode arrays. Ann Otol Rhinol Laryngol Suppl 1998 November;175:1-16.

(24) Whiting BR, Bae KT, Skinner MW. Cochlear implants: three-dimensional localization by means of coregistration of CT and conventional radiographs. Radiology 2001 November;221(2):543-9.

(25) Xu J, Xu SA, Cohen LT, Clark GM. Cochlear view: postoperative radiography for cochlear implantation. Am J Otol 2000 January;21(1):49-56.

(26) van Wermeskerken GK, van Olphen AF, Smoorenburg GF. Intra- and postoperative electrode impedance of the straight and Contour arrays of the Nucleus 24 cochlear implant: relation to T and C levels. Int J Audiol 2006 September;45(9):537-44.

Summary and conclusions

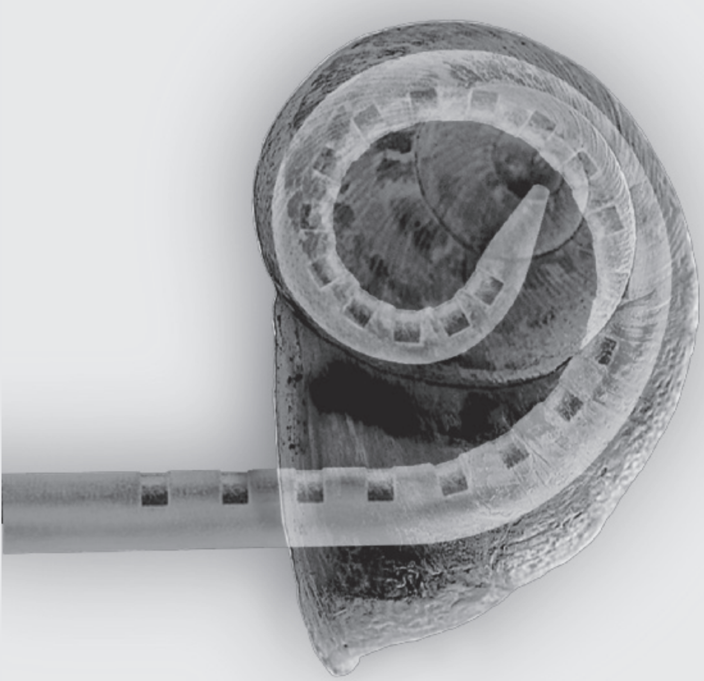

Cochlear implantation (CI) has become an increasingly accepted and effective treatment for profoundly pre- and postlingually deaf patients. The outcomes of CI have improved significantly over the last two decades. This is especially due to technical improvements such as the refinement of electrode designs and speech-processing strategies. The problem of predicting outcomes in CI has preoccupied many researchers. In this thesis we focus our attention on prognostic factors related to electrophysiology, anatomy, and imaging techniques.

Chapter 1 presents an overview of the history of CI and its ongoing development, emphasizing the latest generation of multichannel CI systems and CI candidacy.

Secondly, electrophysiological measurements such as the electrical impedance and the electrically evoked compound action potential (ECAP) are discussed. The electrode is the all-important interface between the electrical stimulus and the auditory nerve fibers that need to be stimulated. The importance of electrode impedance is explained; it provides an indication of electrode integrity and reflects the status of the electrode-tissue interface. Post-implantation effects, such as intracochlear osteoneogenesis or fibrous tissue growth, can negatively influence electrical impedance and thereby increase power consumption. The ECAP came into use with the introduction in 1998 of telemetry in cochlear implants. Nowadays, this method of intracochlear recording is implemented in some speech-processor fitting procedures. It can speed up the fitting procedure by allowing higher stimulation levels than previously applied. This chapter explains the ECAP recording procedure and expands on its possible application in clinical practice.

Thirdly, an overview of the imaging modalities available in the pre-operative work-up for CI is given. High resolution computed tomography (HRCT) provides an exquisitely detailed image of all bony anatomy, including the mastoid, middle ear, cochlea, tegmen, and otic capsule, but also pertinent vascular structures of the temporal bone. However, the cochlear patency may not be as reliably apparent as in magnetic resonance imaging. Radiologically detectable inner ear (IE) malformations have been reported to occur in approximately 5 to 15% of the cases of congenital sensorineural hearing loss. With improvements in HRCT and a better understanding of cochlear malformations, more IE malformations have been identified over the past decade, and in these cases CI has been performed. This development contrasts starkly with previous indications for CI: children with IE malformations used to be excluded on the assumption that they would not perform adequately after implantation. To correlate certain types of IE malformations with surgical aspects of cochlear implantation and rehabilitation outcomes, most reports use the embryogenesis-based classification system described by Jackler et al. Some aspects of classification systems used on IE malformations are described in relation to CI. Unfortunately, hardly any information is available on the relation between the nature of IE malformation and the degree of (dys) function.

At the end of the chapter the overall aims of this thesis are described.

Chapter 2 focuses on various factors influencing electrode impedance. These include the electrically evoked stapedius reflex measurement during surgery, electrode design, stimulation mode, and T and C levels over a nine-month post-operative period. The study includes seventy-five implant recipients, implanted with either a Nucleus straight array or a Contour array. The results show that, during surgery, electrode impedance decreases markedly after electrically evoked stapedius reflex measurements. After surgery, impedance increases in the period without stimulation prior to speech-processor switch-on but decreases after switch-on. The lower impedance values recorded after a period of stimulation are found at the higher T and C levels. This study shows that electrical stimulation results in a lower electrical impedance. This is probably due to the formation of a hydride layer, which effectively increases the surface area of the electrode. In periods without electrical stimulation, we find an increase of impedance, probably due to fibrous tissue growth. The difference in electrical impedance between the two types of implants used in this study corresponds to their respective surface areas. In addition, the Nucleus straight array shows a greater increase of impedance in the apical direction than found for the Contour array, probably as a result of the larger fluid environment around the basal electrodes.

Chapter 3 evaluates the ECAP, which is currently applied in various methods of speech-processor fitting. The ECAP measurements can be performed intra- or postoperatively. To find out whether changes had occurred in ECAP threshold levels after use of the cochlear implant, we compared the ECAP data acquired intra- versus postoperatively. Twenty-five adult patients were included in this study. A high success rate (97.4%) was found when the ECAP threshold was recorded per patient in the intra-operative setting. Measured post-operatively, the success rate per patient was significantly lower (53.4%). Correlations between the intra- versus post-operative ECAP thresholds were statistically significant for all electrodes tested. The ECAP thresholds were not significantly different for the two settings; the effects of changes to the auditory neural periphery are not noticeable.

A limitation of our study was that we could not obtain results in ECAP measurements in all patients postoperatively. To ascertain the presence of biasing factors, we analyzed the differences between three subgroups as to the intra-operative ECAP threshold level and the post-operative C levels. Again, we found no significant differences between these groups. Because the highest success rate for obtaining results of ECAP measurements was in the intraoperative setting, we recommend this setting for acquisition of the ECAP threshold.

Chapter 4 describes a group of children with radiographically detectable IE malformations. Their audiological performance, as assessed by speech-reception tests and ECAP measurements, is compared to the performance of prelingually deafened children at large. At our center, 20% of the congenitally deaf children have IE abnormalities, whereas Jackler et al. report between 5 and 15%. The IE abnormalities include one incomplete partition (IP) type 1, five cases of IP-2, five cases of enlarged vestibular aqueduct, three cases of semicircular canal dysplasia, and two cases of widened internal auditory canal. None of the subjects had the more severe common cavity malformations. The ECAP measurements were successfully recorded in both groups.

The results for open-set speech perception did not differ significantly across the groups, although the variance within both groups differed considerably. Electrode insertion problems were not encountered after cochleostomy in any of these patients. In four out of nine patients with IE malformations, there was minor leakage of cerebrospinal fluid (CSF). Among the children whose inner ear malformations were limited to the IP type, the ability to develop open-set speech perception, as determined after an average follow-up period of two years, was equal to that of prelingually deaf cochlear implant recipients. Intraoperatively, a CSF leak can be expected and managed adequately.

Chapter 5 focuses on postoperative imaging of the temporal bone and the cochlear implant. Recent literature has drawn attention to the importance of intracochlear positioning and reducing intracochlear trauma during insertion of the electrode array. Several imaging modalities are available to assess the position of the electrode array, the main ones being 2-D X-ray approaches, rotational tomography, and HRCT. With the introduction of the 64-slice HRCT scan, thin-slice coverage has improved the quality of the diagnostic images, possibly due to smaller electrode artifacts. We examined a fresh human temporal bone and a fresh human cadaver head, both of which were implanted and then immediately scanned. We were able to identify each electrode individually. Because the electrode artifact was small, after mid-modiolar reconstruction we could locate the intracochlear electrode position relative to the scala tympani and scala vestibuli. This study demonstrates the feasibility of visualization of the electrode position within the intracochlear spaces by means of multislice HRCT scanning.

Chapter 6 investigates the relation between electrophysiological data and the electrode position after cochlear implantation. The development of a new generation of cochlear implant devices as well as modern surgical techniques has to a great extent been aimed at improving stimulus-transferring mechanisms, for example in the modiolus hugging design of the electrode array. In this study we analyzed five adult cochlear implant recipients. In all patients, the electrical impedance and the ECAP were recorded immediately after implantation. The electrode position relative to the modiolus was assessed by means of HRCT, and correlated to the electrophysiological measurements. With HRCT full insertion of all electrode arrays could be visualized and confirmed. The individual electrode distance towards the modiolus could be most precisely analyzed for the basal part of the electrode array. The electrodes in the more apical part of the electrode array could not be identified separately due to image degradation caused by partial volume effects and metallic artifacts of the electrode. We did not find a correlation between the electrical impedance and electrode distance. However, a significant correlation was found between electrode distance and the ECAP. We conclude that the electrode – modiolus distance is of importance in the stimulation of auditory nerve fibers. In the future, further developments of imaging techniques will improve and refine our insight in the relation between electrode positioning and electrophysiological functioning.

General conclusions

1. Electrical stimulation results in a lower electrode impedance.
2. The major difference in electrode impedance between the Nucleus straight and the Contour array electrode is mainly due to their diverse surface areas.
3. The electrically evoked compound action potential is preferably acquired in the intra-operative setting.
4. Improvements in high resolution computed tomography has led to an increased identification of congenital inner ear abnormalities, in cochlear implant candidates.
5. After cochlear implantation, open-set speech perception in congenital inner ear abnormalities is comparable to that found in congenitally deaf patients.

6. Intra-operative complications, such as a cerebrospinal fluid leakage, can be expected in inner ear abnormalities during cochlear implantation.
7. Multislice computed tomography scanning can demonstrate the intracochlear position of the cochlear implant electrode relative to the scala tympani and scala vestibuli.
8. The electrode – modiolus distance is of importance in the stimulation of auditory nerve fibers.

Future developments

During the last two decades, research and development in cochlear implantation has resulted in new implant designs, electrode array configurations and miniaturization of electronics. Besides, great progress has been made in the development of new speech encoding strategies, which has led to a tremendous rise in speech perception scores. Developing a good fitting procedure will be a focus of future research. The conventional fitting procedure, in which behavioral responses are used will be supported by ECAP based fitting procedures. This suggests increasing importance of the routinely use of automated ECAP measurement systems.

Multislice CT scanning has greatly improved the imaging of the inner ear anatomy. With the latest generation HRCT more detailed information on intracochlear electrode positioning has become available as well. Technical improvements in both soft- and hardware will further improve the spatial resolution in HRCT under these extreme contrast conditions.

Samenvatting

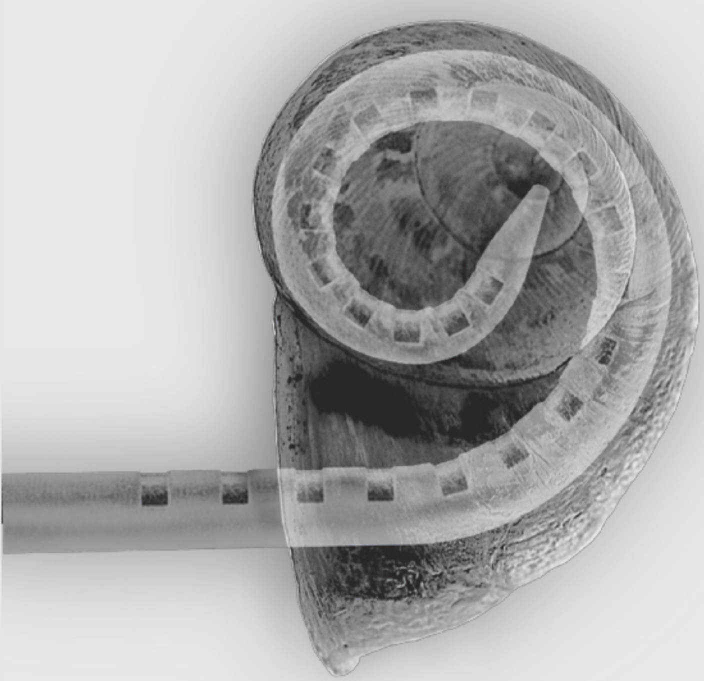

Cochleaire implantatie (CI) is een gangbare en effectieve behandeling voor ernstig pre- en post-linguale slechthorende- en dove patiënten. De resultaten van CI zijn de afgelopen 20 jaar sterk verbeterd. Dit is voornamelijk te danken aan technologische vernieuwingen, bijvoorbeeld op het gebied van elektrode ontwerp en spraakprocessor strategieën. Het voorspellen van resultaten na CI heeft veel onderzoekers bezig gehouden. In dit proefschrift kijken we naar prognostische factoren gerelateerd aan elektrofysiologie, anatomie en beeldvormende technieken.

Hoofdstuk 1 begint met een beknopt overzicht van de geschiedenis van CI en van de voortdurende technologische ontwikkelingen, zoals die van de laatste generatie multikanaals CI systemen.

Het belang van de elektrode impedantie wordt toegelicht; dit geeft een indicatie van de integriteit van de elektrode en reflecteert de status van de overgang van elektrode naar weefsel. Post-implantatie effecten, zoals intracochleaire osteoneogenesis of groei van fibreus weefsel kunnen de elektrische impedantie negatief beïnvloeden en zorgen voor een verhoogd stroomgebruik van het implantaat. De ECAP is sinds de introductie van telemetrie in 1998 een veelgebruikte meetmethode. Tegenwoordig is deze intracochleaire meetmethode geïmplementeerd in een aantal spraakprocessor afregelprocedures. Met de ECAP kunnen deze procedures worden bespoedigd, vergeleken met de conventionele, subjectieve afregelprocedure. In dit hoofdstuk wordt de ECAP procedure uitgelegd en worden toepassingen uit de dagelijkse praktijk beschreven.

In het derde deel van dit hoofdstuk wordt een overzicht gegeven over de verschillende beschikbare beeldvormende technieken in de preoperatieve voorbereiding voor CI. Hoge resolutie computer tomografie (HRCT) is uitermate geschikt om de benige anatomie van het os temporale te bekijken, zoals het mastoid, middenoor, cochlea, tegmen, maar ook die van de grote vaten. De cochleaire doorgankelijkheid kan echter beter worden gevisualiseerd met magnetische resonantie beeldvorming. Radiologisch detecteerbare binnenoor malformaties (IE) hebben een prevalentie van 5 tot 10% in de gevallen van een congenitaal perceptief gehoorverlies. Met verbeteringen in HRCT en een beter begrip van deze cochleaire malformaties worden meer IE malformaties geïdentificeerd in de laatste decade, en in veel gevallen CI uitgevoerd. Deze ontwikkeling staat in scherp contrast met eerdere indicaties voor CI; kinderen met IE malformaties werden voorheen geëxcludeerd op grond van de verdenking van een slechte uitkomst na implantatie.

Het grootste deel van de literatuur betreffende IE malformaties en chirurgische aspecten bij CI is gebaseerd op het classificatie systeem van Jackler. Dit is gebaseerd op embryologische aspecten. Sommige aspecten hiervan worden beschreven in relatie tot CI. Helaas is tot op heden weinig informatie beschikbaar over de relatie tussen het type IE malformatie en de mate van dysfunctie.

Hoofdstuk 2 beschrijft verschillende factoren die van invloed zijn op de elektrode impedantie, te weten het testen van de elektrisch opwekbare stapedius reflex tijdens chirurgie, elektrode ontwerp, stimulatie modus, het drempel niveau (T-level) en aangenaam luidheidsniveau (C-level) in een negen maanden durende postoperatieve fase. Deze studie bevat de gegevens van vijfenzeventig patiënten, geïmplanteerd met een Nucleus straight elektrode of een Contour elektrode. De resultaten laten zien dat tijdens chirurgie de elektrode impedantie afneemt na de elektrisch opwekbare stapedius reflex testen. Na chirurgie neemt de elektrode impedantie toe, zonder elektrische stimulatie, totdat de spraakprocessor wordt aangezet en de impedantie afneemt. Lagere impedantie waarden worden gevonden bij hoge stimulatiewaarden van de T en C niveaus. Deze studie toont dat elektrische stimulatie resulteert in een lagere elektrische impedantie. Dit komt waarschijnlijk door de formatie van een hydride laag, die het elektrode oppervlak effectief vergroot. In periodes zonder elektrische stimulatie wordt een toename van de elektrische impedantie gevonden door de formatie van fibreus weefsel. Het verschil in elektrische impedantie tussen de twee type implantaten correspondeert met hun afzonderlijk elektrode oppervlak. Daarnaast zien we bij de Nucleus straight elektrode een grotere toename in elektrode impedantie in the apicale richting dan bij de Contour elektrode, als gevolg van een groter vloeistofcompartiment rondom de basale elektrodes.

Hoofdstuk 3 evalueert de ECAP, die wordt toegepast in verschillende spraakprocessor afregelprocedures. De ECAP-metingen kunnen zowel intra- als postoperatief worden verricht. Om drempelverschuivingen van de ECAP te evalueren na gebruik van de CI hebben we de ECAP data intra- en post-operatief met elkaar vergeleken. Vijfentwintig volwassen patiënten werden geïncludeerd. Een hoog succespercentage (97.4%) werd gevonden bij het meten van de ECAP drempel intra-operatief per patiënt. Het succespercentage post-operatief was beduidend lager (53.4%). Correlaties tussen de intra- en post-operatieve ECAP metingen waren statistisch significant in alle geteste elektrodes. De drempel ECAP was niet statistisch verschillend op de twee meetmomenten; veranderingen in de perifere banen van de gehoorzenuw zijn niet meetbaar.

Een beperking van onze studie was dat we niet in alle patiënten postoperatief een ECAP drempel konden meten. Om bias factoren in deze groep uit te sluiten hebben we drie verschillende subgroepen gedefinieerd in relatie tot een meetbare ECAP drempel en de postoperatieve C levels. Opnieuw kon geen statistisch significant verschil tussen deze groepen worden gevonden. Omdat het grootste percentage goed meetbare ECAP drempels wordt gevonden in de intra-operatieve groep adviseren wij dit meetmoment om de ECAP te bepalen.

Hoofdstuk 4 beschrijft een groep kinderen met radiologisch detecteerbare IE malformaties. Hun audiologische prestaties, in dit geval gedefinieerd in de vorm van spraaktesten en ECAP metingen, zijn vergeleken met de prestaties van een groep prelinguaal dove kinderen. In onze studie werd een percentage van 20% IE malformaties gevonden in de groep congenitaal dove kinderen. In de literatuur van Jackler wordt een prevalentie van 5-15% beschreven. De IE afwijkingen in deze studie zijn één incomplete partitie (IP) type 1, twee maal een IP-2, vijf maal een vergroot vestibulair acquaduct, drie maal een semicirculair kanaal dysplasie en twee maal een verwijde meatus acusticus interna. Geen van de kinderen in deze studie had de meer ernstige common cavity malformatie. De ECAP metingen waren succesvol in beide groepen.

De resultaten voor de open-spraak testen verschilden niet significant tussen de twee groepen, alhoewel de variabiliteit in beide groepen aanzienlijk was. Problemen bij de elektrode insertie werden niet gezien na de cochleostomie. In vier van de negen patiënten met IE malformaties trad een kleine liquor lekkage op. In onze studie groep, gelimiteerd tot de IP malformatie, vonden we een gelijke spraakontwikkeling na een follow-up periode van twee jaar in vergelijking met een groep prelinguaal dove CI gebruikers. Op de mogelijkheid van intraoperatieve liquorlekkage bij een IE malformatie moet worden geanticipeerd.

Hoofdstuk 5 is gericht op post-operatieve beeldvorming van het os temporale en het cochleaire implantaat. De recente literatuur benadrukt opnieuw het belang van de intracochleaire positie en het verminderen van intracochleair trauma na insertie van de elektrodedraad. Er bestaan verschillende beeldvormende technieken om de intracochleaire elektrode positie te bepalen. De belangrijkste zijn de conventionele 2-D röntgen opnames, rotatie tomografie en HRCT. Met de introductie van de 64 slice HRCT scan lijkt het mogelijk om ultradunne coupes te maken met een hogere resolutie, mogelijk door verminderde elektrode artefacten. In deze studie hebben we een vers humaan os temporale en een humaan kadaver hoofd geïmplanteerd en direct hierna gescand. Het bleek goed mogelijk ieder afzonderlijke elektrode individueel te identificeren met HRCT. Door de kleine elektrode artefacten konden we, na mid-modiolaire reconstructie, de intracochleaire positie van de elektrode bepalen ten opzichte van de scala tympani en de scala vestibuli. Een scanprotocol wordt dan ook beschreven.

Hoofdstuk 6 onderzoekt de relatie tussen elektrofysiologische testen en de elektrode positie na cochleaire implantatie. De ontwikkeling van nieuwe implantaten en moderne operatiemethoden zijn voornamelijk gericht voor het optimaliseren van de signaaloverdracht. Dit wordt bijvoorbeeld gezien bij de zogenaamde *modiolus hugging* implantaat ontwerpen. In deze studie hebben we vijf volwassen patiënten geïncludeerd. Zowel de elektrische impedantie als de ECAP werd bepaald direct na implantatie. De elektrode positie relatief ten opzichte van de modiolus werd vastgesteld middels HRCT en gecorreleerd aan de eerder verkregen elektrofysiologische data. Met HRCT bleek het goed mogelijk de volledige insertie van de elektrodedraad te visualiseren en te bevestigen. De individuele elektrode afstand tot de modiolus kon met name in het basale deel van de elektrodedraad worden bepaald. De meer apicaal gepositioneerde elektrodes konden niet afzonderlijk worden geïdentificeerd door beeld degradatie als gevolg van het *partial volume effect* en metaal artefacten van de elektrode. We hebben geen corelatie kunnen vinden tussen de elektrische impedantie en elektrode afstand. Wel konden we een significante correlatie vinden tussen elektrode afstand en de ECAP. We concluderen dat de elektrode – modiolus afstand van belang is in de stimulatie van de gehoorzenuwvezels. In de toekomst zullen verdere ontwikkelingen in beeldvorming een beter beeld brengen van de relatie tussen elektrode positie en de elektrofysiologische functie.

Conclusies

1. Elektrische stimulatie leidt tot een lagere elektrode impedantie.
2. Het verschil in elektrode impedantie tussen de Nucleus straight elektrode en de Contour elektrode is voornamelijk het gevolg van hun verschillende elektrode oppervlakte.
3. Het meten van de ECAP dienst bij voorkeur plaats te vinden in de intraoperatieve fase.
4. Technologische ontwikkelingen in HRCT hebben geleid tot een verhoogde incidentie van het aantal IE malformaties, in cochleair implantaat kandidaten.
5. Na cochleaire implantatie is het spraakverstaan bij patiënten met een IE malformatie grotendeels vergelijkbaar met congenitaal dove patiënten.
6. Op intraoperatieve complicaties bij patiënten met een IE malformatie, zoals liquorlekkage, dient te worden geanticipeerd.

7. Met HRCT is het mogelijk de intracochleaire positie van de cochleair implantaat elektrode te bepalen ten opzichte van de scala tympani en de scala vestibuli.
8. De elektrode – modiolus afstand is van belang in de stimulatie van de gehoorzenuwvezels.

Toekomstige ontwikkelingen

Gedurende de afgelopen twee decades heeft onderzoek op het gebied van cochleaire implantatie geleid tot nieuw vormgegeven implantaten, elektrode *arrays* en verdere miniaturisatie van elektronica. Daarnaast hebben verbeteringen in spraakprocessor strategieën geleid tot een grote vooruitgang in de spraakverstaan scores van CI gebruikers. De ontwikkeling van nieuwe spraakprocessor afregelprocedures zal een belang onderzoeksdoel zijn. De conventionele aanpassingsprocedure, met subjectieve responsies, zal worden aangevuld met op ECAP gebaseerde afregelprocedures. Hiervoor zal de ontwikkeling van een geautomatiseerd ECAP meetsysteem noodzakelijk zijn.

Ontwikkelingen in HRCT hebben geleid tot een verbeterde beeldvorming van het binnenoor. Met de laatste generatie HRCT scanners blijkt het zelfs mogelijk de intracochleaire elektrode positie te bepalen. Met ontwikkelingen zowel op het gebied van hard- en software zal de spatiële resolutie verder verbeteren onder deze extreme contrast condities.

Dankwoord

Allereerst wil ik alle patiënten bedanken die deel hebben genomen aan dit onderzoek. Hiernaast wil ik een aantal personen in het bijzonder bedanken voor hun hulp bij dit proefschrift.

Prof. Dr. F.W.J. Albers. Voordat u vanuit Groningen naar Utrecht kwam heeft u mijn onderzoek weer op de rails gezet. Zonder uw stimulerende en altijd maar weer opbouwende kritische houding was dit proefschrift nooit tot een goed einde gekomen. Dat uw ziekte u fataal is geworden doet mij en vele anderen nog steeds veel verdriet. Ik ben u nog altijd zeer erkentelijk voor uw bijdrage.

Prof. Dr. K. Graamans, beste Kees, uiteindelijk promoveer ik toch nog bij jou! Ik kan me nog goed herinneren dat ik maar al te graag bij jou onderzoek wilde doen. Jouw vertrek naar Nijmegen indertijd maakte dat helaas niet meer mogelijk. Dat je nu in deze fase van mijn onderzoek wilde inspringen is heel bijzonder. Hiervoor heel veel dank. Dankzij onze feilloze breedbandverbinding en jouw correctiewerk met het potlood kwam het toch allemaal tot een goed einde.

Prof. Dr. G.J. Hordijk, beste Gerrit Jan, dank voor je promotorschap. Na mijn opleidingstijd waarin ik je enthousiasme en kennisoverdracht zeer heb gewaardeerd komt het dan toch eindelijk tot een boekje. Misschien niet altijd meer door iedereen verwacht, maar dankzij jouw eerdere inspanningen tegen het einde van mijn opleiding, kwam het onderzoek weer op de rails. Ik ben blij dat ik ook onder jouw leiding kan promoveren. Dubbel Hordijk.

Prof. Dr. G.F. Smoorenburg, beste Guido. Het opstarten van dit onderzoek heeft enige tijd gekost, het resulteerde uiteindelijk in een stuk waarin ik nog nooit zoveel data aan mijn ogen voorbij heb laten gaan. Dat ik me achteraf realiseerde dat ik het ook allemaal heb ingetypt maakt het een stuk om niet te vergeten. Dank voor onze samenwerking.

Dr. A.F. van Olphen, beste Adriaan. Je hebt er altijd in geloofd dat het tot een goed einde zou komen, en gezorgd voor de nodige morele en inhoudelijke

ondersteuning. Dat motiveerde mij des te meer dit af te ronden, veel dank voor onze samenwerking.

Dr. G.A. van Zanten, beste Bert, dank voor je hulp in mijn onderzoek. We hebben in een korte tijd een fraai stuk geproduceerd waarin mij steeds opviel hoeveel structuur jij eraan kon geven, dat was zeer leerzaam. Je spoedcursus SPSS kwam daarnaast later ook nog goed van pas. Veel dank voor alles.

Prof. Dr. M. Prokop, beste Mathias, op een dag kwam ik bij je binnen gewandeld met de vraag of CT onderzoek nieuwe inzichten zouden kunnen verschaffen na CI. Je enthousiasme om hiermee aan de slag te gaan, tussen al je drukke bezigheden door, heb ik zeer gewaardeerd.

Dr. H. Lubsen, beste Herman, na mijn opleiding heb je mijn wegwijs gemaakt in de hals- en met name parotischirurgie. Wat is dit toch een leuk deel van ons vak, ik ben blij dat je me dit hebt geleerd. Behalve medische zaken besturen we ook graag samen een trein, de volgende keer zal ik de dodemansknop niet meer vergeten!

De leden van de beoordelingscommissie bestaande uit Prof. dr. W.P.T.M. Mali, Prof. dr. H.G. Gooszen, Prof. dr. V.M. Wiegant, Prof. dr. ir. A.F.M. Snik en Dr. G.A. van Zanten dank ik voor de moeite die zij hebben genomen voor de beoordeling van het manuscript.

Mijn paranimfen, Dr. J.A. de Ru en Dr. G.A. Verdoes Kleijn. Sander en Gijs, jullie steun, vriendschap en interesse in dit onderzoek heb ik zeer gewaardeerd. Sander, je wordt nu een echte sheriff! Hou het onderzoek gaande. Gijs, ik ben ooit begonnen jouw proefschrift te lezen, als medicus werd ik toen in het zwarte gat gesleurd en heb het nooit beëindigd. Dat je het nu voor het publiek toegankelijk maakt geeft mijn weer een kans deze materie te begrijpen.

De maatschap KNO Breda, Dr. Koos Plantenga, Paul Briët, Eric Janssen, Ariane Hesselink, Geert Küppers, Antoon van der Rijt en Milou Heiligers. De commissie promotie is van de agenda af! Dank voor al jullie steun om dit af te kunnen ronden. We gaan een fantastische toekomst tegemoet.

De (oud) stafleden en (oud) arts-assistenten van het AZU wil ik bedanken voor de samenwerking en goede tijd gedurende en na de opleiding.

Nancy Smyth-van Weesep, hartelijk dank voor alle snelle en fantastische taalkundige correcties.

Mijn ouders en mijn zus. Lieve papa en mama, Stephanie. Dank voor al jullie liefde, interesse en mogelijkheden die ik altijd heb gekregen om mijzelf te ontplooien.

Lieve Per en Derk, mijn twee helden. Papa wacht voorlopig nog even om dit boek aan jullie voor te lezen, want de boekenkast staat vol met veel leuker leesvoer.

Mijn liefste Sabine, jij bent mijn belangrijkste steunpilaar geweest in dit onderzoek. De continue druk die er was dit af te ronden heb jij goed gemerkt. Je bleef erin geloven. Dank voor al je steun en liefde.

Curriculum vitae

Gijs van Wermeskerken werd geboren op 19 januari 1972 in Leiden. In 1990 behaalde hij het VWO diploma aan het Rijnlands Lyceum te Oegstgeest. Na een verblijf van een jaar aan de Universiteit van Exeter in Engeland begon hij in 1991 met de propedeuse Biomedische Wetenschappen aan de Rijksuniversiteit Leiden. In 1992 startte hij de studie Geneeskunde. Tijdens de studie was de auteur als student-assistent actief (Joshua) op de thorax intensive care afdeling van het Academisch ziekenhuis te Leiden. Daarnaast werd uitvoerig dierexperimenteel onderzoek in het laboratorium voor experimentele chirurgie verricht onder leiding van Dr. P. Schoof, thoraxchirurg. Van 1996 tot halverwege 1997 volgde hij een afstudeerstage aan het department of cardiothoracic surgery van Duke University, North Carolina in de Verenigde Staten. Het artsexamen werd behaald in maart 1999. De opleiding tot KNO-arts vond plaats van mei 1999 tot juni 2005 in het Universitair Medisch Centrum Utrecht, onder leiding van prof. dr. G.J. Hordijk. De B-opleiding werd gevolgd in de Gelre ziekenhuizen, lokatie Lukas te Apeldoorn, onder leiding van drs. J.B. Antvelink en dr. P.P.G. van Benthem. Medio 2000 werd aangevangen met dit promotieonderzoek. Sinds januari 2006 is de auteur toegetreden tot de KNO maatschap van het Amphia ziekenhuis te Breda. De auteur is getrouwd met Sabine van Leeuwen. Zij hebben twee zonen, Per (2006) en Derk (2008).

Publications

- Disproportionate enlargement of the pulmonary autograft in the aortic position in the growing pig. Schoof PH, Hazekamp MG, Van Wermeskerken GK, De Heer E, De Bruijn JA, Gittenberger-de Groot AC, Huijsmans HA.
  J Thorac Cardiovasc Surgery 1998 June;115(6):1264-1272.

- Intraoperative physiologic variables and outcome in cardiac surgery: part I – in-hospital mortality. Hill SE, Van Wermeskerken GK, Lardenoye JH, Phillips-Bute B, White WD, Smith PK, Reves JG, Newman MF.
  Ann Thorac Surg 2000;69:1070-1076.

- Intraoperative physiologic variables and outcome in cardiac surgery: part II – neurological outcome. Van Wermeskerken GK, Lardenoye JH, Hill SE, Grocott HP, Phillips-Bute B, Smith PK, Reves JG, Newman MF.
  Ann Thorac Surg 2000;69:1077-1083.

- Transesophageal echocardiography in quantification of emboli during femoral nailing: reamed versus unreamed techniques. Coles RE, Clements FM, Lardenoye JW, van Wermeskerken GK, Hey LA, Nunley JA, Levin LS, Pearsall AW 4th.
  J South Orthop Assoc 2000 Summer;9(2):98-104.

- Diagnose in beeld: relapsing polychondritis. Van Wermeskerken GK, Van den Bergh WM, Frijns CJ.
  Ned tijdschr Geneeskunde 2004 jan 3:148(1):22.

- Cochleaire implantatie: "Elektrisch horen". Rinia AB, van Wermeskerken GK.
  Ned Tijdschr Geneeskunde-Studenteneditie 2005 jun;8(2):26-8.

- Contributions to the development of Otorhinolaryngology (ORL) in the Netherlands between 1880 and 1920. Huizing EH, van Wermeskerken GKA.
  J Laryngol Otol Suppl. 2005 Aug;(30):67-70.

- Intra- and postoperative electrode impedance of the straight and Contour arrays of the Nucleus 24 cochlear implant: Relation to T and C levels. Van Wermeskerken GK, van Olphen AF, Smoorenburg GF.
  Int J Audiol. 2006 Sep;45(9):537-44.

- A comparison of intra- versus post-operatively acquired electrically evoled compound action potentials. Van Wermeskerken GKA, van Olphen AF, Smoorenburg GF.
  Int J Audiol. 2006 Oct;45(10):589-94.

- Audiological performance after cochlear implantation: a 2 year follow-up in children with inner ear malformation. Van Wermeskerken GKA, Dunnebier EA, van Olphen AF, van Zanten GA, Albers FWJ.
  Acta Otolaryngol. 2007; 127: 252-57.

- Intracochlear assessment of electrode position after cochlear implant surgery by means of multislice computer tomography. Van Wermeskerken GK, Prokop M, van Olphen AF, Albers FW.
  Eur Arch Otorhinolaryngol 2007 Dec; 264(12): 1405-7.

- Imaging of electrode position in relation to electrode functioning after cochlear implantation. Van Wermeskerken GK, van Olphen AF, Graamans K.
  Submitted 2008.

Abbreviations

ACE	Advanced Combination Encoder speech coding strategy
AGF	Amplitude Growth Function
BTE	Behind The Ear speech processor
C level	Most Comfortable Loudness level
CG	Common Ground stimulation mode
CI	Cochlear Implant
CL	Current level
CSF	Cerebrospinal Fluid
CTDI	Computed Tomography Dose Indices
CU	Current Unit
EABR	Electrically evoked auditory brainstem response
EAS	combined Electric and Acoustic Stimulation
ECAP	Electrically evoked compound action potential
EI	Electrical Impedance
ESR	Electrically evoked Stapedius Reflex
EVA	Enlarged Vestibular Aqueduct
HRCT	High Resolution Computed Tomography
IE	Inner Ear
IP	Incomplete Partition
MP1	Monopolar stimulation mode against submuscularly placed reference electrode
MPR	Multi Planar Reformation
MRI	Magnetic Resonance Imaging
MTP test	Monosyllabic Trochee Polysyllabic test
NRI	Neural Response Imaging
NRT	Neural Response Telemetry
NVA test	‘Nederlandse Vereniging voor Audiologie’ open monosyllable test
RF	Radio Frequency
SCD	Semicircular Canal Dysplasia
SNHL	Congenital Sensorineural Hearing Loss
SPEAK	Spectral peak speech coding strategy
T level	Threshold hearing level
WIAC	Widened Internal Auditory Canal